PHARMACOMETRIC MODELING AND SIMULATION OF RANITIDINE IN HUMAN GASTRIC ACID SECRETION

A DISSERTATION
SUBMITTED TO THE FACULTY OF THE GRADUATE SCHOOL
OF THE UNIVERSITY OF MINNESOTA
BY

HYEWON KIM

IN PARTIAL FULFILLMENT OF THE REQUIREMENTS
FOR THE DEGREE OF
DOCTOR OF PHILOSOPHY

Dr. Richard C Brundage

January 2012

AKNOWLEDGEMENTS

First and foremost, I am deeply grateful to God for His support at every step in my life and blessing with wonderful family, friends and mentors. Without Him I believe it was impossible to finish this long journey.

I am especially indebted to my advisor, Dr. Richard Brundage for his guidance, patience and consideration. He helped me to grow as a scientist as well as showed what a great mentorship is. He treated me as one of his friends. His door was open so I always felt free to stop by and ask questions.

I gratefully acknowledge thesis reviewers and committee members: Dr. Richard Brundage, Dr. Esam El-Fakahany, Dr. Mark Kirstein, Dr. Weihua Guan and Dr. Henry Mann. Their valuable comments greatly improved my thesis. A special note of gratitude goes to Dr. Henry Mann for his generosity of letting me use his data for my thesis work.

I would like to acknowledge Dr. Celine Sarr at Novartis and Dr. Brian Corrigan at Pfizer, who were my summer-internship mentors for giving me the opportunities to work on a challenging and interesting projects in the industrial setting.

I am truly indebted to my parents, my sister (Hye Rim), parents-in-law and my husband (Myung Ki) for their unconditional love, trust and support. My strength is deeply rooted in their endless prayer. A special thanks goes to my baby Emily, a precious gift from God, for her waiting to be born after my final defense.

I would like to thank to my friends: Jae Eun, Wonkyung, Varun, Kyle, Amit, Akshanth, Chaitali, Ghada, Jia and Surish. The joyous moments we shared will not be forgotten in my life.

Dedicated to

My parents and their devoted life

ABASTRACT

Stress-related gastric mucosal damage commonly occurs in critically ill patients. Prophylactic therapy has become the standard in patients admitted to intensive care unit to prevent the significant morbidity and mortality associated with acute gastric hemorrhage. Ranitidine has been used widely to prevent the gastric mucosal damage in critically ill patients.

Data previously collected in two clinical trials included repeated measures of both plasma concentrations of ranitidine as well as multiple gastric acid measurements in critically ill patients and healthy volunteers. These studies were designed to answer a specific research question with a standard hypothesis-testing statistical approach, and those results have been reported.

Over the past several years, new research methodologies have been developed or newly applied to analyze this type of data. The aim of this dissertation was to apply new methodologies to develop an appropriate model to simulate the human gastric acid system. A pharmacometric approach places strong statistical and mathematical interpretation to characterize pharmacokinetic and pharmacodynamic behavior and to identify the patient's prognostic factors that cause changes. The pharmacometric analysis showed that 2-compartment pharmacokinetic model, indirect E_{max} exposure-response response model in sequential approach was superior to all other tested models. Creatinine clearance and sex were identified as important covariates for ranitidine pharmacokinetics. Survival analysis provides unbiased estimates from the time-to-event data with differential follow-ups and censoring issues. A parametric survival approach

can then be used to evaluate the model as well as predict observed or simulate future data. It was found that conditional hazard of event increased as time increased. Because it was impossible to discern the thorough exposure-response relationship of ranitidine effect with the range of explored exposure, we concluded that well designed, prospective time-to-event studies were necessary in the future. Simulation implements the physiologically-based mathematical model without invasive and costly experiments. The proposed mathematical model using STELLA® successfully demonstrated physiological gastric acid regulation, the effect of food, and histamine-2 receptor antagonist on gastric acid secretion.

The information from this dissertation can be used to determine an optimal dosing regimen of ranitidine that effectively controls gastric pH and to guide future investigations of stress-related gastric mucosal damage.

TABLE OF CONTENTS

ACKNOWLEDGEMENTS i

DEDICATION ii

ABSTRACT iii

TABLE OF CONTENTS v

LIST OF TABLES xi

LIST OF FIGURES xii

Chapter 1 Introduction 1

1.1 Stress Ulcer 1

1.1.1 Pathophysiology 2

1.1.2 Epidemiology 4

1.1.3 Prophylactic Options 5

1.1.3.1 Histamine 2 Receptor Antagonists 6

1.1.3.2 Proton Pump Inhibitors 7

1.1.3.3 Sucralfate 9

1.1.3.4 Antacid 10

1.1.3.5 Prostaglandin Analogue 10

1.1.3.6 Other Suggestions 10

1.1.3.7 Discontinuation of Prophylaxis 11

1.2 Research Objectives 12

Chapter 2 Simultaneous and Sequential Pharmacokinetic-Pharmacodynamic Models of Ranitidine in Critically Ill Patients and Healthy Volunteers 13

2.1 Introduction 13

2.2 Data 16

2.2.1 Effect of a Priming Dose on the Pharmacodynamic Response to Ranitidine Infusion (Ran-578) 16

2.2.1.1 Study Objectives 16

2.2.1.2 Inclusion and Exclusion Criteria 16

2.2.1.3 Procedures 17

2.2.1.3.1 Prestudy Phase 17

2.2.1.3.2 Study Phase 18

2.2.1.4 Responses to Study Drug 20

2.2.2 Effect of a Priming Bolus Dose on the Pharmacodynamic Response to Ranitidine Infusion in Intensive Care Unit Patients (Ran-591) 21

2.2.2.1 Study Objectives 21

2.2.2.2 Inclusion and Exclusion Criteria 21

2.2.2.3 Procedures 22

2.2.2.3.1 Laboratory Tests 22

2.2.2.3.2 Intragastric pH 22

2.2.2.3.3 Study Drug Administration 23

2.2.2.3.4 Blood Sample Collection 24

2.3 Methods 24

2.3.1 Pharmacokinetic-Pharmacodynamic Models 24

2.3.1.1 Pharmacokinetic-Pharmacodynamic Modeling Approaches: Sequential and Simultaneous Approaches 25

2.3.1.2 Pharmacokinetic-Pharmacodynamic Connecting Structure: Direct and Indirect Models 26

2.3.1.3 Exposure-Response Relationship: Linear and E_{max} models 26

2.3.2 Model Development 26

2.3.2.1 Base Model Development 27

2.3.2.2 Covariate Model Development 29

2.3.3 Model Evaluation 30

2.4 Results 31

2.4.1 Data 31

2.4.2 Patients' Demographics 32

2.4.3 Sequential Approach 32

2.4.3.1 Base Models 32

2.4.3.2 Final Models 33

2.4.3.3 Model Evaluation 34

2.4.4 Simultaneous Approach 35

2.4.4.1 Base Models 35

2.4.4.2 Final Models 36

2.4.4.3 Model Evaluation 37

2.4.5 Comparison of Final Sequential Model with Final Simultaneous Model 38

2.5 Discussion 38

Chapter 3 Population Exposure-Response Analysis Using Time-To-Event Data of the Ranitidine Pharmacodynamic Effect on Gastric Acid Secretion 61

3.1 Introduction 61

3.2 Data and Methods 67

3.2.1 Data 67

3.2.2 Exposure-Response Relationship 68

3.2.3 Time-To-Event Model Development 69

3.3 Results 71

3.4 Discussion 73

Chapter 4 Food and Histamine 2 Receptor Antagonist Effect on Human Gastric Acid Secretion 86

4.1 Introduction 86

4.2 Methods 89

4.2.1 Histology of the Stomach 89

4.2.2 Cell Populations 89

4.2.3 Neural Stimuli 89

4.2.4 Effecters of Acid Secretion 90

4.2.5 Feeding Function 98

4.2.6 Effects of Ranitidine 99

4.2.7 Sensitivity Analysis 100

4.2.8 STELLA® 100

4.3 Results 102

4.3.1 Baseline Conditions 102

4.3.2 Ranitidine Effect 103

4.3.3 Sensitivity Analysis 103

4.4 Discussion 104

Chapter 5 Summary and Future Directions 130

5.1 Pharmacokinetic-Pharmacodynamic Models of Ranitidine 130

5.2 Exposure-Response Analysis Using Time-To-Event Data of the Ranitidine ... 132

5.3 Food and Ranitidine Effect on Human Gastric Acid Secretion 133

REFERENCES 136

APPENDIX 153

LIST OF TABLES

2-1 Patients' demographics 46

2-2 Scheme of (a) base and (b) final pharmacokinetic and pharmacodynamic models in sequential approach 47

2-3 The population parameter estimates and bootstrap results of the final sequential model 48

2-4 Scheme of (a) base and (b) final pharmacokinetic and pharmacodynamic models in simultaneous approach 49

2-5 The population parameter estimates of the final simultaneous model and bootstrap results 51

3-1 Patients' demographics 79

3-2 Final population parameter estimates of the time-to-event model and bootstrap results 80

4-1 Ranitidine indication and dose 111

4-2 Parameter values included in model analysis 112

4-3 Initial conditions 114

4-4 Simulated gastric pH with and without ranitidine infusion 115

4-5 Baseline and peak gastric pH with different dose of ranitidine 116

LIST OF FIGURES

2-1 Scheme of pharmacokinetic and pharmacodynamic models for (a) direct response model and (b) indirect response model 52

2-2 Time course of ranitidine plasma concentrations 53

2-3 Gastric pH versus ranitidine plasma concentration plot 54

2-4 Goodness-of-fit plot of final sequential pharmacokinetic model 55

2-5 Visual predictive check plots of final sequential pharmacokinetic model 56

2-6 Quantified visual predictive check plot of final sequential pharmacodynamic model 57

2-7 Goodness-of-fit plot of final simultaneous pharmacokinetic model..... 58

2-8 Visual predictive check plots of final simultaneous pharmacokinetic model..... 59

2-9 Quantified visual predictive check plot of final simultaneous pharmacodynamic model..... 60

3-1 The probability density function of the Weibull distribution with different values of shape factor, gamma..... 81

3-2 The plot of time to gastric pH > 4 versus the area under the time-concentration curve from the beginning of ranitidine administration to 2 hours (AUC_{0-2})..... 82

3-3 The goodness of fit plots of final time-to-event model..... 83

3-4 The visual predictive plot of the final time-to-event model 84

3-5 The posterior predictive check of the final time-to-event model..... 85

4-1 Histology of stomach 117

4-2 Model diagram of effecter regulation of gastric acid secretion 118

4-3 Feeding function: The volume of food staying in the stomach over time 119

4-4 Baseline gastric pH when food is not given..... 120

4-5 Baseline and peak gastric pH with different dose of ranitidine 121

4-6 Baseline simulation of effecters. (A) Central nervous stimulants and enteric nervous stimulants, (B) Antral and corpal gastrin, (C) Histamine and (D) Antral and corpal somatostatin..... 123

4-7 Baseline simulation of the antral and corpal acid in response to food consumed .. 124

4-8 Ranitidine plasma concentration and gastric pH change 125

4-9 Ranitidine plasma concentration, gastric pH and the volume of food consumed... 126

4-10 Gastric pH change when ranitidine infusion is discontinued 127

4-11 Sensitivity analysis. Gastric pH changes according to the different infusion rate of ranitidine..... 128

4-12 The reciprocal change of gastrin and somatostatin..... 129

CHAPTER 1

INTRODUCTION

1.1 Stress Ulcer

It has long been recognized that severe physical or mental stress can cause upper gastrointestinal mucosal damage. In 1966, Fogelman MJ et al. reported several acute gastroduodenal ulceration cases in seriously ill patients (Fogelman MJ et al., 1966). A few years later, Skillman JJ et al. presented microscopic evidence of acute gastric ulceration in patients with respiratory failure, hypotension, sepsis or jaundice (Skillmann JJ et al., 1969). Although there are a few proceeding studies, Dr. Charles Lucas and colleagues' paper has been regarded as the first publication to coin the term "Stress Gastric Bleeding" (Lucas CE et al., 1971). The terminology in acute gastric bleeding from stress is well defined in virtue of considerable research over the last several decades. The commonly used terms in stress ulcer are the following (Cook DJ et al., 1994; Fennerty MB, 2002).

- Occult bleeding: a guaiac-positive gastric aspirate or guaiac-positive stool
- Overt bleeding: hematemesis, gross blood or "coffee grounds" material in a nasogastric aspirate, hematochezia or melena
- Clinically important bleeding: overt bleeding complicated by one of the following within 24 hours after the onset of bleeding (in the absence of other causes)

- A spontaneous decrease of more than 20 mmHg in the systolic blood pressure
- An increase of more than 20 beats per minute in the heart rate or a decrease of more than 10 mmHg in the systolic blood pressure measured on sitting up
- A decrease in the hemoglobin level of more than 2 g per deciliter and subsequent transfusion, after which the hemoglobin does not increase by a value defined as the number of units transfused minus 2 g per deciliter.

While the Curling's and Cushing's ulcer are recognized for their causes, stress ulcer is a term based on clinical consequences (Navab F et al., 1995). Most of the studies utilized stress-related upper gastrointestinal (UGI) bleeding as an efficacy measure of prophylaxis. Additional outcomes of efficacy or safety were the length of stay in the intensive care unit (ICU), blood transfusion requirements, the incidence of hospital-acquired pneumonia (HAP) and consequent mortality. Although it is not common, *Clostridium difficile*-associated disease was used as an outcome of interest in a few investigations.

1.1.1 Pathophysiology

Dr. Hans Selye defined stress as nocuous endogenous or exogenous stimulus which causes a general alarm reaction to the living organism (Selye H, 1936). Examples of stress include exposure to an extreme environment such as cold or heat, physical injury, poisoning with drugs, mental burden or emotional pressure. The cause of UGI stress ulcer is multi-factorial and its mechanism is not completely understood. Excessive

physiological or mental stress causes the sympathetic nervous system to enhance catecholamine release, vasoconstriction and the sequential hypoperfusion of the gastrointestinal (GI) mucosal layer, the reflux of bile juice and eventually the morphologic change of upper gastrointestinal mucosa results (Lucas CE et al., 1971; Spirt MJ et al., 2006; Quenot JP et al., 2009). Unlike the Curling's or Cushing's ulcer, however, the stress ulcer does not accompany hypersecretion of gastric acid. H^+ ion secretion remains stable or may decrease (Navab F et al., 1995; Fennerty MB, 2002). However, even small amounts of gastric acid can be harmful in combination with other factors. Once a patient undergoes excessive stress, the GI motility and blood perfusion to the GI system are decreased (Dive A et al., 1994; Heyland DK et al., 1996). This hypoperfusion causes the ischemia and the overproduction of nitric oxide and following reperfusion brings inflammatory action to the hypoperfused area (Fennerty MB, 2002; Spirt MJ et al., 2006). Cytotoxic cytokines from dead cells and overproduced oxidative radicals in combination with hypoperfusion cannot be cleared efficiently from the affected site. The mucosal layer also plays a critical role in protecting the gastric epithelial cell by trapping bicarbonate and blocking harmful substances from approaching the epithelium (Spirt MJ et al., 2006; Quenot JP et al., 2009). Thus, when the mucosal layer is damaged, it results in the damaged gastric cells by allowing the hydrogen ions and pepsin to injure the gastric epithelium. Decreased gastric motility causes the gastric cell to be exposed to the aggressive gastric acid longer than usual so that the risk of ulceration is increased. As a result, cell damage is worsened and recovery from a severe UGI stress ulcer sometimes requires medications after being discharged from ICU.

Two independent risk factors of UGI bleeding in critically ill patients are mechanical ventilation for longer than 48 hours and coagulopathy (Cook DJ et al., 1994). In 1999, the American Society of Hospital Pharmacists (ASHP) published risk factors for UGI bleeding. These include the general ICU patient population, patients with thermal injury, head injury, partial hepatectomy, hepatic failure, hepatic or renal transplantation, multiple trauma, spinal cord injury and history of gastric ulceration or bleeding within 1 year with the presence of at least two of the following: sepsis, corticosteroid therapy, occult or overt bleeding for ≥ 6 days (ASHP Therapeutic guideline on stress ulcer prophylaxis, 1999).

1.1.2 Epidemiology

The incidence of gastric bleeding from physiological or mental stress depends on various considerations such as the definition of gastric bleeding, the time of research, the severity of underlying disease and treatment setting. It has been reported that approximately 75 % or more of ICU patients have some gastric mucosal damage within 24 hours of ICU administration (Fennerty MB, 2002; Spirt MJ et al., 2006). Reports of the natural incidence of stress-related gastric bleeding have ranged from 0.6 to 33 % (Czaja MA et al., 1974; Peura DA et al., 1985; Zandstra DF et al., 1993). Clinically important bleeding has been reported to occur in 0.6 to 6% of critically ill patients (Fennerty MB, 2002; Quenot JP et al., 2009). Despite the broad reported incidence, the incidence of stress ulcer in ICU population has decreased significantly over the last decades from 20-30 % in 1970's to single digits in the 1990's (Navab F et al., 1995;

Grube RR et al., 2007). This was attributed to the advanced clinical care for the underlying disease in the ICU, higher availability of trained individuals in hospital, early recognition of the importance of stress ulcer prophylaxis and the introduction of new mechanism-based pharmacotherapeutic options. However, even with these advances the problem remains clinically important.

When the underlying disease or UGI ulcer is not treated properly and intragastric hemorrhage occurs, there is an increase in morbidity and mortality. The mortality rate was more than double (57 % vs 24 %) in patients with ulcer, bleeding or both within 18 hours of ICU admission than patients without these symptoms (Peura DA et al., 1985). Schuster DF and colleagues found higher mortality (64 % vs 9 %) and longer intensive care unit stay (median 14.2 days vs 4.2 days) in the group with gastric bleeding (Schuster DF et al., 1984). Cook DJ et al. also reported a higher mortality rate and longer ICU stay in patients with gastric bleeding than in patients without bleeding (Cook DJ et al., 1994; Cook DJ et al., 2001).

1.1.3 Prophylactic Options

The primary purpose of treatment related to stress ulcer is to prevent clinically important bleeding. The most frequently used medication for stress ulcer prophylaxis for ICU as well as non-ICU population is histamine 2 receptor antagonist (H2RA). Stress ulcer prophylaxis represented 74% of total usage of H2RA in 1998, but diminished to 64% in 2002 (Erstad BL et al., 1999; Daley RJ et al., 2004). In conjunction with this decrease,

the use of proton pump inhibitors (PPI) increased from 5% to 23% (Barletta JF et al., 2002; Daley et al., 2004). Even though the PPI has reduced the H2RA usage recently, H2RA is still the most commonly used agent in stress ulcer prophylaxis (Barletta JF et al., 2002).

1.1.3.1 Histamine 2 Receptor Antagonist

The histamine 2 Receptor Antagonist (H2RA) suppresses gastric acid secretion by competitively binding the histamine 2 receptor on the surface of the acid secreting cell. Although H2RA decreases the acid secretion effectively, the effect of H2RA is reversible based on its mechanism. The adverse effects of H2RA are infrequent but may require secondary medications or discontinuation of treatment. Potential adverse events include hepatitis, thrombocytopenia and central nervous system toxicities (e.g. confusion, delirium, hallucinations, slurred speech and headaches) which are more common in the elderly (Quenot JP et al., 2009). Elimination of H2RA, especially cimetidine, involves metabolism by the cytochrome P450 enzymes. Therefore some drug-drug interactions are of concern with drugs metabolized by the same enzymes such as warfarin, ketoconazole, phenytoin and theophylline (ASHP Therapeutic guideline on stress ulcer prophylaxis, 1999).

The efficacy of H2RA prophylaxis has proven to be superior or equivalent to contemporary alternatives: placebo (Peura DA et al., 1985; Cook DJ et al., 1996), sucralfate (Eddleston JM et al., 1991; Tryba M, 1991; Cook DJ et al., 1998), antacids

(Zeltsman D et al., 1996) and proton pump inhibitors (Levy MJ et al., 1997; Conrad SA et al., 2005; Ojiako K et al., 2008; Miano TA et al., 2009; Lin PC et al., 2010). Cook DJ et al. reported that prophylaxis with H2RA decreased the incidence of clinically important bleeding as well as overt bleeding in comparison to placebo or no therapy (Cook DJ et al., 1996). Dr. Michael Driks and several other researchers suggested that H2RA prophylaxis increased the occurrence of pneumonia (Driks MR et al., 1987; Eddleston JM et al., 1991; Tryba M, 1991; Apte NM et al., 1992; Cook DJ et al., 1996). Other publications demonstrated conflicting results (Simms HH et al., 1991; Prod'hom G et al., 1994; Cook DJ et al., 1998; Kantorova I et al., 2004). To understand this controversy, it has been proposed that several factors in combination with stress ulcer prophylaxis contributed to the incidence of pneumonia. These factors include intragastric volume, severity of underlying disease, bile reflux and oropharyngeal dysfunction (Navab F et al., 1995). It is believed that the relationship between H2RA prophylaxis and the incidence of pneumonia is confounded by uncontrolled factors. H2RA has been commonly used in the ICU as well as outside the ICU. However, tolerance to H2RA develops as early as 48 hours after the start of drug administration (Netzer P et al., 1999). This characteristic makes the H2RA less effective than PPI for long term prophylaxis. Despite sources of discrepancy from multiple studies, H2RA prophylaxis has contributed to the reduction of the incidence of overt GI bleeding and clinically important bleeding in ICU patient population (Cook DJ et al., 1996).

1.1.3.2 Proton Pump Inhibitor

The proton pump inhibitor (PPI) irreversibly binds to the H^+-K^+ ATPase of the gastric parietal cell. The proton pump is the final step of the H^+ ion secreting process so that it is an ideal target for acid suppressive treatment (Spirt MJ et al., 2006). Once the PPI binds to the proton pump, its effect does not disappear until the parietal cell is replaced by a newly differentiated cell. Thus, the PPI is a potent antisecretory agent that provides a long lasting effect. However, comparative studies of the PPIs are limited because the safety and efficacy of the PPI in critically ill patients has not been sufficiently established (Kantorova I et al., 2004). In several recent studies, the effect of the PPI was comparable to that of the H2RA in preventing clinically important bleeding (Levy MJ et al., 1997; Conrad SA et al., 2005; Miano TA et al., 2009; Lin PC et al., 2010). Unlike others, Ojiako K and colleagues found that clinically important bleeding was more common in patients with PPI prophylaxis than H2RA (3.2 % vs 0.38 %, Ojiako K et al., 2008)

The common adverse events of PPI are abdominal pain, nausea, diarrhea and headache (ASHP Therapeutic guideline on stress ulcer prophylaxis, 1999). The first developed PPI, omeprazole, causes a few drug-drug interactions with drugs metabolized by CYP450 whereas a more recent PPI, pantoprozole, has a profile of few drug interactions (Spirt MJ et al., 2006). There are reports that the PPI can be associated with a higher incidence of *Clostridium difficile*-related diarrhea (Dial S et al., 2004) and nosocomial pneumonia (Miano TA et al., 2009; Ran L et al., 2011). However, other publications reported the incidences of nosocomial pneumonia were not different between PPI and

H2RA treated patients (Levy MJ et al., 1997; Conrad SA et al., 2005; Ojiako K et al., 2008). Recent meta-analysis reported that the PPIs were no better than the H2RA in preventing stress related UGI bleeding, pneumonia and mortality among critical care patients (Lin PC et al., 2010).

PPIs are available as an intravenous formula, tablet and an oral suspension that can be given through a nasogastric tube. An immediate-release form of omeprazole powder was approved by FDA to prevent gastric bleeding from stress ulcer in 2005 (Zegerid package insert, 2007). Although the PPIs have been replacing H2RA prophylaxis gradually, more efficacy and safety research is necessary to establish its non-inferiority to the existing prophylaxis in preventing stress ulcer in critically ill patients.

1.1.3.3 Sucralfate

Sucralfate is a sucrose sulfate-aluminum complex which binds to the gastric mucosa. It creates a physical barrier between gastric acid and the mucosal layer. While sucralfate is not absorbed into the systemic circulation, it can impair the absorption of other drugs such as ciprofloxacin, theophylline, tetracycline, phenytoin, ranitidine, levothyroxin, ketoconazole and digoxin (Quenot JP et al., 2009). Other adverse events include constipation and aluminum toxicity. Sucralfate prophylaxis showed a similar effect to either H2RA or antacid in preventing clinically important bleeding (Tryba M, 1991; Cook DJ et al., 1996). However, inconsistent results were reported in sucralfate effect in terms of reducing the incidence of pneumonia and consequent mortality compared to

H2RA prophylaxis (Driks MR et al., 1987; Eddleston JM et al., 1991; Tryba M, 1991; Prod'hom G et al., 1994; Cook DJ et al., 1998; Kantorova I et al., 2004). Sucralfate does not increase gastric pH significantly and its mechanism of action is responsible for the lower incidence of pneumonia compared to H2RA or antacid prophylaxis (Quenot JP et al., 2009). Prod'hom G et al. reported rather complex results; sucralfate prophylaxis reduced the incidence of late onset pneumonia compared with antacid or ranitidine whereas the incidence of early onset pneumonia was not different among groups (Prod'hom G et al., 1994).

1.1.3.4 Antacid

Antacid is available in tablet, solution and suspension formulations. Although antacid presented a significant effect on reducing overt bleeding (Cook DJ et al., 1996), it is rarely recommended as prophylaxis of stress ulcer due to its laborious and frequent dosing and a number of side effects. Side effects of antacid are diarrhea, flatulence, headache, nausea, hepatic dysfunction, electrolyte abnormality, constipation and drug interaction (Spirt MJ et al., 2006)

1.1.3.5 Prostaglandin Analogue

The prostaglandin analogue, misoprostol is not used clinically due to its common side effects: nausea, abdominal pain and diarrhea.

1.1.3.6 Other Suggestions

Additional suggestions for stress ulcer prophylaxis to medications include close clinical and laboratory monitoring, administering sufficient fluid, avoiding non-steroid anti-inflammatory drugs (NSAIDs), narcotics, anti-cholinergics or aspirin or early enteral feeding if appropriate (Fennerty MB, 2002; Spirt MJ et al., 2006; Quenot JP et al., 2009). The efficacy of enteric feeding is still controversial. This controversy is from inadequate study design including small sample size, low statistical power, concurrent use of prophylaxis, inconsistent enteral nutrition regimen and variable definition of gastric bleeding (MacLaren R et al., 2001). Well designed, prospective randomized trials are necessary to determine the efficacy of early enteric feeding in preventing UGI bleeding in seriously ill patients.

1.1.3.7 Discontinuation of Prophylaxis

It is recommended that prophylaxis medication be discontinued once a patient is discharged from the ICU (ASHP Therapeutic guideline on stress ulcer prophylaxis, 1999). However, approximately half of the patients who received stress ulcer prophylaxis continued their medication after being discharged (Barletta JF et al., 2002; Grube RR et al., 2007). It was reported that 26.8-71.4 % of patients on an internal medicine ward received acid suppressive therapy and about half of the inpatients continued to take acid suppressants when they were discharged from the hospital (Gullotta R et al., 1997; Pham CQ et al., 2006). Several studies concluded that the prophylaxis of gastric bleeding in non-ICU setting is unnecessary because the incidence of stress ulcer is low (Grube RR et al., 2007; Amaral MC et al., 2010; Marik PE et al.,

2010). Discontinuation of stress ulcer prophylaxis should be based on the individual and daily evaluation of risk factors

1.2 Research Objectives

Ranitidine is one of the widely used histamine 2 receptor antagonists for stress ulcer prophylaxis in critically ill patients. Data from two clinical trials where pharmacokinetic and pharmacodynamic measurements occurred were available for secondary use. The specific research objectives of this thesis are the following:

1. To model the pharmacokinetic-pharmacodynamic (PKPD) relationship of ranitidine using a pharmacometric data analysis approach from a pooled data set obtained from critically ill patients and healthy volunteers
2. To develop an exposure-response model using a pharmacometric data analysis approach that describes the time to achieve gastric pH greater than 4 after administering ranitidine in critically ill patients and healthy volunteers
3. To test that a physiologically based mathematical model using STELLA® simulation software can describe the human gastric acid secretion, and to test that the current recommended ranitidine dose regimen can control the human gastric pH effectively

Chapter 2

Simultaneous and Sequential Pharmacokinetic-Pharmacodynamic Models of Ranitidine in Critically Ill Patients and Healthy Volunteers

2.1 Introduction

It is common to measure the plasma drug concentrations after a drug is administered. However, what is important to treat or to prevent the disease is the physiologic response of the body. The pharmacokinetic (PK) and pharmacodynamic (PD) models allow the description of the time course of the effect in response to the drug administration. Intensive sampling is necessary to develop the traditional PK and PD models. However, it is not only impractical but unethical to obtain multiple samples in certain populations such as pediatrics, geriatrics or critically ill patients. Thus, it has been common to develop PK and PD models with data from multiple individuals using a population approach. There are two approaches to estimate the PK and PD parameters: sequential and simultaneous approaches. In the sequential approach, the PK parameters are fitted to the PK data, and then the predicted concentrations from empirical Bayes estimates (EBE) of population PK parameters are used to fit the PD parameters to the PD data. The PK parameters of an individual i (i = 1, 2, …, N, where N is the number of individuals) are obtained by minimization of the following objective function ($OFV_{SEQ,PK}$), -2×log-

likelihood of the PK parameters given the observed PK data, assuming that the residual errors in the PK measurements are statistically independent and normally distributed with common variance σ_{PK}^2 for each individual and each measurement (Beal SL et al., 1989; Zhang L et al., 2003a; Proost JH et al., 2007):

$$OFV_{SEQ,PK} = -2 \times \log\left(\prod_i \int p(y_i \mid \theta) p(\theta \mid \Theta) d\theta \right) \tag{2.1}$$

where y_i is the collection of observed PK measurements for i[th] individual, θ is the PK parameters for individual i and Θ is the population PK parameters. The PD parameters of an individual i (i = 1, 2, …, N) are obtained by minimization of the following objective function ($OFV_{SEQ,PD}$), -2×log-likelihood of the PD parameters given the observed PD data and the individually estimated PK parameters, assuming that the residual errors in the PD measurements are statistically independent and normally distributed with common variance σ_{PD}^2 for each individual and each measurement (Beal SL et al., 1989; Zhang L et al., 2003a; Proost JH et al., 2007):

$$OFV_{SEQ,PD} = -2 \times \log\left(\prod_i \iint p(z_i \mid \theta, \phi) p\left(\theta \mid \hat{\Theta}\right) p(\phi \mid \Phi) d\theta \, d\phi \right) \tag{2.2}$$

where z_i is the collection of observed PD measurements for i[th] individual, θ and ϕ are the PK and PD parameters for individual i, respectively, $\hat{\Theta}$ is the estimated population PK parameters and Φ is the population PD parameters. This approach does not account for the possible influence of PD response to PK response (Zhang L et al., 2003a). PK and

PD responses are analyzed separately while conditioning PD response on the estimated PK parameters.

The second PKPD estimation approach is to estimate PK and PD parameters jointly by maximizing following OFV_{SIM} assuming that the residual errors in the PK and PD measurements are statistically independent and normally distributed with common variance σ_{PK}^2 and σ_{PD}^2 for each individual and each measurement, respectively (Beal SL et al., 1989; Zhang L et al., 2003a; Proost JH et al., 2007).

$$OFV_{SIM} = -2 \times \log\left(\prod_i \iint p(y_i \mid \theta) p(z_i \mid \theta, \phi) p(\theta \mid \Theta) p(\phi \mid \Phi) d\theta \, d\phi \right) \tag{2.3}$$

where y_i and z_i are the collection of observed PK and PD measurements for i^{th} individual, θ and ϕ are the PK and PD parameters for individual i, Θ and Φ are the population PK and PD parameters, respectively.

Stress-related gastric mucosal damage commonly occurs in critically ill patients (Duerksen DR, 2003). Prophylactic therapy has become the standard in patients admitted to intensive care unit to prevent the significant morbidity and mortality associated with acute gastric hemorrhage. Ranitidine has been used widely to prevent the gastric mucosal damage in critically ill patients since it was approved by US Food and Drug Administration (FDA) in 1983. To our knowledge, there is no available PKPD research of ranitidine using a population approach. The aim of this analysis was to model the PK-PD relationship of ranitidine, a histamine-2 receptor blocker (H2RA), in the sequential

and the simultaneous approaches from a pooled data set obtained from critically ill patients and healthy volunteers.

2.2 Data

The evidentiary data arose from two previous clinical trials.

2.2.1 Effect of a Priming Bolus Dose on the Pharmacodynamic Response to Ranitidine Infusion (Ran-578)

2.2.1.1 Study Objectives

The purpose of this study was to define the PK and PD relationships of serum concentrations of ranitidine and gastric pH in subjects receiving a bolus dose of ranitidine followed by a continuous infusion and subjects receiving a continuous infusion of ranitidine without a bolus dose.

2.2.1.2 Inclusion and Exclusion Criteria

Healthy volunteers were enrolled in the trial who were aged 18-50 years, nonsmokers, males or non-pregnant females with normal heart rate and blood pressure. Subject's laboratory parameters were within 10 % of normal range and baseline fasting pH was less than 3. The subject's total body weight was within 20% of ideal body weight for height and age as defined by the Metropolitan Life Tables of 1983. Subjects had no

history of cardiovascular, hematological, neurological, respiratory, hepatic or renal diseases nor were they taking any chronic medication. Subjects signed the informed consent documents.

Subjects that presented any of the following were excluded from the study: treatment with a histamine 2 receptor antagonist (H2RA) within 24 hours prior to entering the study, history of hypersensitivity to H2RA, history of esophageal varices, previous ulcer surgery with the exception of a simple oversew, Zollinger-Ellison syndrome or other pathological hypersecretory condition, acute or chronic renal impairment as evidenced by a serum creatinine > 2.0 mg/dL, liver impairment, drug abuse, alcoholism, use of an investigational drug within the past 30 days, use of alcohol or caffeine with 72 hours prior to study initiation.

2.2.1.3 Procedures

2.2.1.3.1 Prestudy Phase

The study population consisted of normal healthy volunteers admitted to the Clinical Research Unit (CRU). Sociodemographic data were obtained from all subjects. These data included age, gender, smoking habits, average alcohol consumption, average caffeine consumption, a medical history and a list of all medication used during the last 30 days. In addition, each patient underwent the following tests within 2 weeks prior to study enrollment: physical examination, laboratory tests and pregnancy test for all women of child bearing potential. Laboratory tests included serum sodium, potassium,

blood urea nitrogen (BUN), serum creatinine (SCr), glucose, aspartate transaminase (AST), alanine transaminase (ALT), alkaline phosphatase, complete blood count (CBC) and urine analysis.

2.2.1.3.2 Study Phase

Phase I

Subjects were admitted to the CRU on the evening prior to beginning the trial and were fed a light snack. At 10 PM the subject began an overnight fast. At approximately 6 AM a properly calibrated intragastric pH probe and nasogastric tube were passed nasally and operation of the intragastric pH monitoring system initiated. Continuous recording and storage of pH data, however was not initiated at this time. At 7 AM the intragastric pH measured with the indwelling pH probe was noted. If intragastric pH was greater than 3, the subject was ineligible to continue on that day. When pH was less than or equal to 3, an intravenous catheter was placed using aseptic technique in one forearm and a solution of 0.9 % sodium chloride was infused at a rate sufficient to keep the intravenous line patent. In the opposite forearm a heparin lock was placed using aseptic technique and flushed with 1-2 ml of a prepared heparin solution. Between 7:30 AM and 8 AM, the pH monitoring system was switched to the continuous recording and storage mode. At 8 AM a baseline blood sample (6 ml) and a baseline gastric fluid sample (5 ml) were obtained and the appropriate study medication as determined by the randomization schedule was given. Intragastric pH was continuously

recorded until 8 AM the following day. In addition, all subjects received 2 liters of 0.45 % sodium chloride containing 10 mEq/liter potassium. This solution was piggybacked over 24 hours into the line delivering study medication. Subjects consumed no food or liquids by mouth during the 24-hour study period.

Phase II

After a period of not less than 36 hours following the completion of Phase I, the subject returned to the CRU for Phase II. The procedures outlined for Phase I was followed except the subject was given the alternate medication as determined by the randomization schedule.

Phase III

After a period of not less than 36 hours following the completion of Phase II, the subject returned to the CRU for Phase III. The procedures outlined for Phase II was followed except the subject was given the alternate medication as determined by the randomization schedule.

During each of three study phases, subject was assigned to one of three treatments according to a randomization schedule generated by the Glaxo Department of Biostatistics. The three treatments were as follows:

Treatment A (Active/Active): 50 mg ranitidine diluted in a volume of 20 ml 0.9 % sodium chloride and delivered via peripheral vein over a period of five minutes.

Initiated simultaneously was an infusion of 75 mg ranitidine made up to 120 ml with 0.9 % sodium chloride and delivered with an infusion pump at a rate of 10 ml/hr.

Treatment B (Placebo/Active): 20 ml 0.9 % sodium chloride delivered via peripheral vein over a period of five minutes. Initiated simultaneously was an infusion of 75 mg ranitidine made up to 120 ml with 0.9 % sodium chloride and delivered with an infusion pump at a rate of 10 ml/hr.

Treatment C (Placebo/Placebo): 20 ml 0.9 % sodium chloride delivered via peripheral vein over a period of five minutes. Initiated simultaneously was an infusion of 120 ml with 0.9 % sodium chloride and delivered with an infusion pump at a rate of 10 ml/hr.

Other medications were not used in any subject during the course of the study. These medications included antacids, anticholinergics, off-protocol H2RA, salicylates and non-steroidal anti-inflammatory agents.

2.2.1.4 Responses to Study Drug

Pharmacokinetic Responses

To evaluate the pharmacokinetic profile of ranitidine, blood and gastric fluid samples were periodically collected for analysis of ranitidine concentration. Six (6) ml of blood and five (5) ml of gastric fluid were obtained immediately prior to the initiation of study medication and at 5, 10, 20, 30 and 45 minutes and at 1, 1.5, 2, 4, 6, 8, 10, 12, 12.5, 13, 14, 16, 18, 20 and 24 hours after beginning infusion. Blood samples were immediately

centrifuged and the serum withdrawn. Both serum and gastric fluid samples were split into two duplicate samples frozen at ≤ - 20 °C, and later sent to Glaxo for analysis of ranitidine concentrations.

Pharmacodynamic Responses

Gastric pH was recorded continuously and monitored at baseline and at 5, 10, 20, 30 and 45 minutes and at 1, 1.5, 2, 4, 6, 8, 10, 12, 12.5, 13, 14, 16, 18, 20 and 24 hours after beginning infusion. The time at which all samples were collected were appropriately recorded in the case report form.

2.2.2 Effect of a Priming Bolus Dose on the Pharmacodynamic Response to Ranitidine Infusion in Intensive Care Unit Patients (Ran-591)

2.2.2.1 Study Objectives

The objective of this study was to determine whether the use of a 50 mg bolus dose of ranitidine administered concurrently with the start of a continuous infusion of ranitidine in intensive care unit (ICU) patients results in a significant difference in the time to reach an intragastric pH of 4 relative to a continuous infusion alone.

2.2.2.2 Inclusion and Exclusion Criteria

All patients were at least 18 years of age, admitted to ICU or scheduled for ICU admission within 24 hours postoperative and required a nasogastric tube and H2RA therapy. Patients were fasting for at least the 8 hours of the study and had a baseline

intragastric pH less than or equal to 3. Patient, patient's spouse or nearest relative signed the informed consent document.

Patients in the following categories were excluded: treatment with an H2RA within 8 hours prior to entering the study, treatment with antacids within 4 hours of study, history of hypersensitivity to H2RA, history of esophageal varices or gastrointestinal bleed, previous ulcer surgery with the exception of a simple oversew, Zollinger-Ellison syndrome or other pathological hypersecretory condition, acute or chronic renal impairment as evidenced by a serum creatinine > 3.0 mg/dL, hospitalization for drug abuse or alcoholism, use of an investigational drug within the past 30 days, females who were pregnant or lactating, any history of upper gastrointestinal malignancy or receiving enteral nutrition.

2.2.2.3 Procedures

Demographic data were obtained from all patients including age, weight, sex, allergies, reason for surgery and concomitant medications.

2.2.2.3.1 Laboratory Tests

Within 12 hours prior to receiving study medication, blood was collected for the following assays: sodium, potassium, chloride, bicarbonate, glucose, blood urea nitrogen (BUN), creatinine, total bilirubin, alkaline phosphatase, aspartate transaminase (AST), alanine transaminase (ALT), hemoglobin, hematocrit, red blood cell and white

blood cell with differential. These laboratory tests were repeated within 24 hours following study treatment.

2.2.2.3.2 Intragastric pH

Intragastric pH was monitored using a gastric pH sensor tube (Graphprobe ST, Zinetics Medical, Salt Lake City, UT) positioned in the antrum of the stomach. Measurements were made from an aliquot of gastric fluid. Proper placement of the tube was confirmed radiographically. Intragastric pH data was recorded continuously with a computerized data acquisition and storage system (Synectics Medical, Irving, TX) and was provided to Glaxo Inc. on floppy disks.

2.2.2.3.3 Study Drug Administration

Patients were randomly assigned to one of the following two treatment groups:

Treatment A (Active/Active): 50 mg ranitidine diluted to a volume of 20 ml with 0.9 % sodium chloride and administered intravenously over a period of five minutes. Initiated simultaneously was an infusion of 50 mg ranitidine made up to 100 ml with 0.9 % sodium chloride and delivered with an infusion pump at a rate of 12.5 ml/hr (6.25 mg/hr) for 8 hours.

Treatment B (Placebo/Active): Placebo 20 ml with 0.9 % sodium chloride and administered intravenously over a period of five minutes. Initiated simultaneously was

an infusion of 50 mg ranitidine made up to 100 ml with 0.9 % sodium chloride and delivered with an infusion pump at a rate of 12.5 ml/hr (6.25 mg/hr) for 8 hours.

Medications were blinded and dispensed by the hospital research pharmacy according to a random code generated by the Glaxo Department of Biostatistics. The precise time of initiation of study drug delivery was indicated on the intragastric pH record. Other medications including antacids, anticholinergics, off-protocol H2RA, salicylates and non-steroidal anti-inflammatory agents were not used in any patient during the course of the study.

2.2.2.3.4 Blood Sample Collection

To evaluate the pharmacokinetic profile of ranitidine, blood samples were periodically collected for analysis of ranitidine concentrations. Six (6) ml of blood was obtained immediately prior to the initiation of study medication and at 1, 2, 4 and 8 hours following the beginning of the infusion. These samples were taken from the arm contralateral to the arm receiving the ranitidine infusion. Blood was immediately centrifuged, serum withdrawn, split into 2 samples and frozen at ≤ - 20°C, and later sent to Glaxo for analysis of ranitidine concentrations.

2.3 Methods

2.3.1 Pharmacokinetic-Pharmacodynamic Models

The total number of tested models in this analysis was eight as a combination of two PKPD modeling approaches (sequential and simultaneous approaches), two PKPD connecting structures (direct and indirect response models) and two exposure-response relationships (linear and E_{max} models). The scheme of PK and PD models are illustrated in Figure 2-1.

2.3.1.1 Pharmacokinetic-Pharmacodynamic Modeling Approaches: Sequential and Simultaneous Approaches

In the sequential approach, pharmacokinetic parameters were estimated first by fitting an appropriate PK model to the drug concentrations in the plasma concentration (C_p) versus time data. One- and two-compartment linear models were evaluated to characterize the time course of the plasmatic concentrations of ranitidine (Figure 2-2). The PK models were parameterized in terms of the clearances (CL and Q) and the volumes of distribution (V_c and V_p). Then, the PK parameters were fixed to the empirical Bayes estimates (EBE) of PK parameters and a PD model was fit to the effect versus predicted C_p data, assuming the PK and PD relationship.

In the simultaneous approach, the plasmatic concentrations of ranitidine and gastric pHs were analyzed together during a single run to allow integrated modeling of PK and PD parameters. The PK model which was inferior in the sequential approach was not tested in the simultaneous model development to save the amount of computational time in NONMEM.

2.3.1.2 Pharmacokinetic-Pharmacodynamic Connecting Structure: Direct and Indirect Models

The direct response model assumed the plasma drug concentration was directly related to the response whereas the indirect response model assumed the plasma concentration was related to the production rate (k_{in}) of response.

2.3.1.3 Exposure-Response Relationship: Linear and E_{max} Models

The exposure-response relationship between ranitidine PK and PD was not clear as presented in Figure 2-3. Gastric pH seemed to either increase proportionally to ranitidine plasma concentration or have the maximum value. Consequently, both the linear and E_{max} models were tested to describe the exposure-response relationship of ranitidine concentrations and gastric pH. Although the pH response is almost certainly expected to reach a plateau, the study design censored higher pHs, and a presumed maximal value was not able to be observed. The PD model was parameterized in terms of the baseline gastric pH (BS), the slope (SLP) of the relationship between gastric pH and ranitidine concentration for the linear model; or the BS, the maximum pH change (E_{max}) due to ranitidine, and the ranitidine concentration at which the ranitidine effect is half of the maximum (EC_{50}) for the E_{max} model.

2.3.2 Model Development

The pharmacokinetic-pharmacodynamic modeling was performed by means of nonlinear mixed-effects approach using NONMEM version 7 (ICON Development Solutions, Ellicott City, MD) with the interface Perl-speaks-NONMEM (PsN version 3.2.12, http://psn.sourcegorge.net/) on a personal computer (Intel® CORE Pro processor). Diagnostic graphics and post-processing of NONMEM output and simulations were performed using the statistical software R (version 2.9.1, http://www.r-project.org/).

In the sequential approach, the subroutines ADVAN1/ADVAN3 and ADVAN6 were used for PK and PD model, respectively. The first-order conditional estimation method (FOCE) with interaction was used for estimating the PK model parameters. Laplacian estimation method with interaction and YUP option was used for estimating the PD parameters due to the censored PD data. In the simultaneous approach, the subroutine ADVAN6 and FOCE estimation method with interaction was used. The YUP option was not used due to a model convergence issue.

Model selection was guided by

- Likelihood Ratio Test (LRT) when competing models were hierarchical
- Akaike Information Criteria (AIC, Akaike H, 1974) when competing models were non-hierarchical
- parameter precision expressed as relative standard error (RSE %) which was calculated as the estimate of standard error divided by the parameter value
- visual inspection of goodness-of-fit plots

- potential plausibility of the relationship between covariates and parameters
- the extent of the Bayesian shrinkage. Large values of shrinkage would be associated with generally poor individual estimates of that parameter.

2.3.2.1 Base Model Development

All PK parameters were assumed to be log-normally distributed and defined as

$$PK_i = TVPK \times exp(\eta_{PK}) \tag{2.4}$$

where $TVPK$ is the typical population value of PK parameter, PK_i is the individual PK parameter value and η_{PK} is the inter-individual variability (IIV) with a mean of zero and estimated variance of ω^2_{PK}. For PD parameters, IIV was assumed to be either normally or log-normally distributed. The following equation describes the case that IIV follows normal distribution.

$$PD_i = TVPD + \eta_{PD} \tag{2.5}$$

where $TVPD$ is the typical population value of PD parameter, PD_i is the individual PD parameter and η_{PD} is the IIV with a mean of zero and estimated variance of ω^2_{PD}. Residual unexplained variability (RUV) was explored using the additive, proportional or combined error model. Combined error models is defined as

$$C_{obs,ij} = C_{pred,ij} + C_{pred,ij} \times \varepsilon_{1,ij} + \varepsilon_{2,ij} \tag{2.6}$$

where $C_{obs,ij}$ and $C_{pred,ij}$ are the jth observed and predicted plasma concentrations in the ith individual, and $\varepsilon_{1,ij}$ and $\varepsilon_{2,ij}$ are random variables which are assumed to be normally distributed with a mean of zero and estimated variance of σ_1^2 and σ_2^2, respectively. The existence of a correlation between the parameters was also tested.

2.3.2.2 Covariate Model Development

From the base model, the effect of covariates on the parameters was tested. Patient specific factors considered for covariate testing included creatinine clearance (CrCL), weight, age, sex and race. Continuous variables were normalized by the median or a clinically relevant approximation to the median and incorporated into the model using a power function as follows:

$$TVP = \theta_P \times \left(\frac{Covariate}{median_{Covariate}} \right)^{\theta_{Covariate,P}} \tag{2.7}$$

where TVP is typical population value of the parameter, θ_P is the parameter for a subject with a covariate of $median_{Covariate}$ value, and $\theta_{Covariate,P}$ is an exponent allowing a nonlinear covariate effect on θ_P. The lack of a relationship would result in this exponent being driven toward zero (the null value). Discrete covariates were modeled as a fractional change to the control group. For example,

$$TVP = \theta_P \times \left(\theta_{Covariate,P}\right)^{Covariate} \tag{2.8}$$

Covariate is given the value of 0 if a patient is in a control group and a value of 1 if a competing group. Thus, θ_P is the parameter for a control group and $\theta_{Covariate,P}$ is the fractional change of θ_P for a competing group. The final model was built through the process of forward selection and backward elimination of clinical covariates. The likelihood ratio test was used to assess the statistical significance of all covariates in the final model. During forward selection, covariates were univariately tested and deemed significant if the OFV decreased by at least 3.8 (χ^2, $p \leq 0.05$, df = 1) with its inclusion in the model. During backward elimination, significance of the covariates was confirmed by removing one covariate at a time from the full model and required an increase in the OFV of at least 10.8 (χ^2, $p \leq 0.001$, df = 1) to remain in the model.

2.3.3 Model Evaluation

To evaluate the precision of the final model parameter estimates, a nonparametric bootstrap was performed, and a visual predictive check (VPC) was performed to assess the ability of the final PK model to predict the observations. For the sequential PKPD model, a total of 1000 bootstrap datasets were generated by repeated sampling with replacement from the original data to form new datasets having the same number of individuals as the original dataset. A total of 200 bootstrap datasets were generated for the simultaneous PKPD model. The smaller number of bootstrap data sets was implemented in the simultaneous PKPD model due to long computational times. The final PK and PD models were fitted to each of the bootstrap datasets to obtain the bootstrap parameter estimates. Bootstrap runs with successful minimization were used in

further analysis. The median, 2.5th and 97.5th percentiles of the bootstrap parameter estimates were obtained for each parameter and compared with the final model estimates from NONMEM. For the VPC of final PK model, 100 datasets using the covariate distributions from the original dataset were simulated using the parameter estimates from the final PK model. The median, 5th and 95th percentiles were compared to those of the observed concentrations. The quantified VPC was implemented to assess the percentage of available data around the simulated median (Post TM et al., 2008).

2.4 Results

The NONMEM codes for the final models are included in the Appendix.

2.4.1 Data

A total of 506 ranitidine plasma concentrations and 405 gastric pH from 16 healthy volunteers, 205 ranitidine plasma concentrations and 586 gastric pH from 51 critically ill patients were available for the analysis. Ranitidine concentrations below the limit of quantification (10 ng/mL) were excluded from the analysis. pH meter which was used for the PD data collection depicted the gastric pH as a fixed level when it was beyond a certain limit. Two investigators read the pH graph and translated the descriptive graph into numeric values. Those investigators recorded the censored value as 8.3 and 8.5,

respectively. One hundred-thirty one gastric pHs were censored in total of 1122 PD data (11.7%) and the censored PD data were excluded from the analysis.

2.4.2 Patients' Demographics

Patient's demographics are presented in Table 2-1. The majority of study subjects were male (70%) and Caucasian (93%). Other than Caucasians, two African-Americans, one Hispanic, one Asian and one Other Race subjects were identified in the study population. Two most frequent types of surgery in critically ill patients were coronary artery bypass (n=30) and aortic valve replacement (n=10). Fifty-eight percent of subjects were older than 50 years and a median (range) age was 57 years (20-76). Median (range) weight was 77.2 kg (37.7-173.9). Renal function within 24 hours of ranitidine administration was widely variable among subjects, with a median (range) CrCL of 88.8 ml/min (28.7-214.4). Of the 67 subjects, 39% (n=26) displayed some degree of renal impairment. Individuals classified with mild, moderate, and severe renal impairment as defined by the FDA regulatory guidelines for PK studies in patients with impaired renal (Food and Drug Administration, 2010) were 27% (n=18), 10% (n=7), and 1.5% (n=1), respectively.

2.4.3 Sequential Approach

2.4.3.1 Base Models

Plasma ranitidine concentration-time data were best described by a two-compartment linear model with inter-individual variability (IIV) on CL, V_c and V_p. Data were insufficient to separately identify the IIV on Q. High correlation was observed between

the inter-individual random effect (η) on CL and V_p, so a covariance between CL the V_p was introduced in the model. Introduction of covariance dropped 10.8 points in the objective function value (OFV) and improved the visual predictive check. Residual unexplained variability was described by combined error model. The relationship of gastric pH and ranitidine concentration was modeled in each combination of PKPD connecting structures and exposure-response relationships. The base PK and PD models in sequential approach are presented in Table 2-2 (a). In AIC comparison, indirect PKPD structure with E_{max} exposure-response relationship was found to be the superior pharmacodynamic base model.

2.4.3.2 Final Models

Creatinine clearance (CrCL) and sex were found to be significant covariates for CL and V_p, respectively. The relationship between covariate and parameters were described by following equations

$$TVCL(L/hr) = \theta_{CL} \times \left(\frac{CrCL}{90}\right)^{\theta_{CrCL,CL}}, \quad TVV_P(L) = \theta_{Vp} \times (Sex)^{\theta_{Sex,Vp}} \tag{2.9}$$

None of the covariates were significant on any of the PD parameters except when PK and PD connected directly and exposure-response had an E_{max} relationship. In the model with direct and E_{max} relationship, CrCL and race were significant covariates on baseline gastric pH (BS). Introducing two covariates in the model dropped 209.354 points of the objective function value (OFV). However, it was the indirect PKPD structure with E_{max}

exposure-response relationship model which was found to be the best pharmacodynamic model in terms of AIC. For convenience, the model with the indirect PKPD structure and E_{max} exposure-response relationship using the sequential approach is called final sequential pharmacodynamic model throughout this chapter. The final sequential PK and PD models are presented in Table 2-2 (b).

The parameter estimates of the final sequential model and the bootstrap results are presented in the Table 2-3. The typical value of CL, V_c, Q and V_p were found to be 25.7 L/hr, 16.6 L, 49.4 L/hr and 59.8 L for a male with a CrCL of 90 ml/min, respectively. The population estimates of ranitidine PK are consistent with the previously reported values in healthy volunteers (McNeal JJ et al., 1981; van Hecken AM et al., 1982). The estimate of elimination half-lives for ranitidine in the distribution and elimination phases was 8.2 minutes and 2.8 hours, respectively. The typical value of k_{in}, baseline gastric pH (BS), EC_{50} and E_{max} were found to be 1.15 ng/ml/hr, 2.13, 44.6 ng/ml and 7.67, respectively. The maximum gastric pH change after ranitidine was administered was 7.67 and 44.6 ng/ml of ranitidine plasmatic concentration was needed to achieve the half of maximum ranitidine effect. The inter-individual variability was found to be 22.8 %, 87.2 % and 14.4% for CL, V_c and V_p, respectively. The covariance between η_{CL} and η_{Vp} was 86.5 %. The goodness of fit plots for the final sequential PK model are presented in Figure 2-4. Residual plots did not show any specific pattern and the observed data seem to be well predicted by the model.

2.4.3.3 Model Evaluation

The visual predictive check (VPC) plots of final sequential pharmacokinetic model are depicted in Figure 2-5. The VPC of final PK model show that the model had adequately described the overall trend and variability in the observed data. No systemic deviation was observed between the observed and simulated data. The quantified visual predictive check (QVPC) plot of final pharmacodynamic model visualized the available observations around simulated median while including the unavailable data at each time point (Figure 2-6). Based on the report of Xu SX et al., the model could not be readily evaluated from 1 to 8 hours after starting the drug infusion because the percentage of the unavailable PD observations was more than 10 % (Xu SX et al., 2011). In the bootstrap analysis (Table 2-3), 905 and 909 runs of final PK and PD model, respectively, minimized successfully. All of the parameter estimates based on original dataset had relative standard errors (RSE) less than 50%. The medians of the bootstrap parameter estimates were similar to the NONMEM estimates based on original dataset. Overall, the bootstrap prediction intervals for the parameters are similar to the asymptotic confidence intervals based on NONMEM estimates.

2.4.4 Simultaneous Approach

2.4.4.1 Base Models

Because the one-compartment model was inferior to the two-compartment in the sequential approach, only two-compartment PK model was applied in the simultaneous approach. The relationship of gastric pH and ranitidine concentration was modeled in each combination of PKPD connecting structures and exposure-response relationships as

in the sequential approach. The base PK and PD models in the simultaneous approach are presented in Table 2-4 (a). In the AIC comparison, the indirect PKPD structure with E_{max} exposure-response relationship was found to be the superior base PD model. In this model, inter-individual variability was incorporated on CL, V_c, V_p, BS, k_{in}, EC_{50} and E_{max}. The covariance between η_{CL} and η_{Vp} was not incorporated due to model instability. Residual unexplained variability (RUV) in PK and PD models were described by combined and proportional error model, respectively.

2.4.4.2 Final Models

The final simultaneous PK and PD models are presented in Table 2-4 (b). In the AIC comparison, an indirect PKPD structure with E_{max} exposure-response relationship was found to be the superior model. For convenience, the model with indirect PKPD structure with E_{max} exposure-response relationship in the simultaneous approach is called the final simultaneous model throughout this chapter. The parameter estimates of the final simultaneous model and the bootstrap results are presented in the Table 2-5. In the final simultaneous PK model, creatinine clearance (CrCL) and sex were found to be significant covariates for CL and V_p, respectively. The typical value of CL, V_c, Q and V_p were found to be 26.4 L/hr, 15.0 L, 49.5 L/hr and 55.4 L for a male with a CrCL of 90 ml/min, respectively. These population PK parameter estimates are consistent with previous report (McNeal JJ et al., 1981; van Hecken AM et al., 1982). The estimate of elimination half-lives for ranitidine in the distribution and elimination phases was 7.3 minutes and 2.5 hours, respectively. The typical value of k_{in}, baseline gastric pH, EC_{50}

and E_{max} were found to be 2.58 ng/ml/hr, 2.02, 91.1 ng/ml and 3.48, respectively. The maximum gastric pH change after ranitidine was administered was 3.48 and 91.1 ng/ml of ranitidine plasmatic concentration was needed to achieve the half of maximum ranitidine effect. The inter-individual variability was found to be 24.2 %, 83.1 %, 19.5 %, 45.7 %, 64.0 %, 164 % and 29.4 % for CL, V_c, V_p, BS, k_{in} EC_{50} and E_{max}, respectively. The goodness of fit plots for the final simultaneous PK model are presented in Figure 2-7. The observed data seem to be well predicted by the model and residual plots do not show any specific pattern.

2.4.4.3 Model Evaluation

The predictive check plots of the final simultaneous pharmacokinetic model are depicted in Figure 2-8. The predictive check plots show that the model had adequately described the overall trend and variability in the observed data. No systemic deviation was observed between the observed and simulated data. The quantified visual predictive check (QVPC) plot of final simultaneous pharmacodynamic model is depicted in Figure 2-9. Similar to the result with the sequential approach, the model could not be readily evaluated from 1 to 8 hours after starting the infusion because the percentage of the unavailable PD observations was more than 10 % (Xu SX et al., 2011). In the bootstrap analysis (Table 2-5), 166 runs in total of 200 bootstraps were minimized successfully. The median of bootstrap parameter estimates was similar to the final model estimates based on the original dataset. Most of the parameter estimates based on final simultaneous model had relative standard error (RSE) less than 50% with two exceptions:

η_{Vc} and η_{Vp}. The RSE of η_{Vc} and η_{Vp} were greater than 50 % and consequently their asymptotic confidence intervals included zero. Overall the bootstrap confidence intervals for the rest of the parameters are similar to the asymptotic confidence intervals based on final model estimates.

2.4.5 Comparison of the Final Sequential Model with the Final Simultaneous Model

Most relative standard errors (RSE%) of the population estimates were larger with the simultaneous approach compared to the sequential approach. That is, the population parameters were estimated more precisely in the sequential approach. Population PK parameter estimates were similar in the two approaches. However, the population PD parameter estimates in the sequential approach were more physiologically reasonable than those in the simultaneous approach.

2.5 Discussion

The data in this analysis derived from two clinical trials which were previously conducted. These studies included repeated measures of both plasma concentrations of ranitidine as well as multiple gastric acid measurements. In this analysis, the pharmacokinetics and pharmacodynamics of ranitidine were evaluated with pharmacometric modeling after administration of ranitidine infusion with or without priming bolus dose in critically ill patients and healthy volunteers. There were two

PKPD modeling approaches (sequential and simultaneous approaches), two PKPD connecting structures (direct and indirect response models) and two exposure-response relationships (linear and E_{max} models) that were evaluated. Consequently, the total number of tested models in this analysis was eight.

Plasma concentrations of ranitidine were well described by a 2-compartment model with first-order elimination. The schemes of final PK model were identical in both the sequential and simultaneous approaches except that the final sequential PK model incorporated the covariance between η_{CL} and η_{Vp}. The covariance was not incorporated in the simultaneous approach because the search of the objective function value did not converge to the global minimum when the covariance was included in the model. We identified creatinine clearance (CrCL) and sex as important clinical covariates impacting ranitidine clearance and the peripheral volume of distribution, respectively, in both the sequential and simultaneous approaches. Ranitidine clearance was predicted to decrease in half when CrCL decreased from normal renal function (90 ml/min) to severe renal impairment (30 ml/min). Female subjects were predicted to have 70 % of the peripheral volume of distribution compared to males according to the final PK model. These covariate effects are consistent with previous reports (McFadyen ML et al., 1983; Garg DC et al., 1986; Pérez FJ et al., 2003) and the results may be used to help guide clinicians and inform better dosing decisions for ranitidine in critically ill patient.

In PD modeling, the interest is the relationship between the exposure to the drug and the pharmacological effect. The direct relationship of drug concentration and its

pharmacological effect is identified when the effect is observed shortly after the beginning of drug administration (Crommelin DJ et al., 2007). If the hysteresis pattern is observed in the effect versus plasma concentration plot, a link model can be characterized which assumes the effect compartment (Sheiner LB et al., 1979; Colburn WA, 1981). Hysteresis plots were not relevant to the current data due to the PK sampling schedule. In most subjects, all PK samples were taken while infusion was proceeding so that the plasma concentrations were theoretically increasing to reach steady state. The first sampling occurred 1 hour post-dose in 76 % of patients which makes it difficult to discern hysteresis pattern if the response occurs relatively quickly in response to drug. Many drug effects can be described as an indirect response model, especially when the mechanism of action of a drug is receptor-mediated. In the indirect exposure-response relationship, there is an accumulation of the drug response following the drug administration which is controlled by the production or dissipation of the endogenous factors (Dayneka NL et al., 1993). The indirect model was more appropriate than the direct model to ranitidine based on its mechanism of action: the pharmacological effect of ranitidine is mediated by the histamine 2 receptor. Despite the known mechanism, the direct model was also tested. It was found that the indirect response relationship was more appropriate given the current data than the direct model in terms of AIC.

The simplest exposure-response relationship is the linear model which assumes that effects are proportional to the concentrations of drug at the active site. The advantage of this model is that it is easy to estimate parameters using linear regression. However, this

model cannot be used to predict effects for concentrations out of the range which were used to estimate the parameters (Meibohm B et al., 1997). The E_{max} model is derived from mechanistic considerations on the interaction of the drug with its receptor (Ariëns EJ et al., 1964) and was more appropriate to the current dataset. The advantage of the E_{max} model is that it can predict a maximum effect. However, it requires nonlinear regression to estimate the parameters. In this analysis, the use of NONMEM satisfied the modeling requirements.

The indirect PKPD connecting structure with an E_{max} exposure-response relationship was the best model of all combinations in the sequential as well as the simultaneous approach in terms of AIC. Although the indirect response model is widely applicable to distinguish the pharmacodynamic response of many drugs, there are some practical limitations in their use (Garg V et al., 2007). It is necessary to understand the pathophysiology of the disease to develop the proper model. The indirect response model can function well when the response reflects the change of the inhibiting or the stimulating factor immediately. In addition, indirect response models require differential equations and numerical integration algorithms to describe the nonlinear drug effect. Although this does take more time to implement and can be numerically instable, NONMEM is a suitable program to deal with the differential equations. Indeed, the indirect exposure-response relationship was successfully implemented in the current analysis.

It was reported that the simultaneous PKPD analysis gave slightly more precise parameter estimates than the sequential PKPD analysis if models were specified correctly (Zhang et al., 2003a). When PK parameters are correlated with PD parameters, the simultaneous approach takes into account the uncertainty of PK data properly by allowing PD responses to adjust the PK fit. Considering the statistical theory, the simultaneous approach is better than the sequential approach because the empirical Bayes estimates of PK parameters are not free from error as they are treated in the sequential approach (Zhang et al., 2003a). However, the computational time is shorter when the sequential approach is applied than when the simultaneous approach is used. Additionally, when either of the PK or the PD model is misspecified, the simultaneous analysis may perform poorly; it adjusts the parameter estimates of the correct model to compensate for the fit of the misspecified model (Proost JH et al., 2007). Simulation study reported that the PK parameters with the simultaneous method were poorly estimated when the PD model was misspecified (Zhang L et al., 2003b). A serious imbalance between the number of PK and PD observations can cause problems in the simultaneous approach. When the PK information overwhelms the PD information, the PD fit can possibly be improved at the expense of PK fit (Proost JH et al., 2007). In the current analysis, critically ill patients (n=51) had much more gastric pH data than blood samples (15 versus 4) while healthy volunteers (n=16) had the same number of PK and PD observations. In addition, the precision of the PK measurements is often markedly better than that of the PD measurements. It was true at least in this analysis because the

gastric pH is defined as -log (H^+) so that 1 unit of gastric pH change actually reflects a 10-fold H^+ ion change.

In our experience, it was found that the sequential approach gave more physiologically reasonable population parameter estimates with the current censored PD data and imbalanced PK observations. Most population PK parameters were estimated more accurately in the sequential approach compared to the simultaneous approach. Although the indirect PKPD connecting structure and E_{max} exposure-response relationship was the best in all tested combinations, it was obvious that the current final PD model was not detailed enough to describe the physiologic processes happening after ranitidine bound on the H2 receptor. The drug effect could have been described better through the effect compartment model. However, the sampling schedule of current studies, unfortunately, was not proper to support the effect compartment model.

In the present analysis, visual predictive check (VPC) was not implemented in final PD model in response to the previous research (Karlsson MO et al., 2007; Post TM et al., 2008; Xu SX et al., 2011). When the original data are censored, it is not always feasible to simulate data correctly and the censoring can mislead the results of a simulation. Karlsson MO et al. suggested that simulation-based model evaluation plots (e.g. VPC, numerical predictive check (NPC), and normalized prediction distribution error (NPDE)) were not appropriate to the censored data (Karlsson MO et al., 2007). In addition, a number of factors are involved in determining the magnitude of spread of data around the line of identity in the individual prediction-based diagnostics. These factors include

censoring, model misspecificantion, unexplained residual variability, unexplained parameter variability and dose range (Karlsson MO et al., 2007). Thus, diagnostics with individual predictions are not applicable to the censored data either. The recommendation is to simulate data properly from the final model and create the reference plot. However, when the responsible factor is unknown, it is not possible to develop additional models for censoring. Consequently, it is not feasible to simulate correctly. A quantified visual predictive check (QVPC) plot displays the available data around the simulated median while including the percentage of the censored data at each time point (Post TM et al., 2008). In QVPC, more unavailable data means less data exist for interpreting the model performance. There are literatures that investigate the impact of data below the limit of quantification on PK parameter estimates (Duval V et al., 2002; Byon W et al., 2008; Xu SX et al., 2011). About 5 to 10% of censored data are regarded as acceptable in a pharmacokinetic model. These guidelines suggested that the simulation-based model evaluation is not appropriate over the time frame of 1-8 hours (Figure 2-6 and Figure 2-9).

In summary, this analysis considered sequential and simultaneous approaches for multiple response models with direct or indirect PKPD connecting structure. The PKPD relationship of ranitidine was reliably described with the use of an indirect response model. Two different (E_{max} and linear) models were tested for the exposure-response relationship and the E_{max} model was superior. The final PK models of sequential and simultaneous approaches were almost identical and their estimated parameters were

similar in the present analysis. For the PD response, an indirect E_{max} model with sequential approach provided more reasonable population parameters for the data.

Table 2-1 Patients' demographics

	Median (range)
Total number of patients	67
No. of patients admitted into an intensive care unit	51
No. of healthy volunteers	16
No. of patients having plasma concentration (PK) data	67
No. of patients having gastric pH (PD) data	59
No. of patients administered ranitidine infusion	40
No. of patients administered ranitidine infusion and bolus	39
No. of patients administered placebo	6
Type of surgical operation (n = 51)[1]	
Coronary artery bypass	31
Aortic valve replacement	10
Femoral bypass	4
Repair of aortic aneurysm	4
Others[2]	9
Male/Female	47/20
Age (years)	57 (20-76)
Weight (kg)	77.2 (37.7-173.9)
Race (Caucasian/non-caucasian)	62/5
Creatinine clearance (ml/min)	88.78 (28.65-214.4)

[1]: patients had multiple reasons, [2]: others included total hysterectomy, cancer related surgery etc.

Table 2-2 Scheme of (a) base and (b) final pharmacokinetic and pharmacodynamic models in sequential approach

(a) Base model

	PKPD connecting structure	Exposure-response relationship	Scheme of PK or PD model	AIC
PD model	Direct	Linear	$BS = \theta_{BS} \times \exp(\eta_{BS}), SL = \theta_{SL} \times \exp(\eta_{SL})$	1705.587
		E_{max}	$BS = \theta_{BS}, EC = \theta_{EC}, \times \exp(\eta_{EC}), E_{\max} = \theta_{E_{\max}}$	2062.667
	Indirect	Linear	$k_{in} = \theta_{k_{in}}, BS = \theta_{BS} + \eta_{BS}, SL = \theta_{SL}$	1826.132
		E_{max}	$k_{in} = \theta_{k_{in}}, BS = \theta_{BS} \times \exp(\eta_{BS}),$ $EC = \theta_{EC} \times \exp(\eta_{EC}), E_{\max} = \theta_{E_{\max}} + \eta_{E_{\max}}$	1294.559
PK model	$CL_i(L/hr) = \theta_{CL} \times \exp(\eta_{CL}), V_{Ci}(L) = \theta_{Vc} \times \exp(\eta_{V_C}),$ $Q(L/hr) = \theta_Q, V_{Pi}(L) = \theta_{Vp} \times \exp(\eta_{V_P})$			5437.974*

*: OFV (objective function value)

(b) Final model

	PKPD connecting structure	Exposure-response relationship	Scheme of PK or PD model	AIC
PD model	Direct	Linear	$BS = \theta_{BS} \times \exp(\eta_{BS}), SL = \theta_{SL} \times \exp(\eta_{SL})$	1705.587
		E_{max}	$BS = \theta_{BS} \times \left(\frac{CrCL}{90}\right)^{\theta_{CrCL,BS}} \times (Race)^{\theta_{Race,BS}},$ $EC = \theta_{EC} \times \exp(\eta_{EC}), E_{\max} = \theta_{E_{\max}}$	1906.316
	Indirect	Linear	$k_{in} = \theta_{k_{in}}, BS = \theta_{BS} + \eta_{BS}, SL = \theta_{SL}$	1826.132
		E_{max}	$k_{in} = \theta_{k_{in}}, BS = \theta_{BS} \times \exp(\eta_{BS}),$ $EC = \theta_{EC} \times \exp(\eta_{EC}), E_{\max} = \theta_{E_{\max}} + \eta_{E_{\max}}$	1294.559
PK model	$CL_i(L/hr) = \theta_{CL} \times \left(\frac{CrCL}{90}\right)^{\theta_{CrCL,CL}} \times \exp(\eta_{CL}), V_{Ci}(L) = \theta_{Vc} \times \exp(\eta_{V_C}),$ $Q(L/hr) = \theta_Q, V_{Pi}(L) = \theta_{Vp} \times (Sex)^{\theta_{Sex,Vp}} \times \exp(\eta_{V_P})$			5388.773*

*: OFV (objective function value)

Table 2-3 The population parameter estimates and bootstrap results of the final sequential model

	Final Model Results		Bootstrap Results	
	Typical Value Estimates	RSE (%)[2]	Median Value	95% Prediction Interval
Population PK Parameters				
θ_{CL}, clearance (L/hr)	25.7	3.1	25.9	24.3, 28.0
$\theta_{CrCL,CL}$, exponent accounting for a continuous CrCL effect on CL	0.554	13.3	0.565	0.415, 0.726
$\theta_{SEX,Vp}$, proportional change of V_P for female	0.719	10.8	0.705	0.466, 0.838
V_C, volume of distribution (central, L)	16.6	15.7	16.4	11.0, 22.3
Q, distribution clearance (L/hr)	49.4	3.7	49.3	46.0, 53.2
V_P, volume of distribution (peripheral, L)	59.8	2.8	59.8	48.8, 63.7
Inter-patient variability (IIV)				
IIV for CL, %CV	22.8	21.9	22.6	17.1, 27.7
Covariance for CL and V_P	86.5	30.3	84.9	68.8, 101.2
IIV for V_C, %CV	87.2	37.1	83.5	47.8, 118.0
IIV V_P, %CV	14.4	47.7	14.3	7.5, 33.8
Residual unexplained variability				
Proportional (%CV)	13.19	14.5	13.1	11.1, 14.9
Additional (SD)	3.592	28.7	3.509	2.427, 4.594
Population PD Parameters				
k_{in} (ng/ml/hr)	1.15	16.7	1.21	0.54, 1.67
BS, baseline gastric pH	2.13	7.7	2.10	1.80, 2.45
EC_{50}, concentration of plasma ranitidine when the effect is half of its maximum (ng/ml)	44.6	9.6	58.2	13.4, 159.0
E_{max}, maximal possible gastric pH change	7.67	6.7	7.67	5.90, 23.3
Inter-patient variability (IIV)				
IIV for BS, %CV	52.4	23.1	51.7	40.6, 66.6
IIV for EC_{50}, %CV	137.5	22.1	126.3	71.2, 217.8
IIV E_{max}, SD	3.435	28.5	3.185	1.543, 14.48
Residual unexplained variability				
Proportional (%CV)	33.76	16.6	33.6	26.8, 38.9

RSE: relative standard error, CV: coefficient of variation, the ratio of the standard deviation to the mean

Table 2-4 Scheme of (a) base and (b) final pharmacokinetic and pharmacodynamic models in simultaneous approach

(a) Base model

PKPD connecting structure	Exposure-response relationship	Scheme of PK and PD model	AIC
Direct	Linear	$CL_i(L/hr) = \theta_{CL} \times \exp(\eta_{CL}),\ V_{Ci}(L) = \theta_{Vc} \times \exp(\eta_{V_C}),$ $Q(L/hr) = \theta_Q,\ V_{Pi}(L) = \theta_{Vp} \times \exp(\eta_{V_P}),$ $BS = \theta_{BS} \times \exp(\eta_{BS}), SL = \theta_{SL} + \eta_{SL}$	7630.666
	E_{max}	$CL_i(L/hr) = \theta_{CL} \times \exp(\eta_{CL}),\ V_{Ci}(L) = \theta_{Vc} \times \exp(\eta_{V_C}),$ $Q(L/hr) = \theta_Q,\ V_{Pi}(L) = \theta_{Vp} \times \exp(\eta_{V_P})$ $BS = \theta_{BS} \times \exp(\eta_{BS}),\ EC_{50} = \theta_{EC} \times \exp(\eta_{EC}),$ $E_{\max} = \theta_{E_{\max}} + \eta_{E_{\max}}$	7483.391
Indirect	Linear	$CL_i(L/hr) = \theta_{CL} \times \exp(\eta_{CL}),\ V_{Ci}(L) = \theta_{Vc} \times \exp(\eta_{V_C}),$ $Q(L/hr) = \theta_Q,\ V_{Pi}(L) = \theta_{Vp} \times \exp(\eta_{V_P})$ $k_{in} = \theta_{k_{in}} \times \exp(\eta_{k_{in}}),$ $BS = \theta_{BS} \times \exp(\eta_{BS}), SL = \theta_{SL} \times \exp(\eta_{SL})$	7434.858
	E_{max}	$CL_i(L/hr) = \theta_{CL} \times \exp(\eta_{CL}),\ V_{Ci}(L) = \theta_{Vc} \times \exp(\eta_{V_C}),$ $Q(L/hr) = \theta_Q,\ V_{Pi}(L) = \theta_{Vp} \times \exp(\eta_{V_P}),$ $k_{in} = \theta_{k_{in}} \times \exp(\eta_{k_{in}}), BS = \theta_{BS} \times \exp(\eta_{BS}),$ $EC_{50} = \theta_{EC} \times \exp(\eta_{EC}), E_{\max} = \theta_{E_{\max}} \times \exp(\eta_{E_{\max}})$	7092.783

(b) Final model

PKPD connecting structure	Exposure-response relationship	Scheme of PK and PD model	AIC
Direct	Linear	$CL_i(L/hr) = \theta_{CL} \times \left(\frac{CrCL}{90}\right)^{\theta_{CrCL,CL}} \times \exp(\eta_{CL}),$ $V_{Ci}(L) = \theta_{Vc} \times \left(\frac{AGE}{57}\right)^{\theta_{Age,Vc}} \times \exp(\eta_{V_C}),$ $Q(L/hr) = \theta_Q \times \left(\frac{CrCL}{90}\right)^{\theta_{CrCL,Q}},\ V_{Pi}(L) = \theta_{Vp} \times \exp(\eta_{V_P})$ $BS = \theta_{BS} \times \left(\frac{Age}{57}\right)^{\theta_{Age,BS}} \times \exp(\eta_{BS}),\ SL = \theta_{SL} \times \left(\frac{Age}{57}\right)^{\theta_{Age,SL}} + \eta_{SL}$	7533.840
	E_{max}	$CL_i(L/hr) = \theta_{CL} \times \left(\frac{CrCL}{90}\right)^{\theta_{CrCL,CL}} \times \exp(\eta_{CL}),$ $V_{Ci}(L) = \theta_{Vc} \times \left(\frac{Age}{57}\right)^{\theta_{Age,Vc}} \times \exp(\eta_{V_C}),$ $Q(L/hr) = \theta_Q \times \left(\frac{CrCL}{90}\right)^{\theta_{CrCL,Q}}, V_{Pi}(L) = \theta_{Vp} \times \exp(\eta_{V_P}),$ $k_{in} = \theta_{k_{in}}, BS = \theta_{BS} \times \exp(\eta_{BS}),$ $EC_{50} = \theta_{EC} \times \exp(\eta_{EC}),\ E_{max} = \theta_{E_{max}} + \eta_{E_{max}}$	7418.725
Indirect	Linear	$CL_i(L/hr) = \theta_{CL} \times \left(\frac{CrCL}{90}\right)^{\theta_{CrCL,CL}} \times \exp(\eta_{CL}),$ $V_{Ci}(L) = \theta_{Vc} \times \exp(\eta_{V_C}),\ Q(L/hr) = \theta_Q,$ $V_{Pi}(L) = \theta_{Vp} \times (Sex)^{\theta_{Sex,Vp}} \times \exp(\eta_{V_P})$ $k_{in} = \theta_{k_{in}} \times \exp(\eta_{k_{in}}),\ BS = \theta_{BS} \times \exp(\eta_{BS}),$ $SL = \theta_{SL} \times \exp(\eta_{SL})$	7388.132
	E_{max}	$CL_i(L/hr) = \theta_{CL} \times \left(\frac{CrCL}{90}\right)^{\theta_{CrCL,CL}} \times \exp(\eta_{CL}),$ $V_{Ci}(L) = \theta_{Vc} \times \exp(\eta_{V_C}), Q(L/hr) = \theta_Q,$ $V_{Pi}(L) = \theta_{Vp} \times (Sex)^{\theta_{Sex,Vp}} \times \exp(\eta_{V_P})$ $k_{in} = \theta_{k_{in}} \times \exp(\eta_{k_{in}}), BS = \theta_{BS} \times \exp(\eta_{BS}),$ $EC_{50} = \theta_{EC} \times \exp(\eta_{EC}),\ E_{max} = \theta_{E_{max}} \times \exp(\eta_{E_{max}})$	7043.105

Table 2-5 The population parameter estimates of the final simultaneous model and bootstrap results

	Final Model Results		Bootstrap Results	
	Typical Value Estimates[1]	RSE (%)[2]	Median Value	95% Prediction Interval
Population Pharmacokinetic Parameters				
θ_{CL}, clearance (L/hr)	26.4	3.9	26.5	24.6, 28.4
$\theta_{CrCL,CL}$, exponent accounting for a continuous CrCL effect on CL	0.586	12.1	0.592	0.458, 0.750
$\theta_{SEX,Vp}$, proportional change of V_P for female	0.709	5.0	0.691	0.478, 0.881
V_C, volume of distribution (central, L)	15.0	10.9	15.3	11.4, 21.6
Q, distribution clearance (L/hr)	49.5	3.5	49.7	46.7, 52.5
V_P, volume of distribution (peripheral, L)	55.4	6.6	55.8	48.7, 60.6
Inter-patient variability (IIV)				
IIV for CL, %CV	24.2	22.9	24.1	18.2, 28.5
IIV for V_C, %CV	83.1	83.1	80.2	47.9, 110.1
IIV for V_P, %CV	19.5	88.7	16.8	6.1, 44.3
Residual unexplained variability				
Proportional , %CV	12.9	15.9	12.9	10.9, 14.4
Additional, SD	3.808	26.6	3.779	2.816, 5.034
Population Pharmacodynamics Parameters				
k_{in} (ng/ml/hr)	2.58	14.0	2.59	1.92, 3.49
BS, baseline gastric pH	2.02	8.1	2.00	1.72, 2.35
EC_{50}, concentration of plasma ranitidine when the effect is half of its maximum (ng/ml)	91.1	48.1	91.6	40.9, 238.8
E_{max}, maximal possible gastric pH change	3.48	12.7	3.53	2.88, 5.03
Inter-patient variability (IIV)				
IIV for BS, %CV	45.7	26.8	44.9	30.4, 57.4
IIV for k_{in}, %CV	64.0	48.1	61.5	32.8, 102.1
IIV for EC_{50}, %CV	164	40.1	155.6	74.0, 226.3
IIV for E_{max}, %CV	29.4	46.0	27.5	11.7, 39.6
Residual unexplained variability				
Proportional , %CV	34.8	16.0	34.7	28.7, 39.7

RSE: relative standard error, CV: coefficient of variation, the ratio of the standard deviation to the mean

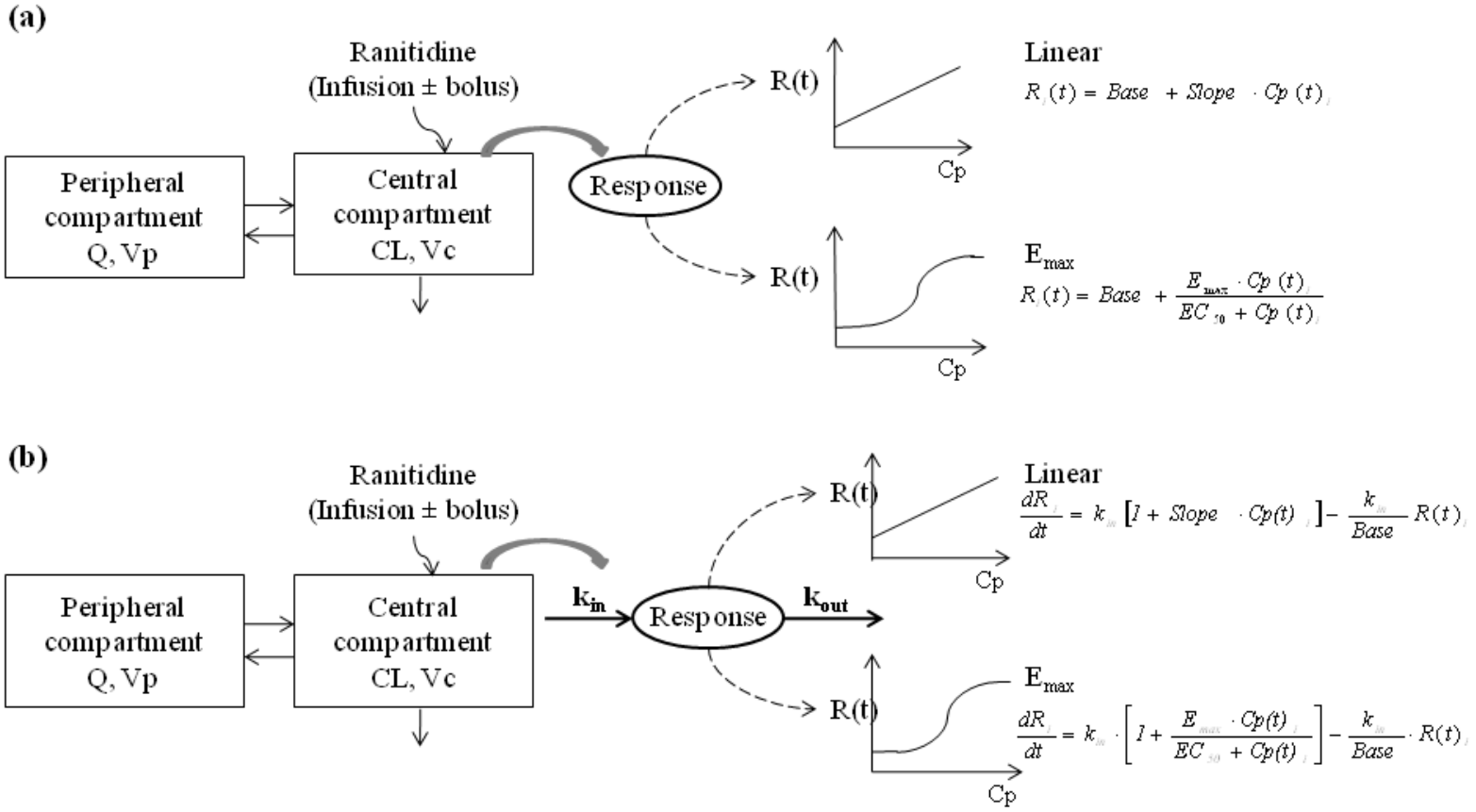

Figure 2-1 Scheme of pharmacokinetic and pharmacodynamic models for (a) direct response model and (b) indirect response model. CL, Q, V_C and V_P are ranitidine clearance, inter-compartmental clearance, the volume of distribution of ranitidine for central and peripheral compartment. k_{in} and k_{out} are the production and elimination rate of response. R(t) and Cp(t) are the response and plasma concentration at time t, respectively.

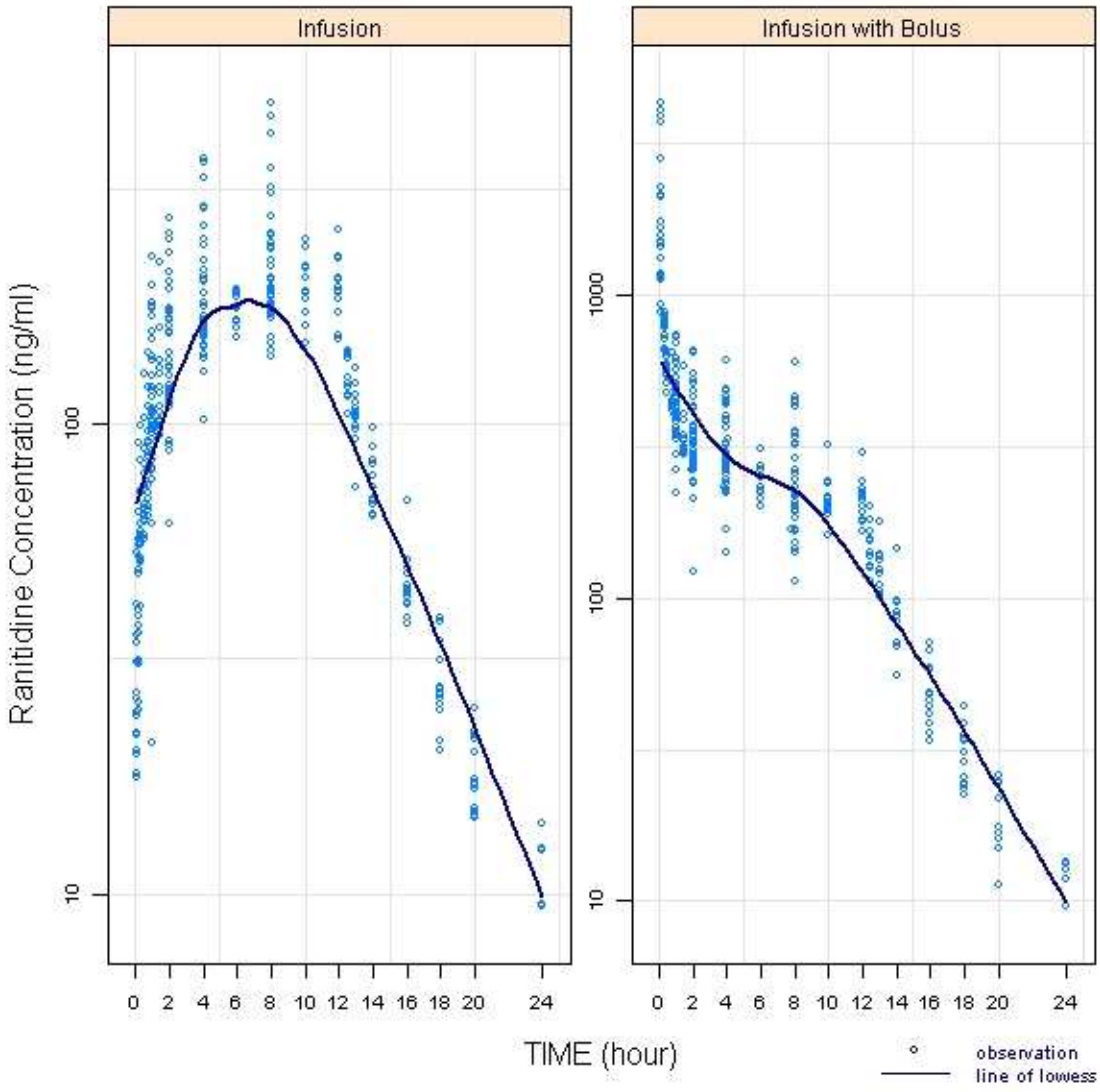

Figure 2-2 Time course of ranitidine plasma concentrations. The number of subjects in the infusion and infusion with bolus group was thirty-nine and forty, respectively.

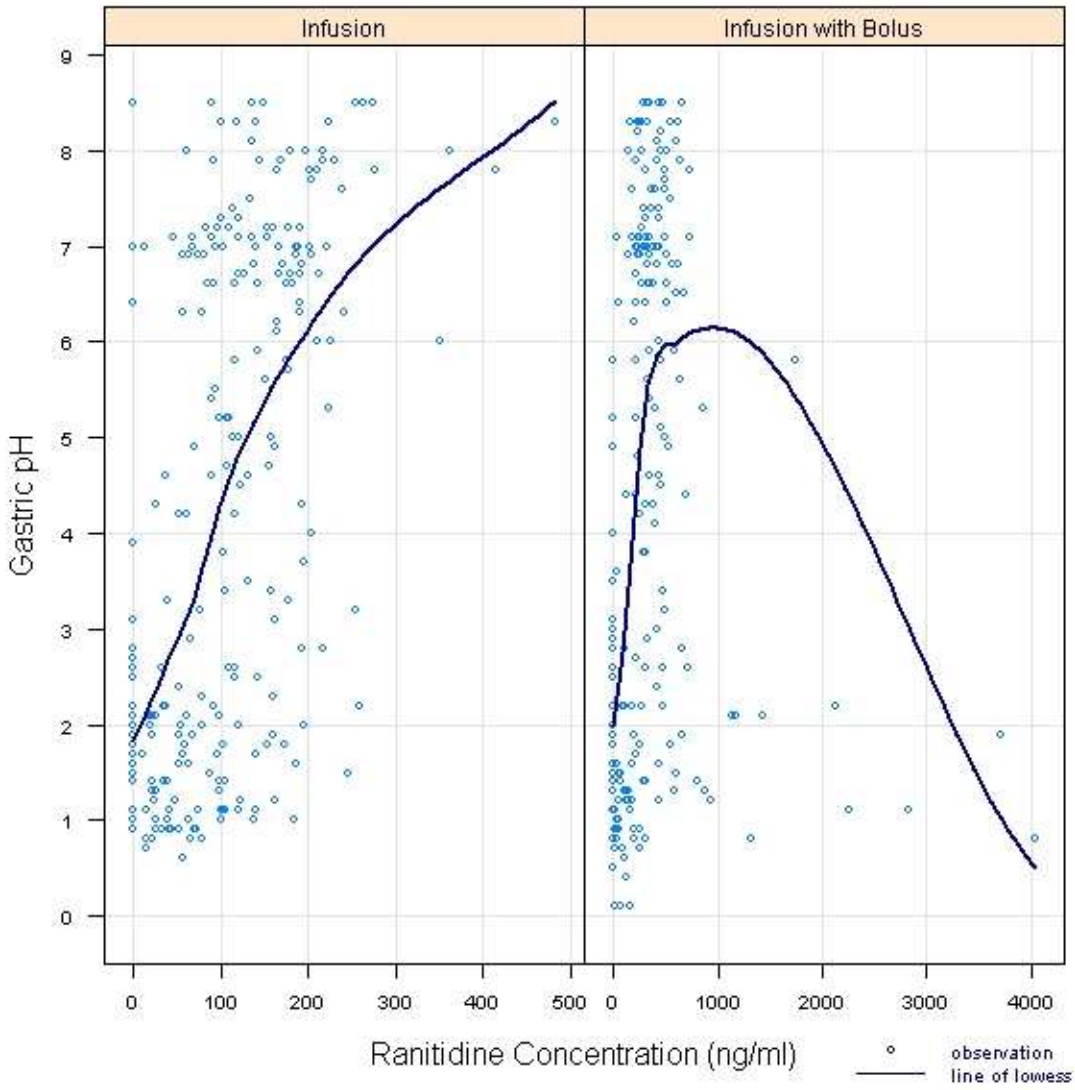

Figure 2-3 Gastric pH versus ranitidine plasma concentration plot. The number of subjects in each group was thirty-two.

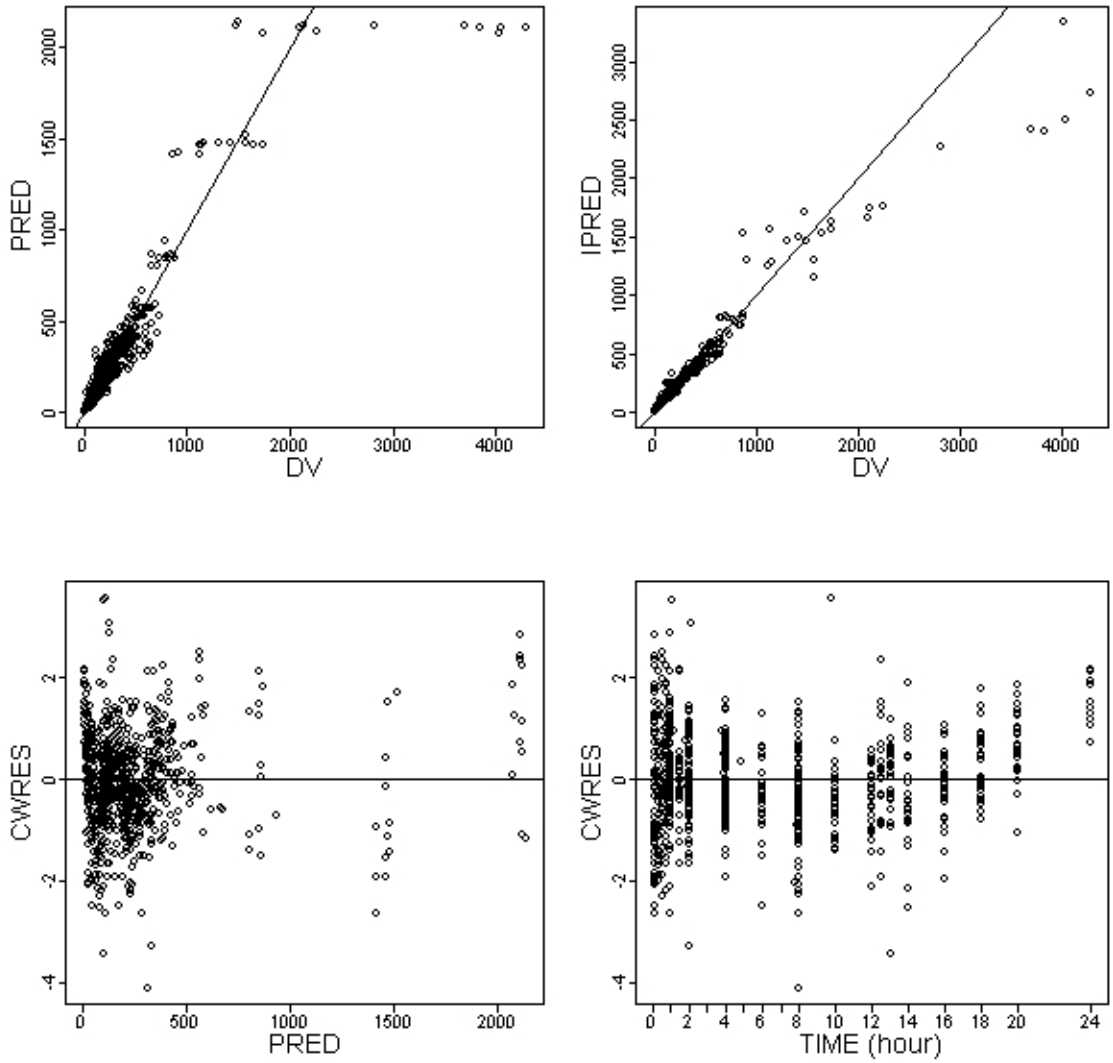

Figure 2-4 Goodness-of-fit plot of final sequential pharmacokinetic model. DV represents observed concentrations, PRED population predicted concentrations and IPRED individual predicted concentrations of ranitidine. CWRES are the conditional weighted residuals under the final seuniquential pharmacokinetic model.

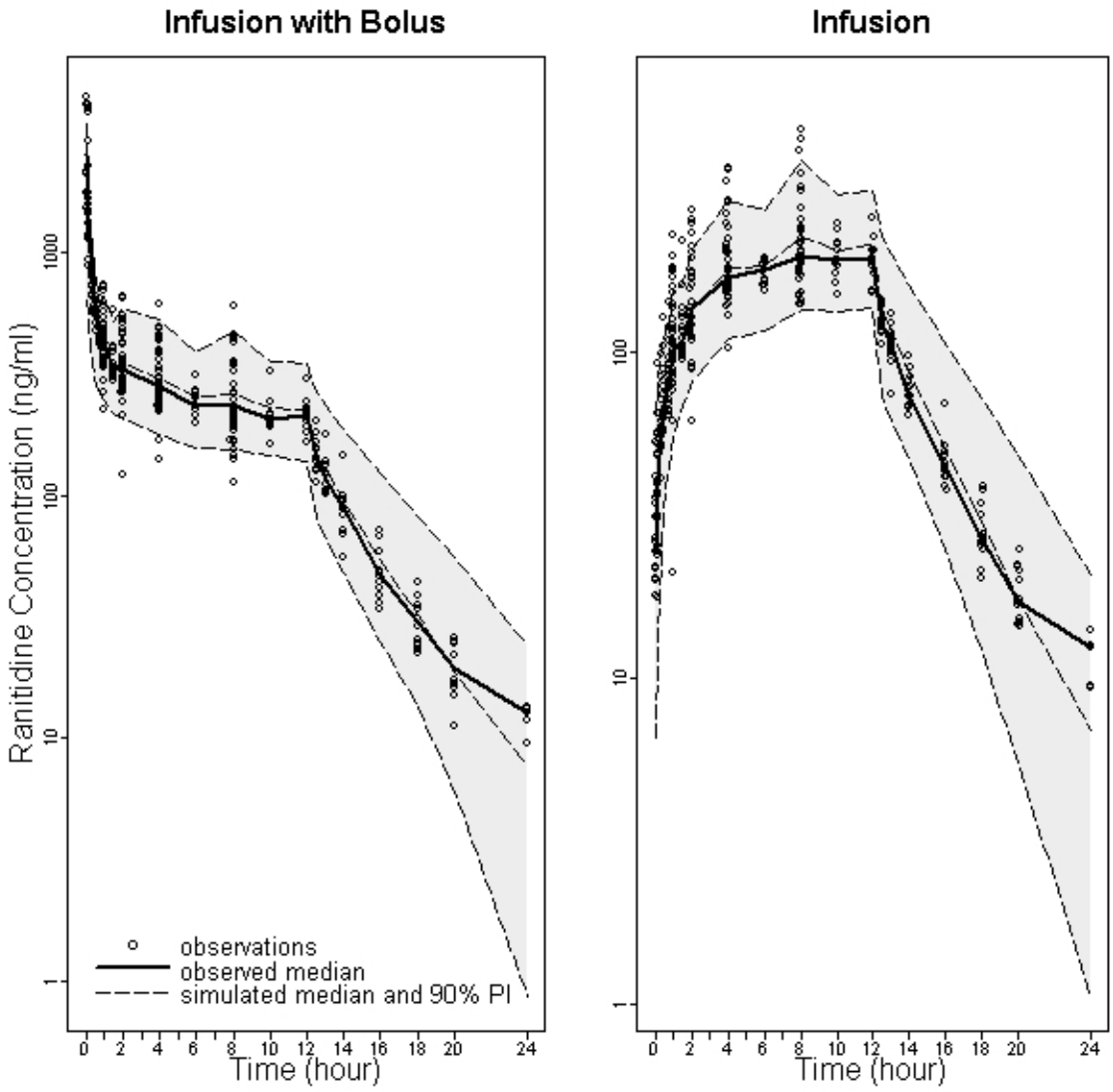

Figure 2-5 Visual predictive check plots of final sequential pharmacokinetic model. PI is the prediction interval.

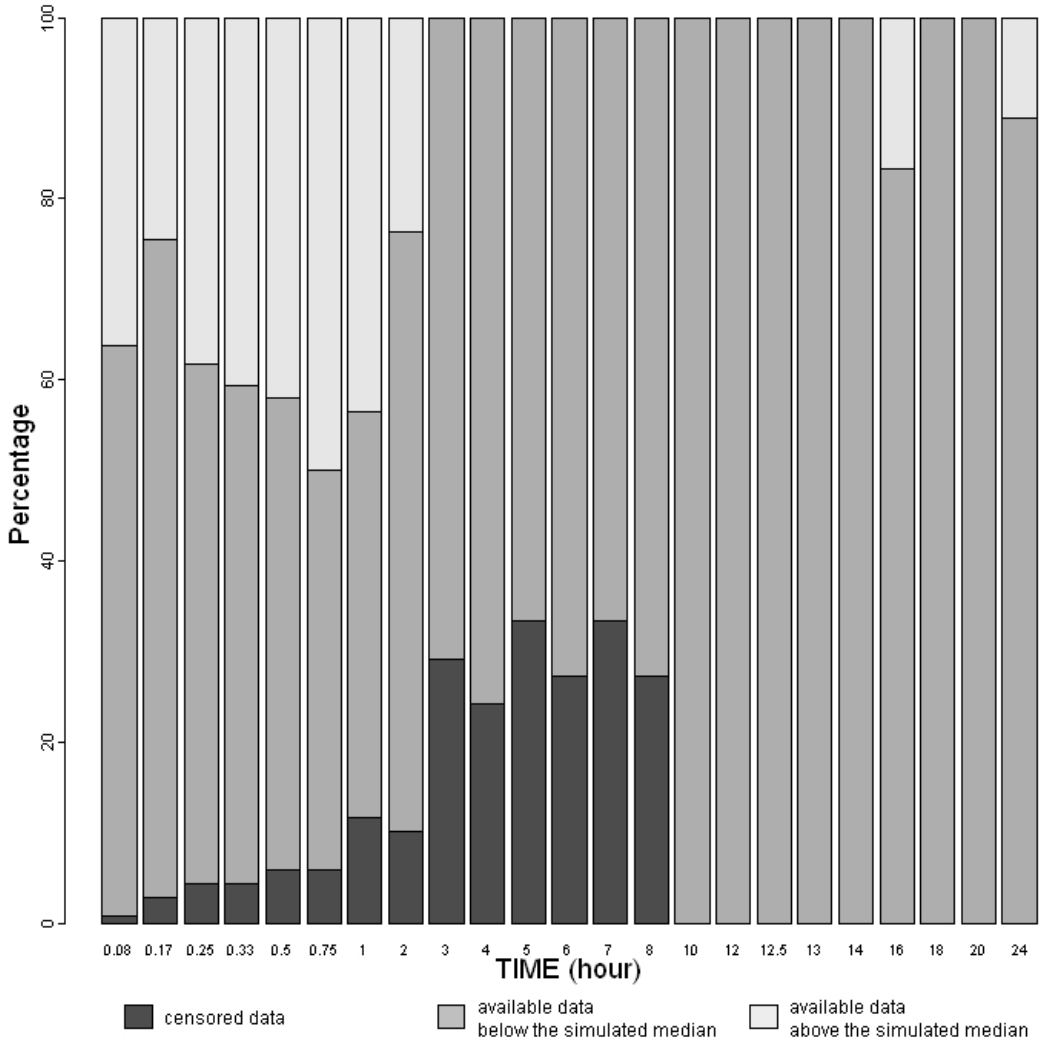

Figure 2-6 Quantified visual predictive check plot of final sequential pharmacodynamic model.

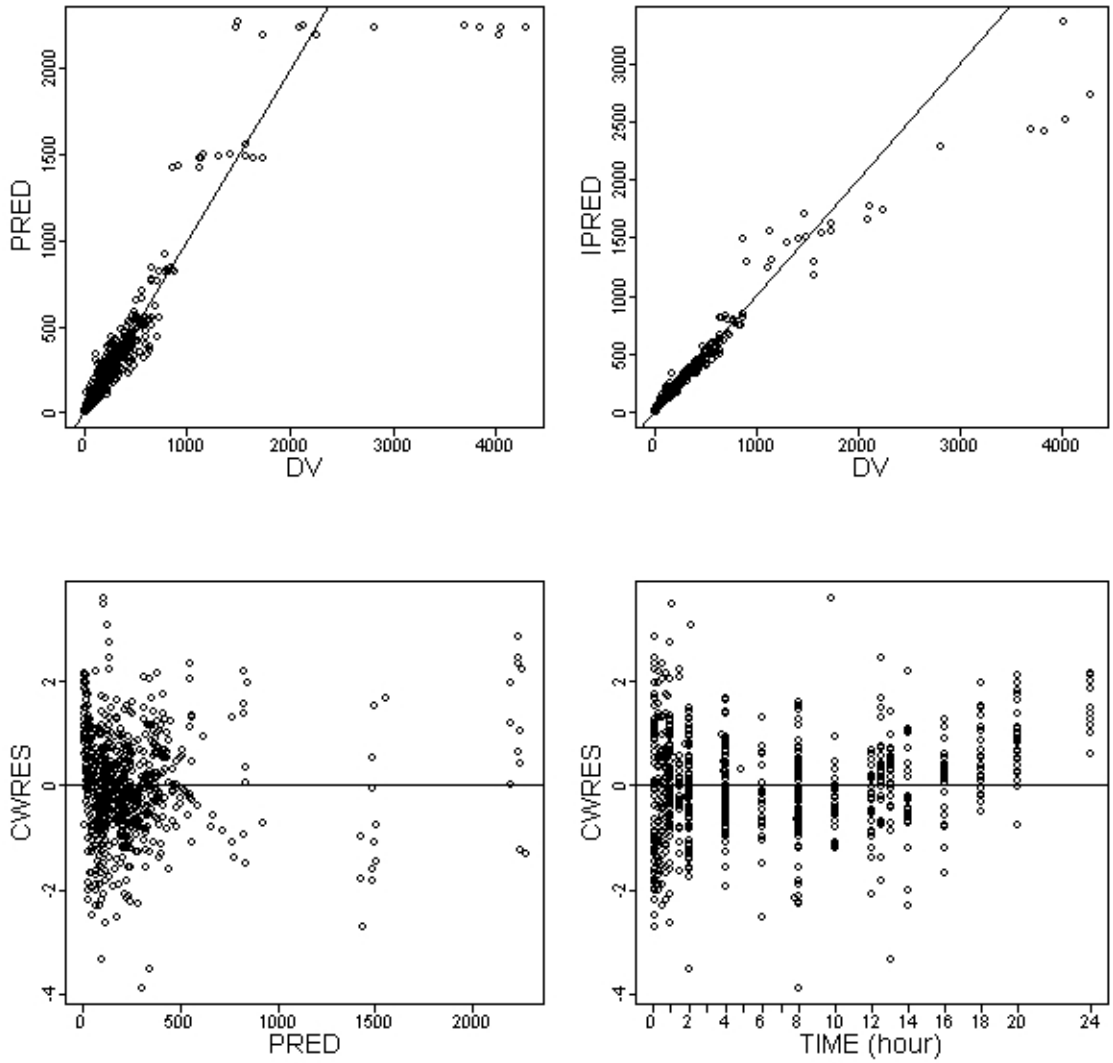

Figure 2-7 Goodness-of-fit plot of final simultaneous pharmacokinetic model. DV represents observed concentrations, PRED population predicted concentrations and IPRED individual predicted concentrations of ranitidine. CWRES are the conditional weighted residuals under the final simultaneous model.

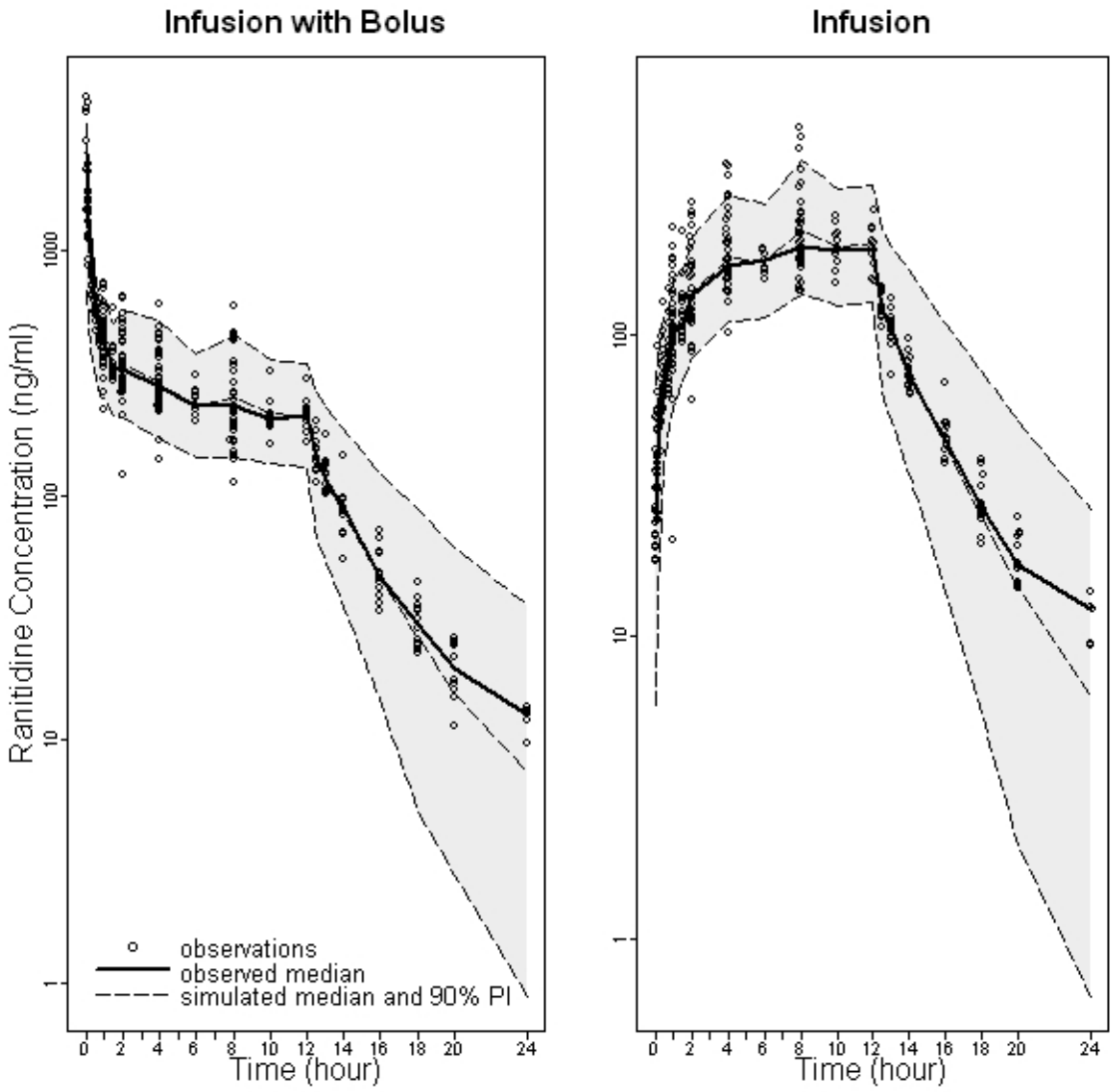

Figure 2-8 Visual predictive check plots of final simultaneous pharmacokinetic model. PI is the prediction interval.

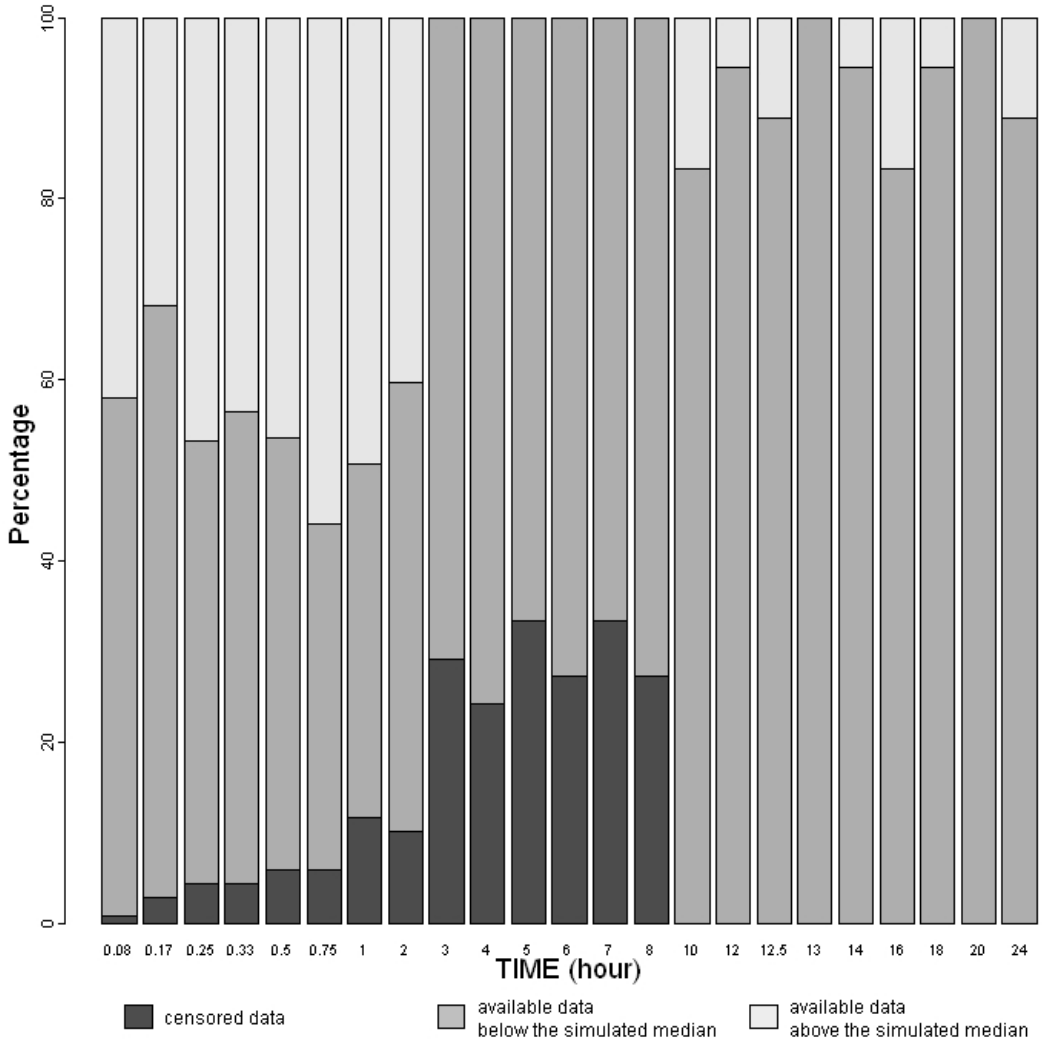

Figure 2-9 Quantified visual predictive check plot of final simultaneous pharmacodynamic model.

Chapter 3

Population Exposure-Response Analysis Using Time-to-Event Data of the Ranitidine Pharmacodynamic Effect on Gastric Acid Secretion

3.1 Introduction

In many clinical trials, researchers are interested in the time to a pre-specified event. The time to the occurrence of an event is called survival time and survival analysis deals with this time. Examples of such survival time include the time to patient's death, the time to respond to a therapy (Cox EH et al., 1999), the time to rescue therapy after having responded to a therapy (Sheiner LB, 1994; Trocóniz IF et al., 2006), or the time to tumor progression (Gieschke R et al., 2003). The analysis of time-to-event data is complicated due to the differential follow up and censoring issue. Each individual may have different follow-up time even when they are from one trial. The other issue, censoring, happens when an individual's survival time is only known to occur within a certain period of time (Klein JP et al., 1997; Ette EI et al., 2007). That is, the exact time of event is unknown. The survival time is said to be right censored when the subject has not experienced the event by the end of the observation period. Right censoring may occur when the event does not occur by the end of the study, the subject experiences the event of interest from a reason other than intervention, the subject drops out at one's will, or the subject is lost

to follow-up during the study period. Unlike right censoring, left censoring happens when the event of interest has already occurred before the subject is enrolled in a study. Interval censoring occurs when the event of interest happens within an interval of time. Censoring and variable follow-up causes unique difficulties in the analysis of time-to-event data that cannot be handled properly by standard statistical methods. When survival data is analyzed in traditional methods, summary statistics may not reflect the true characteristics of the data due to the censoring (Klein JP et al., 1997; Ette EI et al., 2007). For example, the sample mean is no longer an unbiased estimator of the population mean. Thus, alternative methods are needed for analyzing the data such as characterizing the underlying true distribution of time to an event so that summary survival statistics from the estimated distribution have the desired properties of time-to-event data.

Time-to-event data can be analyzed in different approaches: nonparameteric, semiparameteric and parametric approaches. The Kaplan-Meier (KM) estimator is an intuitive and simple descriptor presenting the properties of survival data in a nonparametric approach. However, the usefulness of the KM estimator is limited to describing the observations. It is not plausible to infer the response outside of the range of predictors or to simulate data for evaluating the KM estimator. Proportional hazard analysis, the semi-parametric approach of survival analysis, assumes a baseline hazard and covariate effects. It is exceptionally useful when one is interested in comparing two or more groups. A baseline hazard model determines the risk when all covariates are set

to the reference levels while the covariate effect model assesses the effect of each covariate of interest on the event risk. Therefore, the covariate effect is always expressed in the form of comparison to the reference level. For instance, the female gender effect on an event risk is represented as the proportional change compared to the reference gender, in this example, male. Lastly, parametric survival analysis assumes that the event times follow a specific distribution and aims to estimate the necessary parameters to describe the underlying distribution. When the parametric model fits the data well, it is possible to estimate characteristics of interest more precisely with fewer parameters. There are several distributions that are commonly used in the parametric analysis including exponential, Weibull, gamma, log normal, normal and Gomperz distributions. Although each distribution has its strength, exponential and Weibull distribution are more widely used than the others. An exponential distribution is useful for its simplicity and a Weibull distribution is commonly adopted because it can describe different shapes of distributions.

Let T be the time from start of drug administration until a subject has an event. Three functions characterize the distribution of T: the survival function, the hazard function and the probability density function (Klein JP et al., 1997). There is a one-to-one relationship among these three functions. Thus, if one knows any of three functions, the other two will be determined uniquely. The survival function, the probability of an individual surviving beyond time t, is defined as

$$S(t) = Pr[T > t] = \int_{t}^{\infty} f(t)dt \tag{3.1}$$

where, T is a survival time and $f(t)$ is the probability density function. The survival function is a nonincreasing function which is equal to 1 at time zero and 0 as time approaches infinity.

The hazard function, sometimes called a risk function or hazard risk, is the chance an individual at time *t* experiences the event in the next instant given that the individual does not have the event until time *t*. The hazard function $h(t)$ is defined as following equation.

$$h(t) = \lim_{\Delta t \to 0} \frac{P[t \le T < (t + \Delta t) \mid T \ge t]}{\Delta t} \tag{3.2}$$

This function is also known as the conditional failure rate. The hazard rate is a probability rate, not a probability so that it is possible for a hazard rate to exceed 1. The only restriction on $h(t)$ is that it is nonnegative, $h(t) \ge 0$.

The probability density function is the unconditional probability of the event at time *t*.

$$f(t) = \lim_{\Delta t \to 0} \frac{P[t \le T < t + \Delta t]}{\Delta t} \tag{3.3}$$

The probability density function $f(t)$ is a nonnegative function with the area under $f(t)$ being equal to one. From the equations above, it can be shown that the relationship between the probability density function and the survival function is given by

$$f(t) = h(t) \cdot S(t) = -\frac{dS(t)}{dt} \tag{3.4}$$

The Weibull model is one of the distributions which are widely used in survival analysis where the survival function is given by

$$S(t) = exp\left(-ln2 \times \left(\frac{t}{\varphi} \right)^{\gamma} \right) \tag{3.5}$$

where *S(t)* is the survival function of the event, φ is the median time-to-event and γ is shape factor.

The hazard function *h(t)*, for the Weibull distribution is given by

$$h(t) = ln2 \times \frac{\gamma}{t} \times \left(\frac{t}{\varphi} \right)^{\gamma} \tag{3.6}$$

The Weibull distribution can describe data with a constant hazard (γ = 1), increasing hazard (γ >1) or decreasing hazard (0 < γ < 1). The probability density function plot of the Weibull distribution with different values of gamma is presented in Figure 3-1.

If the hazard rate is constant $h(t) = \lambda$, for all t $\geq$ 0, then the survival function $S(t) = \exp(-\lambda t)$. This distribution is the exponential distribution with constant hazard λ. The exponential distribution is a special type of Weibull distribution.

Ranitidine is approved by US Food and Drug Administration (FDA) to inhibit gastric acid production and thus prevent stress-related gastric damage. Most stress-related gastric bleedings are observed when the intragastric pH is less than 4. Thus the primary objective of acid suppressive treatment is to prevent stress-related mucosal damage by raising intragastric pH to greater than 4 (Gedeit RG et al., 1993; Netzer P et al., 1999). The pharmacokinetics and pharmacodynamics of ranitidine and their relationship have been investigated extensively in the prevention and treatment of gastric acid over-secretion related disease (McFadyen ML, 1981; McNeil JJ et al., 1981; Mignon M et al., 1982; van Hecken AM et al., 1982). Complex modeling techniques such as time-to-event data analysis have been used with increasing frequency in biomedical analyses, but have not been applied to investigate the exposure-response relationship of ranitidine.

Standard survival analysis can be performed using commercially available software such as R, S-PLUS, SAS, BMDP, STATA, GLIM and SPSS (Lee ET et al., 1997). Although there are facilities in the software for fitting mixed models to data, these tools are not appropriate to the data collected hierarchically. A time-to-event analysis using a nonlinear mixed effect modeling approach such as NONMEM is different from standard survival analysis. NONMEM is commonly used for modeling and simulation in population pharmacokinetic-pharmacodynamic analysis and is considered a very

powerful tool in clinical pharmacology (Ette EI et al., 2007). The non-linear mixed effect modeling approach in NONMEM includes additional random effect terms that are appropriate when data are collected over time on the same individuals. However, to the author's knowledge, there are no publications available using NONMEM in the analysis of time-to-event data of ranitidine. The current analysis aimed to demonstrate the performance of NONMEM in analyzing survival data and address the following questions: (a) Does ranitidine reduce the time it takes for a patient to achieve gastric pH greater than 4? (b) If ranitidine has an acid-reducing effect, how effective is it? (c) Which covariates, if any, are related with parameters describing the baseline time-to-event and the ranitidine efficacy?

3.2 Data and Methods

3.2.1 Data

The data arose from two clinical trials designed to investigate if rapidly achieving therapeutic concentrations with a bolus dose (50 mg) in addition to an infusion (6.25 mg/hr) would produce an increase in gastric pH more quickly than administering the infusion alone. A total of 50 patients were enrolled in this analysis: 41 critically ill patients and 9 healthy volunteers. Concentration-time data and pH data from two previous ranitidine studies were combined and analyzed using a nonlinear mixed-effects survival analysis approach. Details of the two studies are presented detailed in chapter 2.

The primary objective of the treatment was to achieve gastric pH greater than 4. The response considered for the exposure-response relationship modeling was defined as the first time that gastric pH exceeded 4. It was clear from a visual inspection of the data the pH responded fairly rapidly to ranitidine. Hence, a partial area under the time-concentration curve from 0 to 2 hours ($AUC_{0\text{-}2}$) was used as a relevant metric of exposure rather than a more conventional $AUC_{0\text{-}\infty}$. Only the first time to achieve the treatment goal was taken into the analysis. Patients whose gastric pH was greater than 4 at time 0 i.e. at the start of ranitidine infusion were excluded from analysis.

3.2.2 Exposure-Response Relationship

The ranitidine pharmacologic effect of time to achieve gastric pH > 4 was modeled according to the Hill equation. The relationship between the median time to achieve gastric pH 4 and the exposure to ranitidine was described by following equation.

$$\varphi = \textit{Time-to-event}_{NoDrug} \times \left(1 - \frac{AUC_{0\text{-}2}^{\alpha}}{EA_{50}^{\alpha} + AUC_{0\text{-}2}^{\alpha}} \right) \tag{3.7}$$

where φ is the median time-to-event, $\textit{Time-to-event}_{NoDrug}$ is the time to achieve gastric pH > 4 when ranitidine is not given to a patient, $AUC_{0\text{-}2}$ is the area under the time-concentration curve from the beginning of drug administration to 2 hours, EA_{50} is the $AUC_{0\text{-}2}$ when the inhibitory effect of ranitidine is half of its maximum and α is the sigmoidicity coefficient.

The final pharmacokinetic model in the sequential approach developed in chapter 2 was adopted to predict subject specific AUC_{0-2} on the basis of covariates in the original dataset.

3.2.3 Time-to-Event Model Development

A time-to-event analysis was performed by means of nonlinear mixed-effects approach using NONMEM version 7 (ICON Development Solutions, Ellicott City, MD) with the interface Perl-speaks-NONMEM (PsN version 3.2.12, http://psn.sourcegorge.net/) on a personal computer (Intel® CORE vPro processor). Diagnostic graphics and post-processing of NONMEM output and simulations were performed using the statistical software R (version 2.9.1, http://www.r-project.org/). The Laplacian approximation method was used to estimate the time-to-event model parameters. Censoring was taken into account in the likelihood formula.

The baseline hazard ($Time\text{-}to\text{-}event_{NoDrug}$) and the inhibitory E_{max} effect (EA_{50}) of ranitidine were modeled first without any covariate. Once the model provided an adequate description of the data, covariate effect was incorporated in the model. The model development process was guided by the likelihood ratio test, visual inspection of diagnostic plots and the potential biological plausibility of a relationship between covariates and responses. Covariates of interest included weight, age, sex and patient's condition (critically ill versus healthy). The effect of covariate was tested on the time-to-event parameters: $Time\text{-}to\text{-}event_{NoDrug}$ and EA_{50}. Continuous variables were normalized

by the median or a clinically relevant approximation to the median and incorporated into the model. Discrete covariates were modeled as a fractional change to the control group. The final model was built through the process of forward selection and backward elimination with the level of significance set at 0.05 for forward selection and at 0.001 for backward elimination, respectively. The likelihood ratio test was used to assess the statistical significance of all covariates in the final model.

As a model evaluation technique, goodness of fit plots were made comparing model predicted data with observations. A box and whiskers plot of residuals was created in which residuals were defined as the difference between the observation and model prediction. A thousand data sets were simulated based on final parameter estimates and descriptive Kaplan-Meier plot was created with the raw data and superimposed simulated data. A posterior predictive check plot of the number of patients experiencing an event at each time was also created with simulated data. Lastly, a thousand bootstrap runs were performed to assess the precision of the final model parameter estimates. The median, 2.5^{th} and 97.5^{th} percentiles of the parameter estimates were computed form the bootstrap runs with successful minimization and compared to the point estimates and 95% confidence intervals from the original dataset.

The following assumptions were made in the current analysis. First, the censoring of data was non-informative and all censorings were right censored. Second, the time to an event followed the Weibull distribution. Third, the pharmacologic effect of ranitidine followed

inhibitory sigmoid E_{max} model. Fourth, the occurrence of an event is independent of study endpoint.

3.3 Results

A total of sixty two observations from fifty patients were used in this analysis: 41 critically ill patients and 9 healthy volunteers. The majority of study subjects were male (70 %) and critically ill patients (82 %). Patients' demographics are presented in Table 3-1. The median (range) age and weight were 56.5 years old (20-76) and 78.3 kg (37.7-173.9), respectively. Renal function within 24 hours of ranitidine administration was widely variable among subject with a median (range) creatinine clearance of 88.7 ml/min (28.7-214.4). The range of exposure (AUC_{0-2}) was 0.0593-1.8746 mg·hr/L when the drug was given. The plot of AUC_{0-2} versus time to achieve gastric pH > 4 is presented in Figure 3-2.

The inhibitory sigmoid E_{max} model was successfully implemented to explain ranitidine effect on the median time to achieve gastric pH greater than 4. The estimated parameters of the final model with their relative standard errors are presented in Table 3-2. The time to achieve gastric pH > 4 was 19.4 hours when ranitidine was not given to a patient. AUC_{0-2} of 0.000125 mg·hr/L was needed to achieve the half of the maximal inhibitory ranitidine effect on the median time-to-event. The sigmoidicity coefficient 0.423 implied that the inhibitory effect of ranitidine was moderate. The shape factor was 1.41

indicating an increased conditional probability of event risk with time. That was, it was more likely that the gastric pH would eventually increase over 4 given the patient did not have event until time *t*. None of the demographic and clinical characteristics had clinical relevant effect on the time-to-event parameters.

The goodness of fit plots of the final time-to-event model are presented in Figure 3-3. There was one outstanding outlier. The area excluding the outlier was magnified to make the comparison of predicted values to observed ones more clear. The model predictions agreed well with the observed data (Figure 3-3 (a)). Residual plot (Figure 3-3 (b)) clustered around zero with tight interquartile range. No systemic deviation was observed between the predictions and the observations. The visual predictive check plot of final time-to-event model is depicted in Figure 3-4. The simulated data showed a similar pattern with observed data in terms of the Kaplan-Meier plot. However, the final model overestimated the survival probability compared to the observations from 0 to 6 hours post-dose. Figure 3-5 shows the histogram of the number of event at each time point with the vertical bar representing the observed number of event. Because 80 % of events happened within 1 hour of starting the ranitidine infusion, the events after 1 hour were combined. The final model predicted fewer patients having an event than actual data at every time points until 1 hour after starting drug administration. In the bootstrap analysis, 937 runs in 1000 bootstraps minimized successfully. The median of bootstrap parameter estimates was similar to the final model estimates based on the original dataset as presented in Table 3-2. The relative standard error (RSE) of $Time-to-event_{NoDrug}$

and EA_{50} were greater than 50% and consequently their asymptotic confidence intervals included zero. And the bootstrap confidence intervals of $Time-to-event_{NoDrug}$ and EA_{50} were close to the null value, zero (Table 3-2).

3.4 Discussion

Survival analysis deals with the time to the occurrence of an event. One of the special characteristics of time-to-event data is that the exact time to an event is usually not known for the entire study population (Klein JP et al., 1997; Ette EI et al., 2007). In addition, each individual in a trial can have a different follow-up period. Thus, the analysis of survival experiments is complicated by these characteristics and a traditional hypothesis testing approach is not appropriate due to the censoring. On the other hand, a time-to-event analysis method allows the comparison of the entire survival experience despite the different follow-up times for each individual and potential right-sided censoring. Nonlinear mixed effect modeling tool, NONMEM has become an increasingly pharmacokinetic-pharmacodynamic analysis method recently (Ette EI et al., 2007). Thus, a time-to-event data analysis using NONMEM became one of the alternatives of the traditional analysis in estimating parameters, predicting and simulating survival data.

Maintaining gastric pH at 4 or above is important to reduce intragastric mucosal damage and to prevent possible gastric bleeding in critically ill patients (Fennerty MB, 2002).

Ranitidine, one of the histamine 2 receptor antagonists has been reported to be effective in preventing acute gastric bleeding in critically ill patient with high risk of gastric bleeding (Cook DJ et al., 1996). The pharmacokinetics and pharmacodynamics of ranitidine have been studied extensively. However, there are few studies relating the exposure of ranitidine to the time required to achieve effective pH control. The aim of this analysis was to develop an exposure-response model that described the time to achieve gastric pH greater than 4 after administering ranitidine in critically ill patients and healthy volunteers. Concentration-time data and pH data from two previous studies that evaluated whether a bolus plus infusion regimen lead to more rapidly attaining therapeutic ranitidine plasma concentrations than an infusion alone, were used for this study.

Drug exposure was defined as the area under the time-concentration curve of ranitidine from the start of drug administration to 2 hours (AUC_{0-2}). The choice of 2 hours was arbitrary and was chosen because the event happened at an early time point in most subjects. The pharmacokinetic sampling schedules also needed to be considered in defining the exposure. The PK samples were taken before the drug was given and at 1, 2, 4 and 8 hours post-dose in 75% of subjects. AUC_{0-1} and AUC_{0-2} were tested for the measure of exposure. The final parameters of AUC_{0-2} were more reasonable than those of $AUC_{0-1.}$ And AUC_{0-2} was chosen as a measure of the exposure for the analysis.

Survival analysis using NONMEN was successfully implemented to analyze the time-to-event data. The placebo time-to-event of 19.4 hours was reasonable considering some

events were observed at 1 hour when placebos were given while others were censored at 24 hours. An inhibitory sigmoid E_{max} model described well the exposure-response relationship for the ranitidine effect in this analysis. The model predicted a patient needed EA_{50} of 0.000125 mg·hr/L to achieve half of maximal ranitidine effect on increasing gastric pH. That was, 0.00321 mg of ranitidine was needed to produce EA_{50} of 0.000125 mg·hr/L for a subject with clearance of 25.7 L/hr, population estimate of clearance. All subjects received much more amount of ranitidine than the dose needed to achieve EA_{50}. Each individual received 6.25 mg/hr of ranitidine for 8 or 12 hours with or without 50 mg preceding bolus according to the protocol. The estimated individual clearance clustered narrow range, 11.6-50.4 L/hr. Therefore, the estimated AUC_{0-2} banded tightly; 0.0593-1.8746 mg·hr/L. In fact, none of the observed AUC_{0-2} values were less than estimated EA_{50} except when placebo was given. It was necessary to test wide range of exposure to establish relationship of ranitidine exposure and its effect on time-to-event response. It was not feasible to distinguish the thorough exposure-response relationship with the tight range of ranitidine exposure explored in the current studies. Consequently, we found fairly weak exposure-response relationship which is difficult to discern whether it is from true lack of relationship or insufficient range of exposure. The sigmoidicity coefficient of 0.486 indicated that the inhibitory effect of ranitidine on the median time to gastric pH > 4 was more gradual than steep as would be seen with sigmoidicity > 1.0. Considering the mechanism of action of ranitidine, competitive inhibition on receptor binding, this result is plausible.

The somewhat weak relationships between systemic exposure and drug effect was reflected into the high variability of $Time-to-event_{NoDrug}$ and EA_{50}. The variability of estimated EA_{50} was larger than 400 %. It may be due to the fact that AUC_{0-2} of ranitidine in plasma does not necessarily reflect the exposure of gastric tissue where response actually occurs. The ranitidine concentration at the effect site would be a better measure of the exposure but it could not be directly measured. Other measurements of exposure such as ranitidine plasma concentration (C_p) at time of event, AUC_{0-1} or dose were tested but they performed worse than AUC_{0-2} in terms of the plausibility of final parameters, the goodness of fit plots and predictive check plots. Especially C_p at time of event was not reasonable based on the mechanism of action of ranitidine. Dose was not a good measure either because all subjects were received ranitidine in same bolus dose and same infusion rate.

Karlsson KE et al. reported that the bias of a parameter is notably significant when the responses were skewed and Laplacian estimation method was used (Karlsson KE et al., 2011). In this analysis, the response was highly skewed and Laplacian method was used. Seventy-seven percent of responses occurred within one hour of the beginning of drug administration. Jönsson S et al. suggested that the model with biased parameter estimates could not reproduce important features of the original data in the simulations (Jönsson S et al., 2004). A discrepancy was observed in our simulation. Final model overestimated survival probability to the observation as depicted in Figure 3-4. While the proportion of censored patients was higher in the simulation than in observed data, the number of

simulated events was less than the observed at every time point until 1 hour after starting infusion. The limitation may come from the study design. The original two studies were designed to test whether ranitidine infusion with preceding bolus regimen achieves gastric pH > 4 faster than the infusion-alone regimen. In these studies, frequent blood samples were not only unnecessary but also would have introduced ethical issues in the critically ill patients. However, estimating the exposure was crucial in developing the exposure-response relationship in the current analysis.

It was reported that critically ill patients and the elderly were exposed to higher risk of developing stress-related mucosal lesions than healthy subjects or young individuals (Yang YX et al., 2003; Franceschi M et al., 2009). However, none of covariates including age and patient's condition was associated with any of the time-to-event parameters. The patients' demographics might indeed be related to the development of disease but they might not be associated with the effect of ranitidine on acid secretion. The elderly showed a considerably slower rate of gastric pH recovery to the previous steady state level after a meal than young and healthy subjects (Russell TL et al., 1993). The recovery from ranitidine effect after the discontinuation of infusion was not studied in this analysis.

In summary, the survival analysis was successfully implemented to analyze the time-to-event data in NONMEM. An inhibitory sigmoid E_{max} model well described the exposure-response for the ranitidine effect in this analysis. The placebo time-to-event was 19.4 hours and the conditional hazard of event increased as time increased.

However, the estimated dose of ranitidine to achieve half of maximal inhibitory effect, 0.00321 mg, was much less than the dose actually administered to subjects in the current study. And the range of explored exposure, AUC_{0-2}, was too tight to discern the thorough exposure-response relationship of ranitidine effect. Consequently, well designed, prospective time-to-event trials are necessary to establish the exposure-response relationship of ranitidine in the future.

Table 3-1 Patients' demographics

	Count or Median (range)
Critically ill patients/Healthy volunteers	41/9
Male/Female	35/15
Age (years)	56.5 (20-76)
Weight (kg)	78.3 (37.7-173.9)
Creatinine clearance (ml/min)	88.7 (28.7 – 214.4)

Table 3-2 Final population parameter estimates of the time-to-event model and bootstrap results

	Final Model Results		Bootstrap Results	
	Typical Value Estimates	RSE (%)	Median Value	95% Confidence Interval
$Time-to-event_{NoDrug}$, time to achieve gastric pH > 4 when ranitidine was not given (hour)	19.4	85.6	15.3	2.51, 66.81
EA_{50}, $AUC_{0\text{-}2}$ of plasma ranitidine when the effect is half of its maximum (mg·hr/L)	0.000125	456	0.00053	1.4×10^{-6}, 0.0752
α, sigmoidicity	0.423	44.4	0.485	0.253, 0.854
γ, shape factor of Weibull distribution	1.41	12.1	1.46	1.17, 1.89
Interindividual variability (IIV) for $Time-to-event_{NoDrug}$, % CV	84.7	33.3	85.6	49.2, 111.6

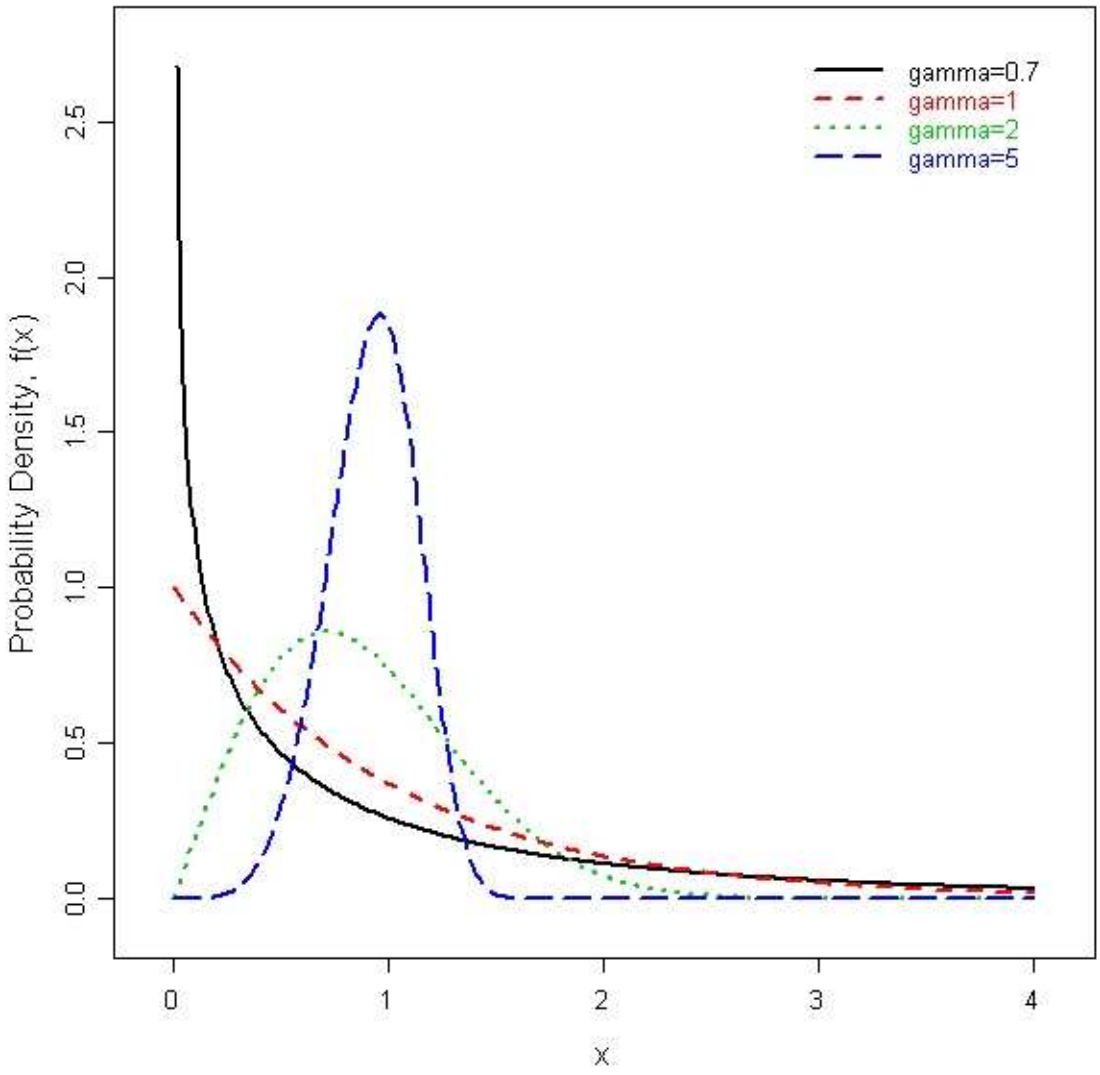

Figure 3-1 The probability density of the Weibull distribution with different values of shape factor, gamma.

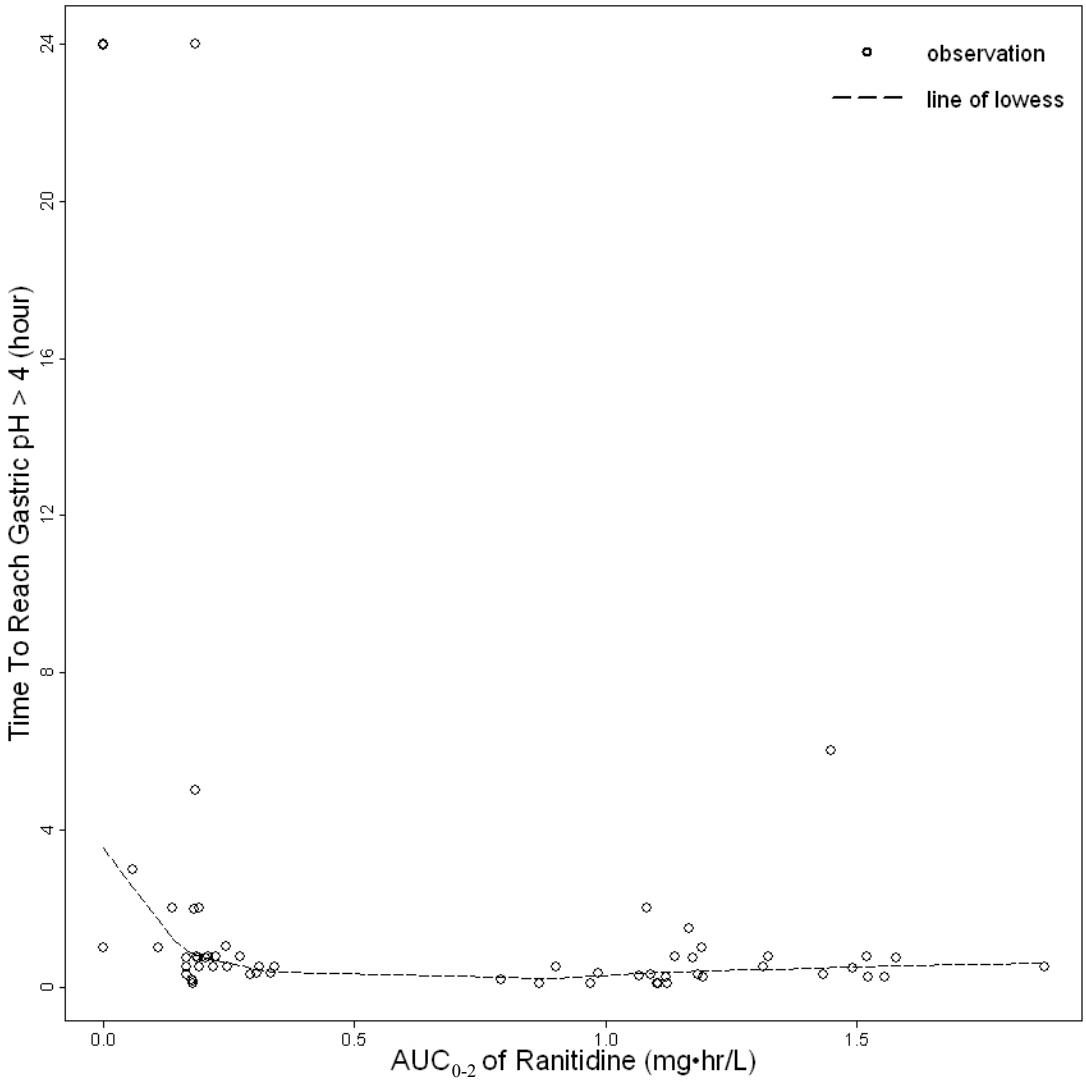

Figure 3-2 The plot of time to gastric pH > 4 versus the area under the time-concentration curve from the beginning of ranitidine administration to 2 hours (AUC_{0-2})

(a)

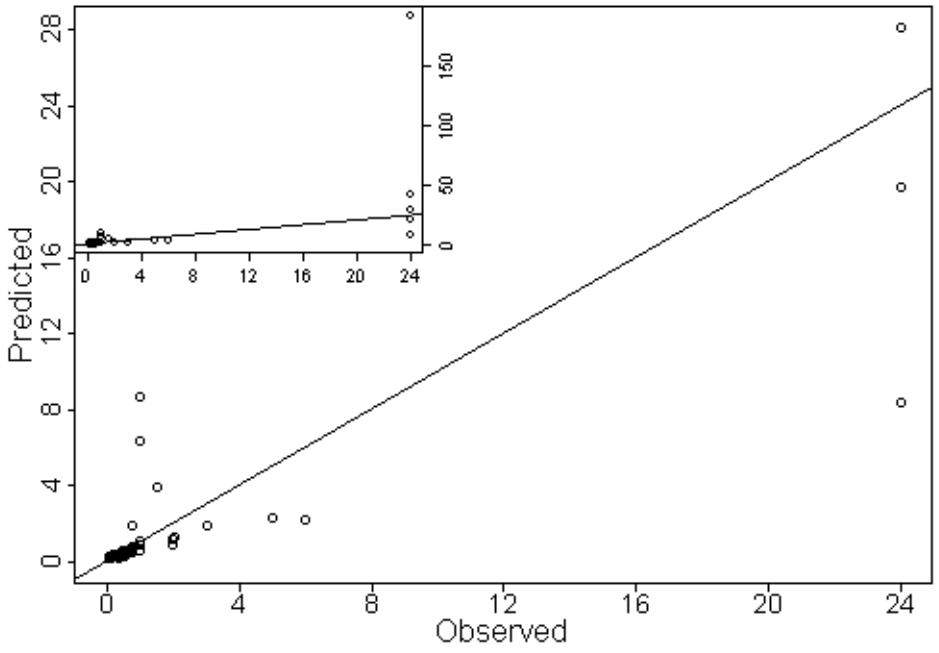

(b)

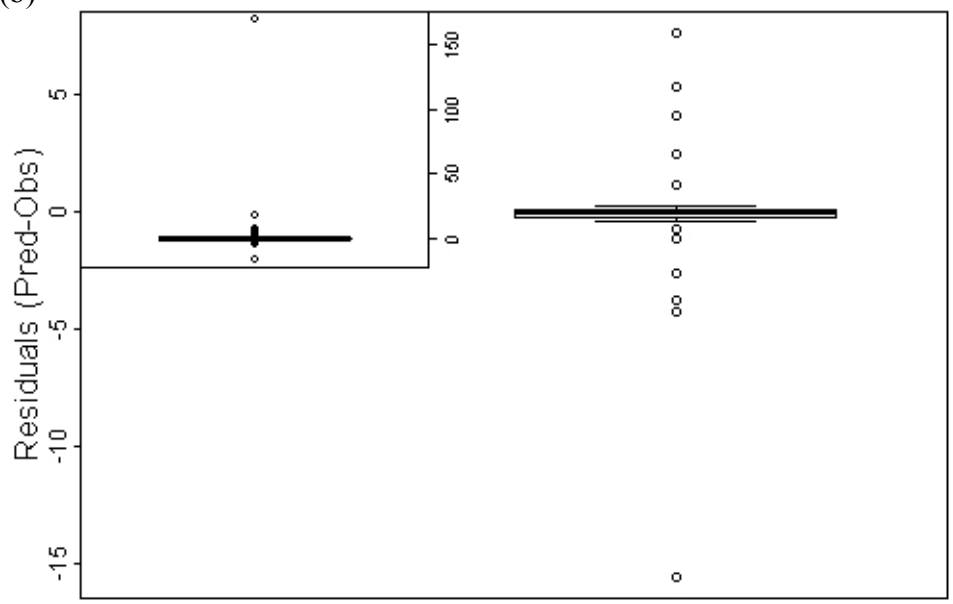

Figure 3-3 The goodness of fit plots of final time-to-event model. (a) Model prediction versus observation. (b) Box and whisker plot of residuals

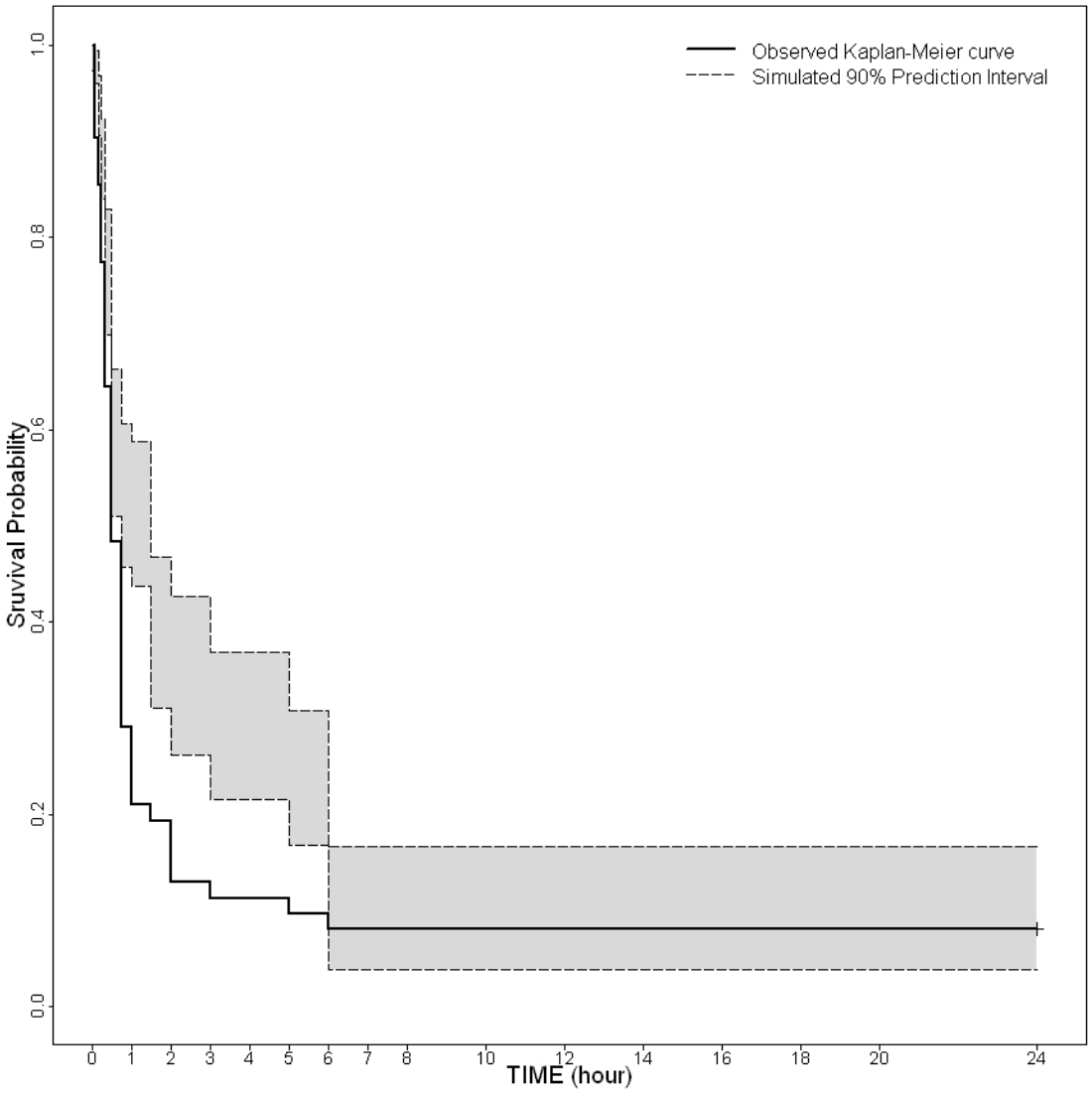

Figure 3-4 The visual predictive plot of the final time-to-event model. Kaplan-Meier plot shows the survival probability which is the fraction of the subjects remaining in the study at least time *t*.

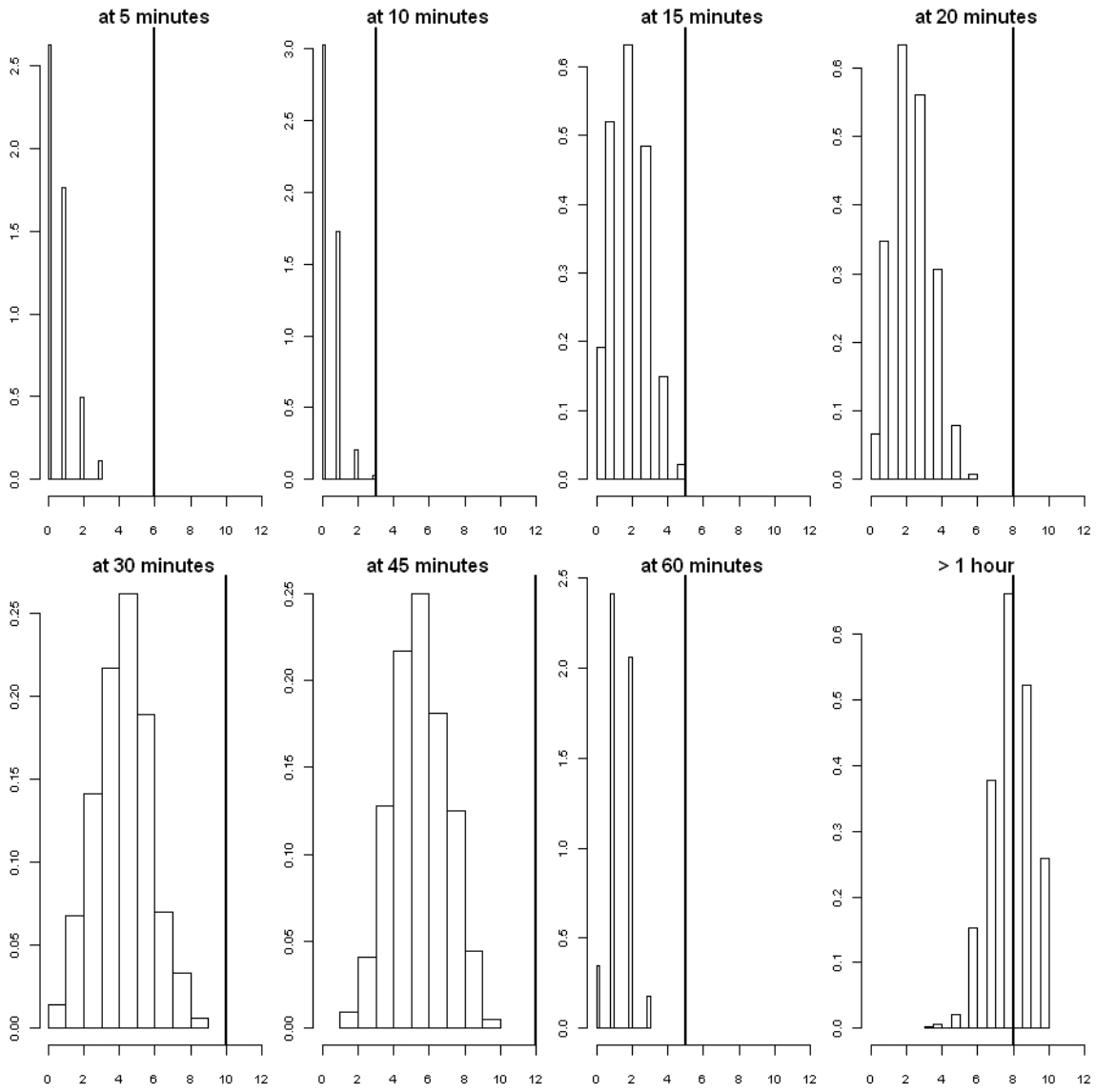

Figure 3-5 The posterior predictive check of the final time-to-event model. The histograms show the distribution of the number of patients experiencing event at each time from a thousand simulated data set of the final model. Vertical bar is the observed number of patients having event.

Chapter 4

Food and Histamine 2 Receptor Antagonist Effect on Human Gastric Acid Secretion

4.1 Introduction

Gastric acid control in human is a "complex, highly regulated and dynamic process" (Joseph IM et al., 2003). It involves neural stimuli, endocrine, paracrine control and food ingestion (Johnson LR, 2006). Parietal cells secrete gastric acid in response to gastrin, histamine and acetylcholine. Gastrin triggers the parietal cell to release gastric acid not only directly but also indirectly including the secretion of histamine from enterochromaffin-like (ECL) cells. Histamine augments gastric acid secretion from parietal cell by binding on histamine 2 (H2) receptors. Neural excitation stimulates the ECL cell to release histamine and provokes parietal cells to secrete gastric acid. Somatostatin inhibits the parietal cell to secrete acid in response to histamine. It also antagonizes histamine release from ECL cell which is driven by gastrin. Antral somatostatin regulates its own secretion through a negative feedback mechanism and suppresses gastrin release from the antral gastrin (G) cell. The entire hormonal and neural process is optimized to digest food. Food consumption disturbs the central and enteric nervous system, drives the change in gastric pH and distends stomach. However,

the disturbed gastric pH provokes a negative feedback mechanism so that the system eventually restores the balance.

The majority of significant upper gastrointestinal bleeding incidents occur in patients whose intragastric pH drop below 4. Thus, maintaining intragastric pH above this critical level is a principle therapeutic objective (Gedeit RG et al., 1993; Netzer P et al., 1999). H2 receptor antagonists have shown high potency in inhibiting gastric acid secretion by competing with histamine for binding on the H2 receptor. Ranitidine is one of the most commonly used H2 receptor antagonists and is available over-the-counter in the United States.

Over the past several years, a number of genetically engineered animals have been generated. Research in gastric acid secretion has benefited from these transgenic animals in investigating the key elements and pathways in the gastric acid secretion system (Samuelson LC et al., 2003). However, no matter how close the animal model is to human, there are no animal models which completely mimic the human physiology due to species differences. While the transgenic animal models have provided opportunities to assess the gastric acid regulation, the controlled experiment is the preferred research approach to understand the complexity of the gastric acid system in humans. However, the benefits of clinical trial are also limited due to the possible invasiveness of methodology, the financial burden, ethical reasons and availability of subjects. Mathematical modeling is a non-invasive method to explore the mechanisms of the gastric acid control. Mathematical modeling is independent from the unexpected

variability that is commonly accompanied with a clinical trial. In addition, a mathematical modeling approach allows testing the system under extreme conditions which cannot be implemented in an experimental study (Ličko V et al., 1992). It is a powerful tool that allows the investigation of each individual element of the model as well as a system's response (Joseph IM et al., 2003).

Mathematical models of gastric acid secretion have previously been published. de Beus AM and colleagues had developed an extensive mathematical model of gastric acid and bicarbonate secretion (de Beus AM et al., 1993). Ličko and Ekblad had built a combined experimental and modeling analysis of gastric acid secretion (Ličko V et al., 1992). An integrative model of human gastric acid secretion was developed using a mathematical modeling approach (Joseph IM et al., 2003). Marino S et al. introduced an inter-compartmental delay between two parts of stomach in the integrative model of human gastric acid secretion (Marino S et al., 2003). In these previous mathematical models, gastric acid secretion was developed successfully but the effect of a gastric antisecretory drug was not incorporated.

In this study, it was hypothesized that a mathematical model using STELLA® could predict reasonable gastric acid secretion without carrying out invasive pH monitoring. Hence, a physiologically-based mathematical model was developed to describe the gastric acid secretion in humans and the responses to multiple doses of ranitidine were simulated to evaluate gastric acid reduction after drug administration.

4.2 Methods

4.2.1 Histology of the Stomach

The stomach was divided into four portions based on their function: fundus, corpus, antrum and pylorus (Johnson LR, 2006). Because the fundus and pylorus were a small portion of stomach and their major function was not gastric acid regulation, both regions were excluded from gastric acid secretion model. The simple anatomy of the stomach is depicted in Figure 4-1.

4.2.2 Cell Populations

Human gastric acid secretory process consists of four cell populations and their products (Joseph IM et al., 2003; Marino S et al., 2003). These cells were the gastrin (G) cell, somatostatin secreting (D) cell, enterochromaffin-like (ECL) cell and parietal cells (PC). The cell populations were assumed to be at steady state in this simulation. The diagram of cell populations is presented in Figure 4-2.

4.2.3 Neural Stimuli

The disturbances of central nervous system (CNS) and the enteric nervous system (ENS) were driven by food intake. There were few of kinetic data describing the effect of food consumption on neural activity. Thus the neural activities were assumed to increase in a Michaelis-Menten manner with food volume as Joseph IM et al. suggested (Joseph IM et

al., 2003). It was also assumed that the central and enteric nervous systems functioned independently. The dynamics for neural stimuli were defined by using the following equations:

$$\frac{d[N_C(t)]}{dt} = \left(\frac{N_{\max_1}[Fd(t)]}{([Fd(t)] + k_{Fd_1})\left(1 + \frac{[A_C(t)]^2}{[A_C(t)]^2 + k_{AN_1}^2}\right)} \right) - \kappa_{N_C}[N_C(t)] + Bas_1 \quad (4.1)$$

$$\frac{d[N_E(t)]}{dt} = \left(\frac{N_{\max_2}[Fd(t)]}{([Fd(t)] + k_{Fd_2})\left(1 + \frac{[A_C(t)]^2}{[A_C(t)]^2 + k_{AN_2}^2}\right)} \right) - \kappa_{N_E}[N_E(t)] + Bas_2 \quad (4.2)$$

where $N_C(t)$ and $N_E(t)$ are the concentrations of the central and enteric neural stimulant at time *t*, N_{max1} and N_{max2} are the maximal CNS and ENS stimulant secretion rates, Fd(t) is the volume of food remaining in the stomach at time *t*, k_{Fd1} and k_{Fd2} are the dissociation constants of food from food receptor on the CNS and ENS, $A_C(t)$ is the corpal acid concentration at time *t*, k_{AN1} and k_{AN2} are the dissociation constants of acid from acid receptor on the CNS and ENS, κ_{NC} and κ_{NE} are the clearance rates of the CNS and ENS stimulant, Bas_1 and Bas_2 are basal neural activities in the CNS and ENS, respectively.

4.2.4 Effecters of Acid Secretion

The G cells and ECL cells released effecters stimulating gastric acid secretion while the product of D cells inhibited the acid secretion. It was assumed that the stimulants were secreted in Michaelis-Menten manner (Joseph IM et al., 2003; Marino S et al., 2003). On the other hand, somatostatin acted in a noncompetitive manner as supported by the experimental evidence (Chew CS, 1983). Thus, an inhibitory term was included where needed: $\left(1+\frac{[I(t)]}{k_I}\right)$, where $[I(t)]$is inhibitor concentration at time t and k_I is dissociation constant of inhibitor from its receptor. If two inhibitors existed on the same receptor, they were assumed to have a multiplicative inhibitory effect.

Gastrin

Food intake directly triggered G cells to secrete gastrin, which was released into antral blood capillaries and diffused into the corpus (Lindström E et al., 2001). Thus, there was a delay between the gastrin secretion from the antral G cells and the gastrin effect observed in the corpus. Marino S et al. suggested this delay was approximately 30 minutes (Marino S et al., 2003). A delay function was employed to account for this delay in the simulation model (equation 4.4). Besides the food, intragastric acid controlled the gastrin secretion through negative feedback while CNS and ENS excitation promoted acid secretion. Gastrin also stimulated the D cells and increased somatostatin leaded gastrin secretion decreased. The antral gastrin was diffused to corpus or washed out to duodenum. The dynamics of antral and corpal gastrin were defined by the following equation:

$$\frac{d[Gtn_A(t)]}{dt} = G_A \left(\begin{array}{l} \dfrac{K_{NG_1}[N_E(t)]}{([N_E(t)]+\alpha_{NG_1})\left(1+\dfrac{[S_A(t)]}{k_{SG}}\right)\left(1+\dfrac{[A_C(t)]^2}{[A_C(t)]^2+k_{AG}^2}\right)} \\ + \dfrac{K_{NG_2}[N_C(t)]}{([N_C(t)]+\alpha_{NG_2})\left(1+\dfrac{[S_A(t)]}{k_{SG}}\right)\left(1+\dfrac{[A_C(t)]^2}{[A_C(t)]^2+k_{AG}^2}\right)} \\ + \dfrac{K_{FG}[Fd(t)]}{([Fd(t)]+\alpha_{FG})\left(1+\dfrac{[S_A(t)]}{k_{SG}}\right)\left(1+\dfrac{[A_C(t)]^2}{[A_C(t)]^2+k_{AG}^2}\right)} \end{array} \right) - \kappa_{Gtn}[Gtn_A(t)] \quad (4.3)$$

$$Gtn_C(t) = \int_{t-0.5}^{t} Gtn_A(t)dt = \int_0^t Gtn_A(t)dt - \int_0^t Gtn_{A,delayed}(t)dt \quad (4.4)$$

where Gtn_A and Gtn_C are the antral and corpal gastrin concentrations at time *t*, G_A is the population of antral G cell, $N_C(t)$ and $N_E(t)$ are the concentrations of the central and enteric neural stimulant at time *t*, $S_A(t)$ is the antral somatostatin concentration at time *t*, $A_C(t)$ is the corpal acid concentration at time *t*, Fd(t) is the volume of food remaining in the stomach at time *t*, K_{NG1}, K_{NG2} and K_{FG} are the maximal rates of the gastrin secretion due to ENS stimulant, CNS stimulant and food intake, α_{NG1} and α_{NG2} are the concentrations of ENS and CNS stimulant at which the rate of gastrin secretion is half-maximal, α_{FG} is the volume of food at which rate of gastrin secretion is half-maximal, k_{SG} and k_{AG} are the dissociation constants of somatostatin and acid from each receptor on the G cell and κ_{Gtn} is the clearance rate of gastrin, respectively.

Somatostatin

Somatostatin was the primary inhibitor of acid secretion and secreted by the D cells in both the antrum and corpus. Antral acid, ENS stimulant, CNS stimulant and antral somatostatin were involved in antral somatostatin secretion (equation 4.5). The corpus gastrin and ENS acted on the corpus D cell to activate somatostatin release (equation 4.6). Corpus somatostatin secretion was inhibited by its own concentration and CNS stimulation. The CNS suppressed somatostatin secretion while it activated gastrin release. Increased gastrin promoted corpal D cell to release more somatoatatin so that the system could eventually recover steady state (equation 4.6).

$$\frac{d[S_A(t)]}{dt} = D_A\left(\frac{K_{AS}[A_A(t)]}{([A_A(t)]+\alpha_{AS})\left(1+\frac{[S_A(t)]}{k_{SS}}\right)\left(1+\frac{[N_C(t)]}{k_{NS}}\right)} + \frac{K_{NS_1}[N_E(t)]}{([N_E(t)]+\alpha_{NS_1})\left(1+\frac{[S_A(t)]}{k_{SS}}\right)\left(1+\frac{[N_C(t)]}{k_{NS}}\right)}\right) - \kappa_S[S_A(t)] \qquad (4.5)$$

$$\frac{d[S_C(t)]}{dt} = D_C\left(\frac{K_{GS}[Gtn_C(t)]}{([Gtn_C(t)]+\alpha_{GS})\left(1+\frac{[S_C(t)]}{k_{SS}}\right)\left(1+\frac{[N_C(t)]}{k_{NS}}\right)} + \frac{K_{NS_2}[N_E(t)]}{([N_E(t)]+\alpha_{NS_2})\left(1+\frac{[S_C(t)]}{k_{SS}}\right)\left(1+\frac{[N_C(t)]}{k_{NS}}\right)}\right) - \kappa_S[S_C(t)] \qquad (4.6)$$

where $S_A(t)$ and $S_C(t)$ are the antral and corpal somatostatin concentrations at time *t*, D_C and D_C are the populations of the antral and corpal D cell, $A_A(t)$ is the antral acid concentration at time *t*, $Gtn_C(t)$ is the corpal gastrin concentration at time *t*, $N_C(t)$ and

$N_E(t)$ are the concentrations of the central and enteric neural stimulant at time *t*, K_{AS} and K_{GS} are the maximal rates of somatostatin secretion due to antral acid and corpal gasrin, K_{NS1} and K_{NS2} are the maximal rates of the antral and corpal somatostatin secretion due to ENS stimulation, α_{AS} and α_{GS} are the acid and gastrin concentrations at which the rate of somatostatin secretion is half-maximal, α_{NS1} and α_{NS2} are the concentrations of ENS stimulant at which rate of antral and corpal somatostatin secretion is half-maximal, k_{SS} and k_{NS} are the dissociation constants of somatostatin and central neural stimulant from its receptor on the G cell and κ_S is the clearance rate of somatostatin, respectively.

Histamine

Corpus gastrin and ENS excitation stimulated ECL cell to secrete histamine while corpal somatostatin inhibited the histamine secretion. The dynamics of histamine was defined by the following equation:

$$\frac{d[H_C(t)]}{dt} = ECL\left(\begin{array}{c}\dfrac{K_{GH}[Gtn_C(t)]}{([Gtn_C(t)]+\alpha_{GH})\left(1+\dfrac{[S_C(t)]}{k_{SH}}\right)} \\ +\dfrac{K_{NH}[N_E(t)]}{([N_E(t)]+\alpha_{NH})\left(1+\dfrac{[S_C(t)]}{k_{SH}}\right)}\end{array}\right) - \kappa_H[H_C(t)] \qquad (4.7)$$

where $H_C(t)$ is the corpal histamine concentration at time *t*, ECL is the population of the enterochromaffin-like cell, $Gtn_C(t)$ is the corpal gastrin concentration at time *t*, $S_C(t)$ is the corpal somatostatin concentration at time *t*, $N_E(t)$ is the concentration of the ENS

stimulant at time *t*, K_{GH} and K_{NH} are the maximal rates of histamine secretion due to gastrin and ENS stimulant, α_{GH} and α_{NH} are the gastrin and ENS stimulant concentrations at which the rate of histamine secretion is half-maximal, k_{SH} is dissociation constant of somatostatin from its receptor on the ECL cell and κ_H is the clearance rate of histamine, respectively.

Acid

Gastrin, histamine and the neural stimulant were the most important physiologic regulators on the acid secretion (Debas HT et al., 1994; Hersey SJ et al., 1995; Lindström E et al., 2001). Corpal gastrin which was diffused from antral region directly stimulated parietal cells to secrete acid in the corpus. Histamine acted in a paracrine manner enhancing acid secretion and also augmented gastrin secretion of parietal cells (Shankley NP et al., 1992). The proximity of ECL cells to the parietal cells permitted histamine to diffuse so as to stimulate acid secretion. As in gastrin and histamine control, somatostatin inhibited the acid secretion noncompetitively. Acid was lost through transport, buffering or washout. Transport of gastric acid from the corpus to antral region and loss to duodenum occurred at a rate of β_A and κ_A, respectively. Buffering of acid by bicarbonate and food is represented in equation 4.8. Antral acid was modeled by the corpus acid transferred to the antrum, based on assumption that the antrum did not have any parietal cells (equation 4.9).

$$\frac{d[A_C(t)]}{dt} = P\left\{\left(\frac{[H_C(t)]}{[H_C(t)]+\alpha_{HA}}\right)\left(\frac{K_{GA}[Gtn_C(t)]}{([Gtn_C(t)]+\alpha_{GA})\left(1+\frac{[S_C(t)]}{k_{SA}}\right)}\right)\right.$$
$$\left.+\left(\frac{K_{HA}[H_C(t)]}{([H_C(t)]+\alpha_{HA})\left(1+\frac{[S_C(t)]}{k_{SA}}\right)}\right)+\left(\frac{K_{NA}[N_C(t)]}{([N_C(t)]+\alpha_{NA})\left(1+\frac{[S_C(t)]}{k_{SA}}\right)}\right)\right\} \quad (4.8)$$
$$-[A_C(t)][B_C(t)]-[A_C(t)]\left(\frac{K_{Fd_{\max}}Fd(t)}{Fd(t)+\alpha_{FA}}\right)-\beta_A[A_C(t)]$$

$$\frac{d[A_A(t)]}{dt} = \beta_A[A_C(t)]-\kappa_A[A_A(t)]-[A_A(t)][B_A(t)] \quad (4.9)$$

where $A_A(t)$ and $A_C(t)$ are the antral and corpal acid concentrations at time *t*, P is the population of the parietal cell, $H_C(t)$ is the corpal histamine concentration at time *t*, $Gtn_C(t)$ is the corpal gastrin concentration at time *t*, $S_C(t)$ is the corpal somatostatin concentration at time *t*, $N_C(t)$ is the concentration of the CNS stimulant at time *t*, $B_A(t)$ and $B_C(t)$ are the antral and corpal bicarbonate concentrations at time *t*, Fd(t) is the food volume remaining in the stomach at time *t*, K_{GA}, K_{HA} and K_{NA} are the maximal rates of acid secretion due to gastrin, histamine and CNS stimulant, K_{Fdmx} is the maximal buffering capacity due to food intake, α_{GA}, α_{HA} and α_{NA} are the gastrin, histamine and CNS stimulant concentrations at which the rate of acid secretion is half-maximal, α_{FA} is the food volume remaining in the stomach at which rate of acid secretion is half-maximal, k_{SA} is the dissociation constant of somatostatin from its receptor on the P cell

and β_A is the transfer rate of acid from corpus to antral region and κ_A is the washout rate of acid, respectively.

Bicarbonate

Gastric acid is destructive to gastric epithelial cells. To protect gastric cells, mucus and bicarbonate ions are produced. For modeling purposes, it was assumed that gastric acid was buffered by bicarbonate ions alone. The behavior of bicarbonate secretion was assumed to follow Michaelis-Menten kinetics. CNS stimulated the bicarbonate secretion in antral and corpal region. Loss of bicarbonate occurred via buffering of acid, transport to the antrum from the corpus or washout to duodenum. The buffering of acid was incorporated by a mass action term, $[A(t)][B(t)]$as suggested by Joshep IM et al. (Joshep IM et al., 2003).

$$\frac{d[B_A(t)]}{dt} = \left(\frac{K_{B_A}[N_C(t)]}{[N_C(t)] + \alpha_{NB}} \right) - [A_A(t)][B_A(t)] - \kappa_B[B_A(t)] \tag{4.10}$$

$$\frac{d[B_C(t)]}{dt} = \left(\frac{K_{B_C}[N_C(t)]}{[N_C(t)] + \alpha_{NB}} \right) - [A_C(t)][B_C(t)] - \beta_B[B_C(t)] \tag{4.11}$$

where $B_A(t)$ and $B_C(t)$ are the antral and corpal bicarbonate concentrations at time *t*, $A_A(t)$ and $A_C(t)$ are the antral and corpal acid concentrations at time *t*, $N_C(t)$ is the concentration of the CNS stimulant at time *t*, K_{BA} and K_{BC} are the maximal rates of antral and corpal bicarbonate secretion due to CNS stimulant, $\alpha_{NB\ is}$ the CNS stimulant concentration at which the rate of base secretion is half-maximal, β_B is the transfer rate of bicarbonate

from corpus to antral region and κ_B is the clearance rate of bicarbonate to duodenum, respectively.

4.2.5 Feeding Function

The standard American diet of three meals a day was used to describe the volume of food consumed. Breakfast, lunch and dinner were given at 6:30 am, 12:30 pm and 6:30 pm, respectively with one liter being the maximal capacity of the stomach. The volume of food remaining in the stomach over time is depicted in Figure 4-3. Hyperbolic tangent function was used to implement the feeding function in the simulation as presented in equation 4.12. Food buffered acid and raised gastric luminal pH (Dressman JB et al, 1990). It was assumed that the dilution following food ingestion was the primary and unique reason of increasing gastric pH. Therefore, effective food volume was determined jointly by the volume of gastric juice and the water in the meal (equation 4.13). The average volume of gastric juice over 24 hour period was reported to be 25 ± 5 ml in healthy volunteers (Dubios A et al., 1977). The volume of gastric juice in the empty stomach was assumed to be 25 ml in the simulation. Since the diluting ability also depends on the contents of consumed food, each meal would have a different buffering capacity. For the modeling purpose, it was assumed that food had ten times buffering capacity of its volume. Gastric pH was calculated according to the equation 4.14.

$$
\begin{aligned}
Fd(t) = {} & 1.6(1+\tanh(\pi[t-(24\times day+19)]))e^{-\frac{1}{2}(1+5[t-(24\times day+19)])} \\
& +(1+\tanh(\pi[t-(24\times day+13)]))e^{-\frac{1}{2}(1+5[t-(24\times day+13)])} \\
& +0.5(1+\tanh(\pi[t-(24\times day+7)]))e^{-\frac{1}{2}(1+5[t-(24\times day+7)])}
\end{aligned} \tag{4.12}
$$

$$
H_{adj}(t) = \frac{Vol_{GF}}{Vol_{GF}+10\cdot Fd(t)}\cdot H(t) \tag{4.13}
$$

$$
pH = -\log\left[H^{+}_{adj}(t)\right] \tag{4.14}
$$

where, *day* is the greatest integer which is less than *t/24*, $tanh(x) = \frac{e^{x}-e^{-x}}{e^{x}+e^{-x}}$, $H^{+}_{adj}(t)$ is the adjusted H^{+} ion at time *t*, Vol_{GF} is the volume of gastric fluid in the empty stomach, H(t) is the acid ions in the stomach at time *t*, Fd(t) is the volume of food remaining in the stomach at time *t*.

4.2.6 Effects of Ranitidine

Ranitidine was assumed to be administered intravenously using the study design introduced in chapter 2. Typical male with creatinine clearance of 90 ml/min was assumed for calculating ranitidine plasma concentrations. In addition, the final population pharmacokinetic parameters in the sequential approach which were developed in chapter 2 were adopted. These parameters were clearance (25.7 L/hr), inter-compartmental clearance (49.4 L/hr), the volume of distribution of central compartment (16.6 L) and the volume of distribution of peripheral compartment (59.8 L). Ranitidine

competes with histamine for binding on H2 receptor located on the surface of parietal cell. In the model, ranitidine effect was incorporated where histamine influencing the acid secretion (equation 4.15).

$$\frac{d[A_C(t)]}{dt} = P\left\{\left(\frac{[H_C(t)]}{[H_C(t)]+\alpha_{HA}\left(1+\frac{C_P(t)}{k_d}\right)}\right)\left(\frac{K_{GA}[Gtn_C(t)]}{([Gtn_C(t)]+\alpha_{GA})\left(1+\frac{[S_C(t)]}{k_{SA}}\right)}\right)\right.$$
$$\left.+\left(\frac{K_{HA}[H_C(t)]}{([H_C(t)]+\alpha_{HA})\left(1+\frac{C_P(t)}{k_d}\right)\left(1+\frac{[S_C(t)]}{k_{SA}}\right)}\right)+\left(\frac{K_{NA}[N_C(t)]}{([N_C(t)]+\alpha_{NA})\left(1+\frac{[S_C(t)]}{k_{SA}}\right)}\right)\right\} \quad (4.15)$$
$$-[A_C(t)][B_C(t)]-[A_C(t)]\left(\frac{k_{Fd_{\max}}Fd(t)}{Fd(t)+\alpha_{FA}}\right)-\beta_A[A_C(t)]$$

where $C_P(t)$ is the ranitidine plasma concentration at time *t*, k_d is the second-order rate constant for interaction between parietal cell and ranitidine. Other abbreviations are identical with those in equation 4.8.

4.2.7 Sensitivity Analysis

In the simulation, sensitivity analysis was implemented to determine the appropriate dose based on current recommendations. The recommended ranitidine dose for adults is presented in Table 4-1 (Grant SJ et al., 1989). Because Zollinger-Ellison syndrome is a cancerous condition, its recommended dose was excluded from the sensitivity analysis.

4.2.8 STELLA®

Physiologically-based mathematical model was developed using STELLA® (Isee Systems, Lebanon, NH), a software for the modeling and simulation of dynamic systems (Sawchuk RJ, 2010). STELLA® is an intuitive and straight forward program for both differential and integral equations. Importantly, sensitivity analysis in STELLA® allows the user to evaluate the sensitivity of the system in response to the change of a specific parameter. Simulation outcomes can be presented as graphs, tables or animation. STELLA® is a useful software program for presenting a complex pharmacokinetic or pharmacodynamic system and for studying the behavior of the system when a change is introduced.

Differential equations were solved by numerical approximation using Runge-Kutta 2nd order method (equation 4.16). In Runge-Kutta 2nd order method, when a starting point x_0, y_0 and an equation $\frac{dy}{dx} = f(x, y)$ are given, the value of y_{i+1} for $x_{i+1} = x_i + h$ is given approximately by

$$y_{i+1} = y_i + \frac{(k_1 + k_2)}{2} \tag{4.16}$$

where, $k_1 = hf(x_i, y_i)$, $k_2 = hf(x_i + h,\ y_i + k_1)$.

Parameters, cell populations and the initial conditions for the simulation were adopted from published experimental data. They are presented in Table 4-2 and Table 4-3. Data from experiments in human were used primarily when possible. Animal data were used

when no human data were available. In the absence of available data, parameters were estimated based on biological feasibility and sensitivity analysis.

4.3 Results

4.3.1 Baseline Conditions

The resting gastric pH when food was not consumed is presented in Figure 4-4. It took about 3 hours to stabilize the system. The estimated baseline gastric pH of 1.97 was within the physiologic gastric pH range, pH 1 - 2 (Dressman JB et al., 1990). Gastric pH change was consistent with the volume of food remaining in the stomach (Figure 4-5). The peak gastric pH after breakfast, lunch and dinner was 4.05, 4.34 and 4.53, respectively. While the gastric pH responded according to the volume of food, the baseline gastric pH was tenable as pH 1.97 when there was no food in the stomach. Food ingestion provoked neural change, release of gastrin and other hormonal and paracrine secretion resulted in gastric acid secretion. Baseline simulations of effecters are depicted in Figure 4-6. While corpal gastrin responded with a delay, the central and enteric nervous system, ECL cell and antral G cell reacted immediately to the food intake. The reciprocal behavior of gastrin and somatostatin in the simulation agreed with previous reports. The bilateral curbing relationship between somatostatin and gastrin has been observed in *in vitro* as well as *in vivo* experiments (Zavros Y et al., 1999; Zavros Y et al.,

2002). The antral and corpal acid change in response to food consumed is presented in Figure 4-7.

4.3.2 Ranitidine Effect

Ranitidine competes with histamine in binding to the H2 receptor and inhibits H^+ ion secretion from the parietal cell. Figure 4-8 displays the gastric pH and plasma concentration of ranitidine when 12.5 mg/hr (300 mg/day) dose was continuously infused over 24 hours. The baseline pH became stable (pH 3.10) when plasma ranitidine concentration achieved steady-state level. Endocrine and paracrine effecters changed similarly to the case when ranitidine was not infused (data not shown). When food was given on top of the ranitidine infusion, the peak gastric pH was 5.18, 5.47 and 5.67 after breakfast, lunch and dinner, respectively (Figure 4-9). The baseline and peak gastric pH with and without ranitidine infusion is presented in Table 4-4.

An abrupt drug discontinuation scenario was also simulated. Based on the previous simulation, it was verified that new steady state was achieved within 24 hours of ranitidine infusion. Figure 4-10 supports that resting gastric pH restored to the original condition within 24 hours if ranitidine infusion was ceased unexpectedly after reaching steady state.

4.3.3 Sensitivity Analysis

Four doses of ranitidine were tested to determine the appropriate dose to achieve gastric pH greater than 4. The doses ranged 8.33-25 mg/hr which are dose for the prophylaxis of acute gastric bleeding, low, medium and high recommended doses. The tested dose, the baseline and peak gastric pH are presented in Table 4-5. The infusion rate of 25 mg/hr of ranitidine yielded the highest resting gastric pH as well as the highest peak gastric pH when food was ingested (Figure 4-11). However, none of the tested achieved resting gastric pH greater than 4. To maintain the baseline gastric pH above 3, at least 300 mg of ranitidine was needed to be administered per day.

4.4 Discussion

Human gastric acid secretion was simulated using a mathematical model with 11 differential equations and a feeding function. In the simulation, it was assumed that food intake alone could bring the disturbance in gastric acid regulation system. Endocrine and paracrine effecters, central and enteric nervous stimuli were connected to each other to maintain the homeostasis. Simulation model was successfully characterized the fasting gastric condition and produced physiologically compatible outcomes with gastric acid controlling agent.

The stomach consists of anatomically and histologically distinct regions: fundus, corpus, antrum and pylorus. The major role of fundus is to store stomach gases released from chemical digestion of food (Johnson LR, 2006). The pylorus is the bottom of stomach

connected with the duodenum and passes food down to the small intestine. Although fundus and pylorus have some gastric cells, they are not profoundly involved in the gastric acid control. Therefore, these two regions were excluded in the current simulation. Gastric cells other than ECL cells proliferate from stem cell through mitosis (Tielemans Y et al., 1990). The ECL cells replicate from themselves as other somatic cells do. Under the normal condition and in a short period, the change of the cell number was negligible (Joseph IM et al., 2003). Thus, cell populations were assumed to be at steady state in this simulation.

The observed gastric pH from the simulation at fasting condition was 1.97 agreed with the literature value (Dressman JB et al., 1990). Maintaining appropriate gastric pH is critical not only for the optimal function but also for the aseptic condition of the stomach (Johnson LR, 2006). Simulation model presented these characteristics by preserving homeostasis once it achieved steady state and returning back quickly when it was disturbed. When food came into the stomach, food triggered neuronal responses, buffered acid and increased gastric luminal pH. The patterns of the neural and effecter activities (Figure 4-6) were consistent with the feeding function (Figure 4-3). Food ingestion promoted release of gastrin in antrum, which was diffused to the corpal region. This diffusion caused the delay between antral gastrin secretion and its observed effect at corpus. The delay between antral and corpal gastrin was clearly observed in the current simulation (Figure 4-6 (B)). The response of somatostatin was reciprocal of other effecter's response which was in accordance with the experimental data (Zavros Y et al.,

1999). The representative reciprocal behavior of gastrin and somatostatin in corpus is presented in Figure 4-12. This emphasized the antagonistic relationship between the two hormonal effecters (Chew CS, 1983; Zavros Y et al., 2002). Histamine release started immediately after each meal (Figure 4-6 (C)). This prompt response of histamine can be explained by the direct ENS effect provoking ECL cell to release histamine. Only a few agents directly stimulate the parietal cells to secrete acid. While ENS acts indirectly on promoting acid release, CNS directly stimulates acid release (Debas HT et al., 1994). Corpal acid and delayed antral acid change that is presented in Figure 4-7 agrees with the experimental outcomes (Dressman JB et al. 1990).

The H2 receptor antagonist effects were investigated by incorporating different doses of ranitidine in the model. Gastric pH change caused by ranitidine usage was closely related to the ranitidine concentration at effect site. Plasma ranitidine concentration was used as a substitute of the concentration at effect site in the current simulation. Because ranitidine competes with histamine for binding on H2 receptor, the higher dose was necessary to achieve higher resting gastric pH. Figure 4-11 suggests that resting gastric pH depends on the rate of infusion of ranitidine. Commonly recommended infusion rate of 12.5 mg/hr (300 mg/day) yielded a baseline gastric pH of 3.10. This outcome needed to be improved to achieve clinically desirable endpoint, resting gastric pH greater than 4. At least infusion rate of 112.5 mg/hour was needed to achieve resting gastric pH greater than 4. The resting and peak gastric pH with different doses of ranitidine is presented in Table 4-5. The simulation also presented that if a patient stopped ranitidine infusion

abruptly, the resting gastric pH will be recovered in 24 hours (Figure 4-10). The rate of recovery depends on the pharmacokinetic characteristics of ranitidine: total body clearance and the volume of distribution at terminal phase. The changes of endocrine, paracrine and neurocrine effecters with and without ranitidine infusion were similar (data not shown).

Although none of the tested doses showed satisfactory outcome in terms of the fasting gastric pH in this simulation, it has been reported that ranitidine increases the gastric pH greater than 4 in the clinical setting (Amsden GW et al., 1994; Orenstein SR et al., 2002). Part of this discrepancy is attributed to the parameters in the simulation. Some parameters were from animal studies due to the lack of reported values in human. These animal estimates could not be free from species differences. Current model assumed a healthy male subject to calculate plasma ranitidine concentration. Ranitidine concentration can be increased when patient population is changed to the other population such as elderly, children or critically ill patients.

Due to the limited studies of food effect on nervous system as well as effecters, a couple of parameters related with food were estimated. For instance, maximal buffer capacity of food was determined through sensitivity analysis. Reported buffer capacity of some dark and light beef, pork and poultry muscles ranged from 40 to 60 mmol H^+/pH·kg (Puolanne E et al., 2000). Within explored range of 5 - 100 mmol H^+/pH·kg, the effect of buffer capacity of food on gastric pH was minimal. The choice of a few parameters for example, dissociation constants of food from food receptor on nervous system (k_{Fd1} and

k_{Fd2}) were arbitrary due to the lack of related reported values. The influence of these parameters on gastric pH and the pattern of effecters were limited to the simulated range. Unlike other parameters, K_{HA} was very influential on the resting pH demonstrating the significant role of histamine in the gastric acid secretion. Histamine is known to be critically involved in the stimulation of gastric acid secretion with gastrin and acetylcholine in the so called gastrin-ECL cell-parietal cell axis (Barocelli E et al., 2003).

Despite the convincing outcomes of the simulation, this model should be applied with great caution. One of the aims of this study was to predict gastric acid secretion. To achieve this, many of the complicated parts consisting actual physiology of gastric acid control were neglected. For example, the simulation model assumed that all gastric cells were at steady state over the study period however, it was rather unrealistic. The number of gastric cells had reported to fluctuate over several days during an experiment, although it was stable in a short period. There are studies presenting that gastrin concentration was correlated with the ECL cell proliferation (Häkanson R et al., 1976; Borch K et al., 1986). The growth of the gastric cells is influenced by non-gastrointestinal hormones and factors associated with the ingestion or digestion of a meal (Johnson LR, 2006). Furthermore, long-term administration of the H2 receptor antagonist may cause the ECL cell to overgrow or parietal cell to degenerate (Feurle GE, 1994; Karam SM et al., 2001). Disease state and stress can also affect the gastrointestinal system. The classical examples are stress ulcer, gastroesophageal reflux disease and inflammatory bowel disease (Harty RF et al., 2006; Kamolz T et al., 2006; Farhadi A et al., 2007). In

addition, different food contents have dissimilar acid buffering capacities which were not considered in the model. In general, a meal with more amino acid sources has a higher buffering capacity because amino acids have one or more anionic, cationic group and a lateral chain that may be ionizable (Cuvale RA, 2009). Also food with more amino acid, especially aromatic amino acids, stimulated antral G cell to secrete more gastrin than when food with carbohydrate or lipid was taken (Peterson WL 1996). Neuronal control on gastric acid was so strong and complicated that its own stimulus could drop the pH regardless of food ingestion (Feldman M, 1985; Debas HT et al., 1994). It was also reported that significant distention of the antral portion of the stomach resulted in enhanced release of gastrin (Schiller LR et al., 1980). Lastly, the possible interactions of effecters in acid secretion were ignored in the simulation. It was reported that the combination of histamine with CNS stimulus induced a more increase in the gastric acid secretion than the addition of the effects of histamine and CNS stimulus separately (Kleveland PM et al, 1987). As another example, histamine not only stimulated acid secretion, but also enhanced gastrin-stimulated acid release in a dose dependent manner (Lindström E et al., 2001).

Although the main purpose of this study was to develop a mathematical model to predict gastric acid secretion and antisecretory effect of a H2 receptor antagonist, this model can be applied to design gastric acid secretion in a disease condition such as *H. pylori* infection or partial gastrectomy. Antisecretory agents other than H2 receptor antagonist can also be incorporated into a simulation as well.

In summary, the proposed mathematical model successfully demonstrated physiological gastric acid regulation, the effect of food, and H2 receptor antagonist on gastric acid secretion. This model can be applied to determine optimal dosing regimens of antisecretory agents other than H2 receptor antagonist and to predict gastric acid profiles under disease conditions.

Table 4-1 Ranitidine indication and dose

Indication	Dose
Stress ulcer, prophylaxis	50 mg qid
Duodenal ulcer	150 mg bid, 300 mg qd
Gastric ulcer	150 mg qd - bid, 300 mg qd
Peptic ulcer	150 mg bid
Erosive esophagitis	150 mg bid
Gastroesophageal reflux disease	150 mg bid / 300 mg qd
Pulmonary acid aspiration, prophylaxis	50 mg before operation - 150 mg qid
Helicobacter pylori infection	150 mg bid
Zollinger-Ellison syndrome	150 mg bid - 6 g/day

qd: once a day, bid: twice a day, qid: four times a day

Table 4-2 Parameter values included in model analysis.

Parameters	Description	Unit	Value
α_{AS}[1,2]	Acid concn at which rate of somatostatin secretion is half-maximal	M	0.05
α_{FA}[*]	Food volume at which rate of acid secretion is half-maximal	L	0.01
α_{FG}[*]	Food volume at which rate of gastrin secretion is half-maximal	L	0.05
α_{GA}[1]	Gastrin concn at which rate of acid secretion is half-maximal	M	1.8×10^{-10}
α_{GH}[1]	Gastrin concn at which rate of histamine secretion is half-maximal	M	3×10^{-10}
α_{GS}[1,2]	Gastrin concn at which rate of corpal somatostatin secretion is half-maximal	M	5.20×10^{-12}
α_{HA}[1,*]	Histamine concn at which rate of acid secretion is half-maximal	M	3.2×10^{-9}
α_{NA}[1]	Concn of CNS stimulant at which rate of acid secretion is half-maximal	M	5×10^{-6}
α_{NB}[*]	Concn of ENS stimulant at which rate of bicarbonate secretion is half-maximal	M	10^{-10}
α_{NG1}[1,2]	Concn of ENS stimulant at which rate of gastrin secretion is half-maximal	M	10^{-10}
α_{NG2}[1,2]	Concn of ENS stimulant at which rate of gastrin secretion is half-maximal	M	10^{-10}
α_{NH}[1]	Concn of ENS stimulant at which rate of histamine secretion is half-maximal	M	3.25×10^{-8}
α_{NS1}[1,2]	Concn of ENS stimulant at which rate of antral somatostatin secretion is half-maximal	M	6.28×10^{-7}
α_{NS2}[1,2]	Concn of ENS stimulant at which rate of corpal somatostatin secretion is half-maximal	M	8.98×10^{-11}
β_{A}[1]	Transfer rate of acid from corpus to antral region	/hr	2.72
β_{B}[2]	Transfer rate of bicarbonate from corpus to antral region	/hr	2.72
κ_{A}[1]	Washout rate of acid	/hr	2.72
κ_{B}[2]	Clearance rate of bicarbonate	/hr	2.72
κ_{H}[1]	Clearance rate of histamin	/hr	11.89
κ_{G}[1,2]	Clearance rate of gastrin	/hr	11.88
κ_{Nc}[2]	Clearance rate of CNS stimulant	/hr	12
κ_{Ne}[2]	Clearance rate of ENS stimulant	/hr	12
κ_{S}[1,2]	Clearance rate of somatostatin	/hr	11.88
k_{AG}[2,*]	Dissociation constant of acid from acid receptor on G cell	M	10^{-9}
k_{AN1}[*]	Dissociation constant of acid from acid receptor on CNS	M	10^{-11}
k_{AN2}[*]	Dissociation constant of acid from acid receptor on ENS	M	10^{-11}
k_{Fd1}[*]	Dissociation constant of food from food receptor on CNS	L	0.1
k_{Fd2}[*]	Dissociation constant of food from food receptor on ENS	L	0.5
k_{NS}[1,2]	Dissociation constant of GRP from somatostatin receptor on D cell	M	10^{-9}
k_{SA}[2]	Dissociation constant of somatostatin from somatostatin receptor on parital cell	M	9×10^{-10}
k_{SG}[1]	Dissociation constant of somatostatin from somatostatin receptor on G cell	M	9×10^{-11}
k_{SH}[1]	Dissociation constant of somatostatin from somatostatin receptor on ECL cell	M	9×10^{-10}
k_{SA}[1]	Dissociation constant of somatostatin from somatostatin	M	9×10^{-11}

	receptor on parietal cell		
k_{SS}[1]	Dissociation constant of somatostatin from somatostatin receptor on antral D cell	M	9×10^{-11}
K_{AS}[1,2]	Maximal rate of somatostatin secretion due to antral acid	M/hr/cell	8.04×10^{-15}
K_{Ba}[3]	Maximal rate of antral bicarbonate secretion due to CNS stimulant	M/hr/cell	2.8818×10^{-5}
K_{Bc}[3]	Maximal rate of corpal bicarbonate secretion due to CNS stimulant	M/hr/cell	0.1059×10^{-2}
K_{FG}[1,2]	Maximal rate of gastrin secretion due to food intake	M/hr/cell	9.39×10^{-18}
K_{Fdmax}[4]	Maximal buffering capacity of food consumed	M/L/pH	0.01
K_{GA}[1]	Maximal rate of acid secretion due to gastrin	M/hr/cell	4.98×10^{-11}
K_{GH}[1]	Maximal rate of histamine secretion due to gastrin	M/hr/cell	7.77×10^{-16}
K_{GS}[1,2]	Maximal rate of somatostatin secretion due to gastrin	M/hr/cell	2.54×10^{-18}
K_{HA}[1]	Maximal rate of acid secretion due to histamine	M/hr/cell	1.5×10^{-10}
K_{NA}[1]	Maximal rate of acid secretion due to nervous stimulant (ACh)	M/hr/cell	2.33×10^{-11}
K_{NG1}[1,2]	Maximal rate of gastrin secretion due to CNS stimulant	M/hr/cell	8.75×10^{-17}
K_{NG2}[1,2]	Maximal rate of gastrin secretion due to ENS stimulant	M/hr/cell	6.28×10^{-17}
K_{NH}[1]	Maximal rate of histamine secretion due to ENS stimulant	M/hr/cell	7.59×10^{-16}
K_{NS1}[1,2]	Maximal rate of antral somatostatin secretion due to ENS stimulant	M/hr/cell	1.14×10^{-15}
K_{NS2}[1,2]	Maximal rate of corpal somatostatin secretion due to ENS stimulant	M/hr/cell	1.54×10^{-17}
k_d[5,6]	Dissociation constant of ranitidine from H2 receptor on ECL cell	M	10^{-7}
N_{max1}*	Maximal rate of CNS stimulant secretion	M/hr	10^{-9}
N_{max2}[2]	Maximal rate of ENS stimulant secretion	M/hr	10^{-8}

1: Joseph IM et al., 2003

2: Marino S et al., 2003

3: Feldman M, 1983

4: Puolanne E et al., 2000

5: Lin JH 1991

6: Coruzzi G et al., 1996

*: estimated

Table 4-3 Initial conditions

Initial conditions	Unit	Value
Initial antral bicarbonate concentration[1]	M	2.8818×10^{-6}
Initial antral gastrin concentration[1]	M	1.0213×10^{-12}
Initial antral acid concentration[1]	M	0.2605×10^{-3}
Initial antral somatostatin concentration[1]	M	8.4402×10^{-12}
Initial corpal bicarbonate concentration[1]	M	0.1059×10^{-3}
Initial corpal gastrin concentration[1]	M	0.1289×10^{-12}
Initial corpal acid concentration[1]	M	10.9×10^{-3}
Initial corpal somatostatin concentration[1]	M	66.56×10^{-12}
Initial histamin concentration[1]	M	1.1074×10^{-9}
Iinitial CNS stimulant concentration[1]	M	0.57309×10^{-9}
Initial ENS stimulant concentration[1]	M	55.588×10^{-12}
Antrum D cell[2]	count	3.7×10^{6}
Antrum G cell[2]	count	8.75×10^{6}
Corpus D cell[2]	count	2.69×10^{8}
Corpus EC cell[2]	count	8.68×10^{8}
Corpus PC cell[2]	count	1×10^{9}

1: Marino S et al., 2003

2: Joseph IM et al., 2003

Table 4-4 Simulated gastric pH with and without ranitidine infusion

		No ranitidine	Ranitidine infusion
Baseline gastric pH		1.97	3.10
Peak gastric pH	Breakfast	4.05	5.18
	Lunch	4.34	5.47
	Dinner	4.53	5.67

Table 4-5 Baseline and peak gastric pH with different dose of ranitidine

Infusion rate (daily dose)	Baseline	Breakfast	Lunch	Dinner
8.33 mg/hr (200 mg)	2.95	5.03	5.32	5.51
6.25 mg/hr (150 mg)	2.84	4.92	5.21	5.41
12.5 mg/hr (300 mg)	3.10	5.18	5.47	5.67
25 mg/hr (600 mg)	3.37	5.45	5.75	5.94

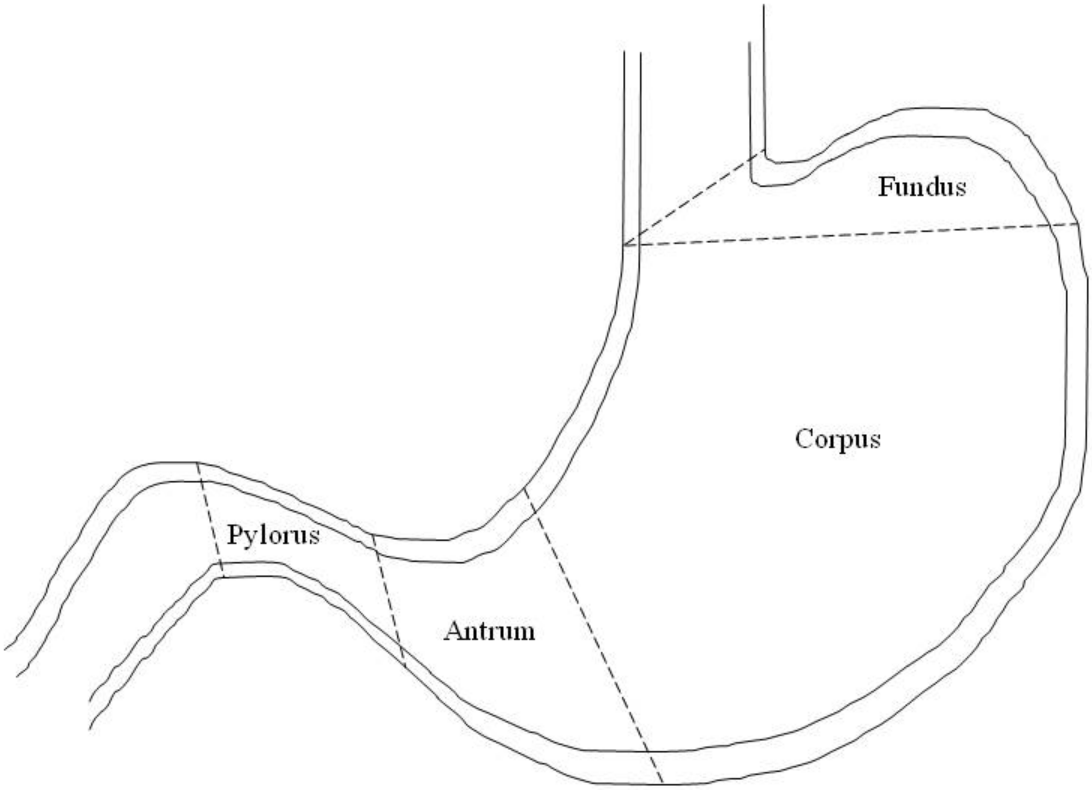

Figure 4-1 Anatomy of stomach (Johnson LR, 2006)

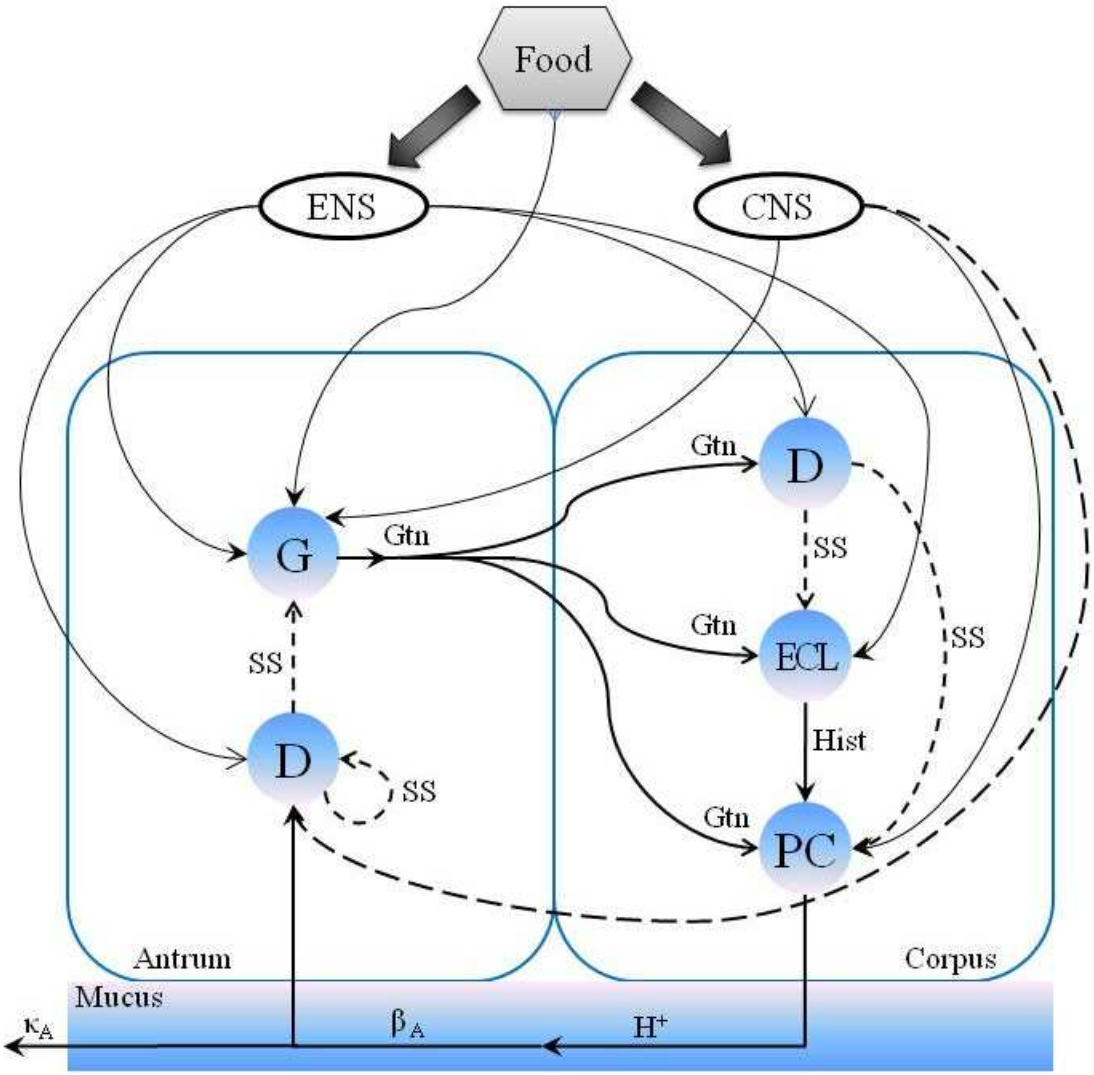

Figure 4-2 Model diagram of effecter regulation of gastric acid secretion. Solid line represents the stimulating action whereas dashed line the inhibiting action. G cells secrete gastrin (Gtn) which stimulates the secretion of histamine (Hist) from enterochromaffin-like (ECL) cells, gastric acid (H^+) from parietal cells (PC) and somatostatin (SS) from D cells. CNS and ENS mean central and enteric nervous system, respectively. β_A and κ_A represents transport rate of acid from corpus to antrum and washout rate of acid with gastric emptying, respectively (Joseph IM et al., 2003; Marino S et al., 2003).

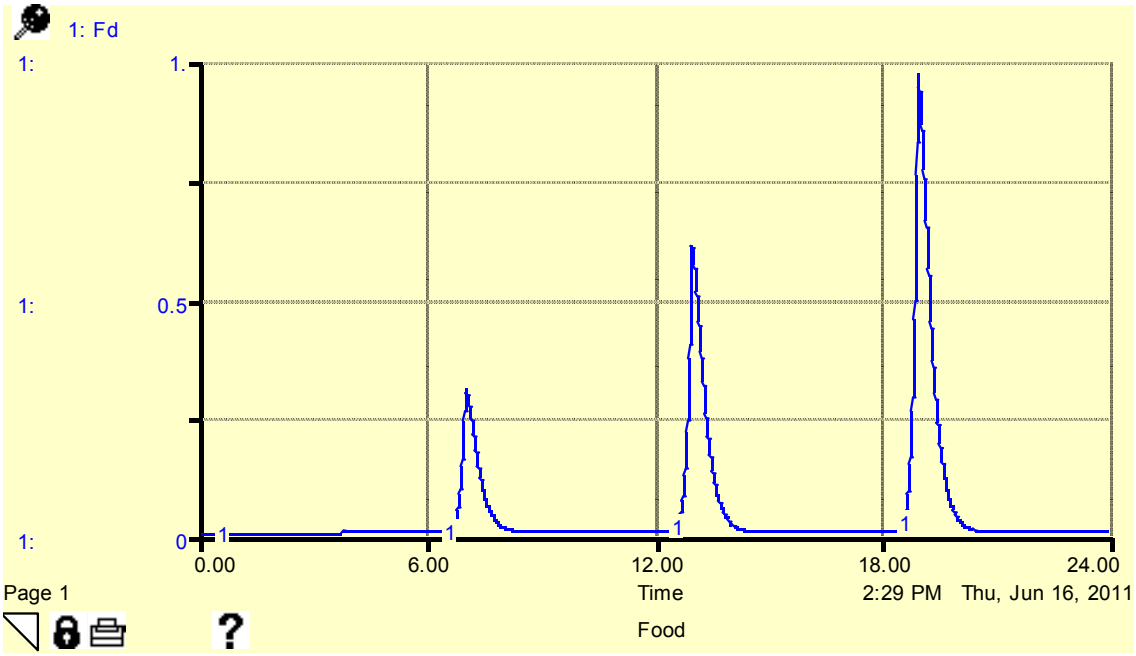

Figure 4-3 Feeding function: The volume of food staying in the stomach over time.

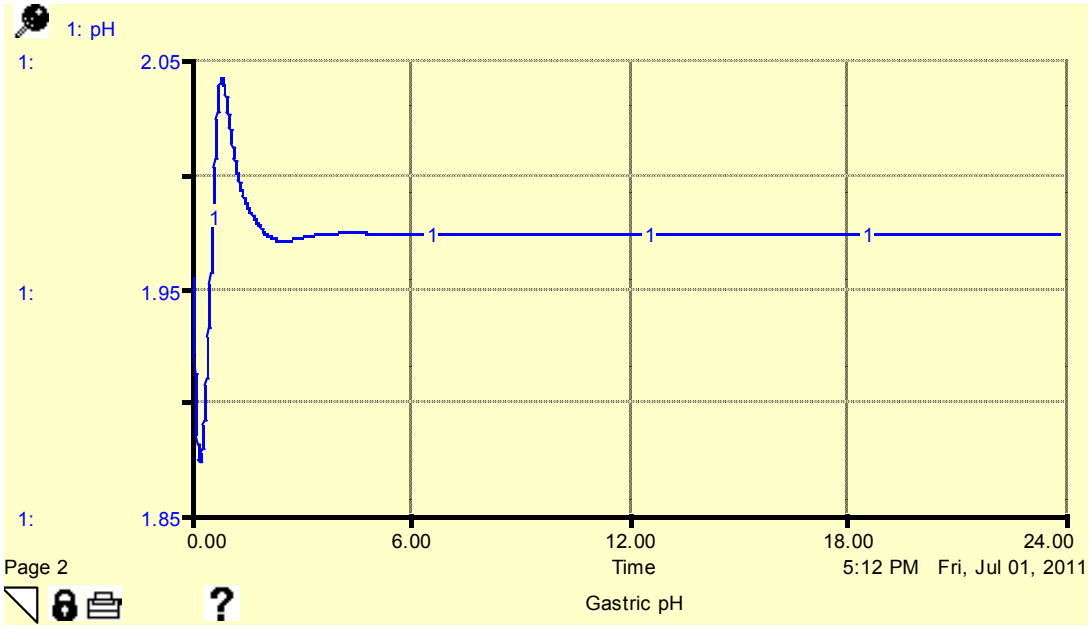

Figure 4-4 Baseline gastric pH when food is not given

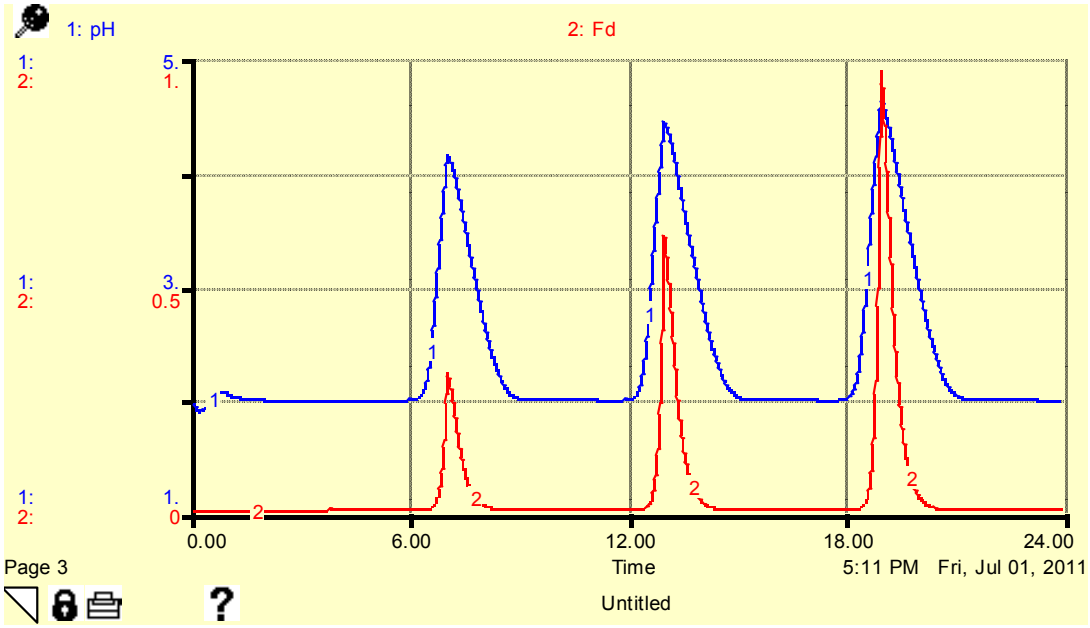

Figure 4-5 Baseline gastric pH and feeding function over time

(A)

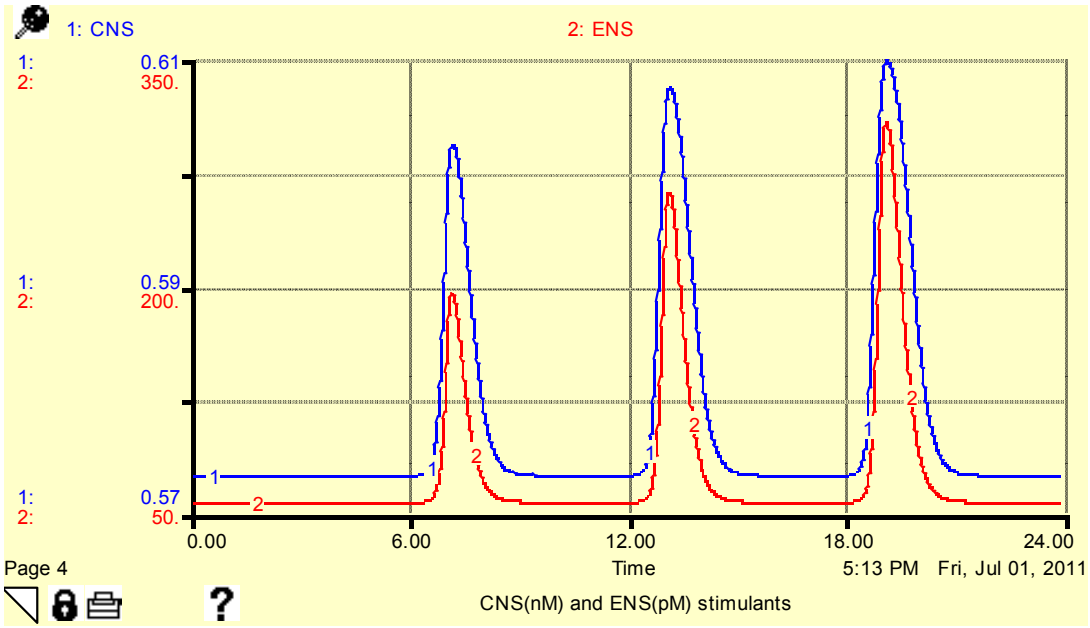
1: CNS
2: ENS
1: 0.61
2: 350.
1: 0.59
2: 200.
1: 0.57
2: 50.
0.00
6.00
12.00
18.00
24.00
Time
Page 4
5:13 PM Fri, Jul 01, 2011
CNS(nM) and ENS(pM) stimulants

(B)

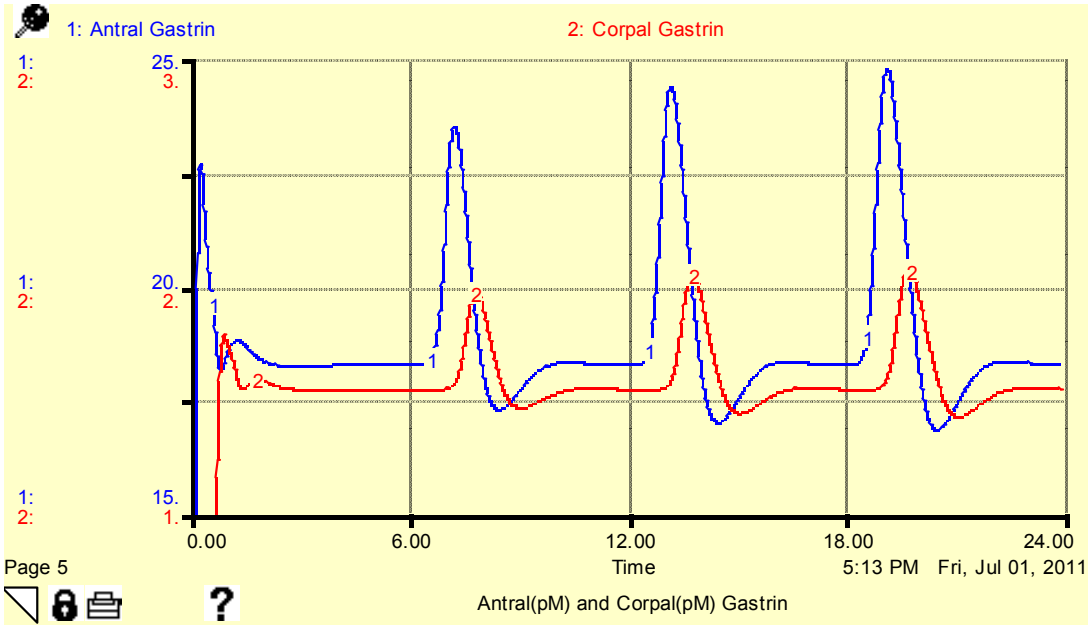
1: Antral Gastrin
2: Corpal Gastrin
1: 25.
2: 3.
1: 20.
2: 2.
1: 15.
2: 1.
0.00
6.00
12.00
18.00
24.00
Time
Page 5
5:13 PM Fri, Jul 01, 2011
Antral(pM) and Corpal(pM) Gastrin

(C)

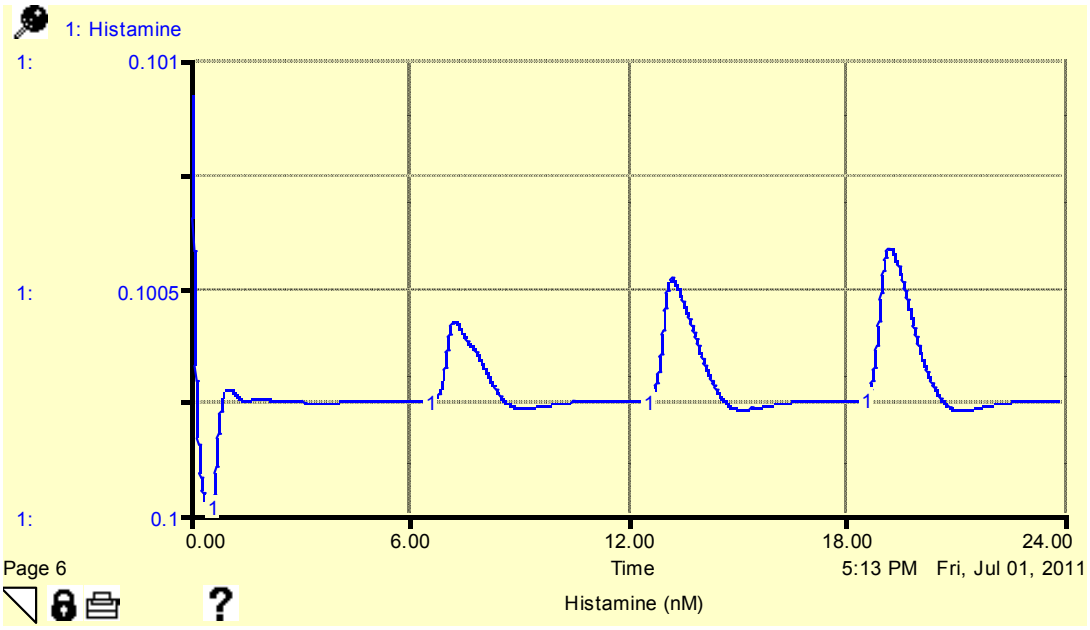

(D)

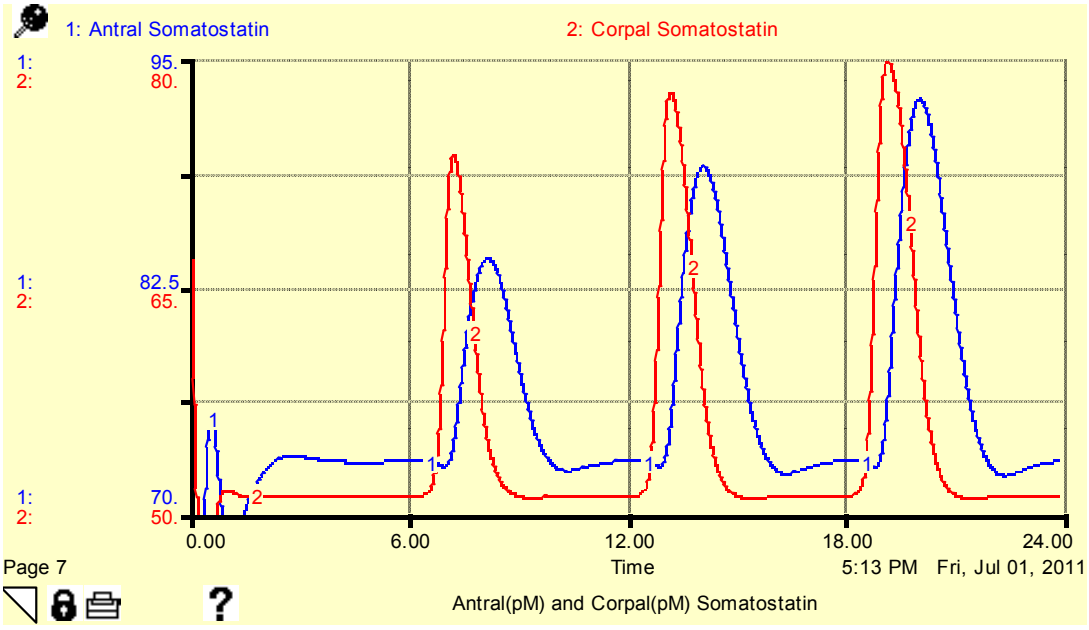

Figure 4-6 Baseline simulation of effecters. (A) Central nervous stimulants and enteric nervous stimulants, (B) Antral and corpal gastrin, (C) Histamine and (D) Antral and corpal somatostatin

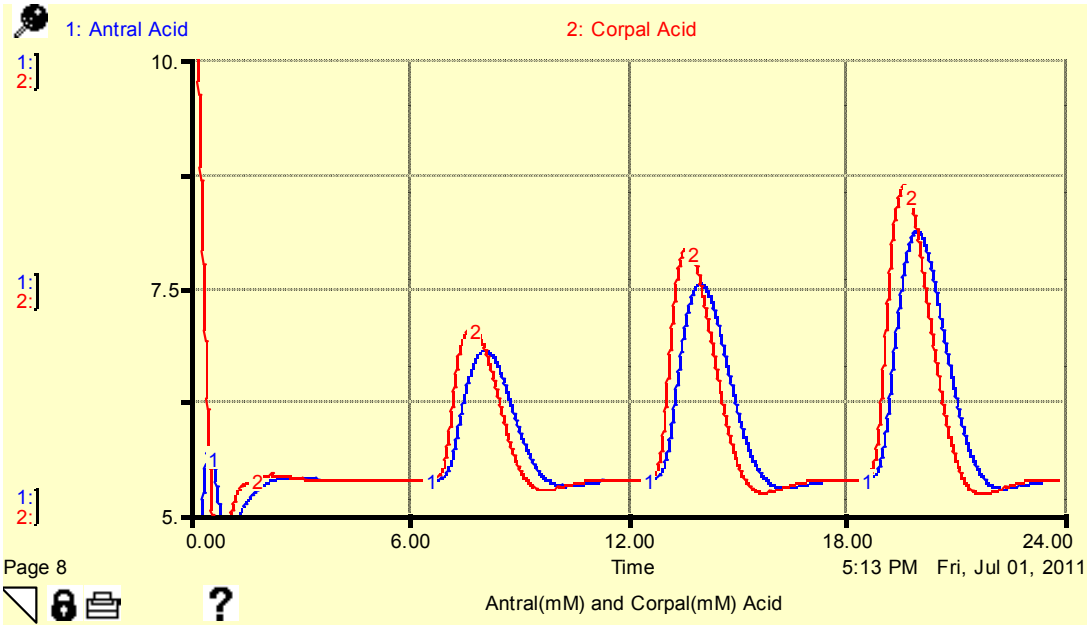

Figure 4-7 Baseline simulation of the antral and corpal acid in response to food consumed.

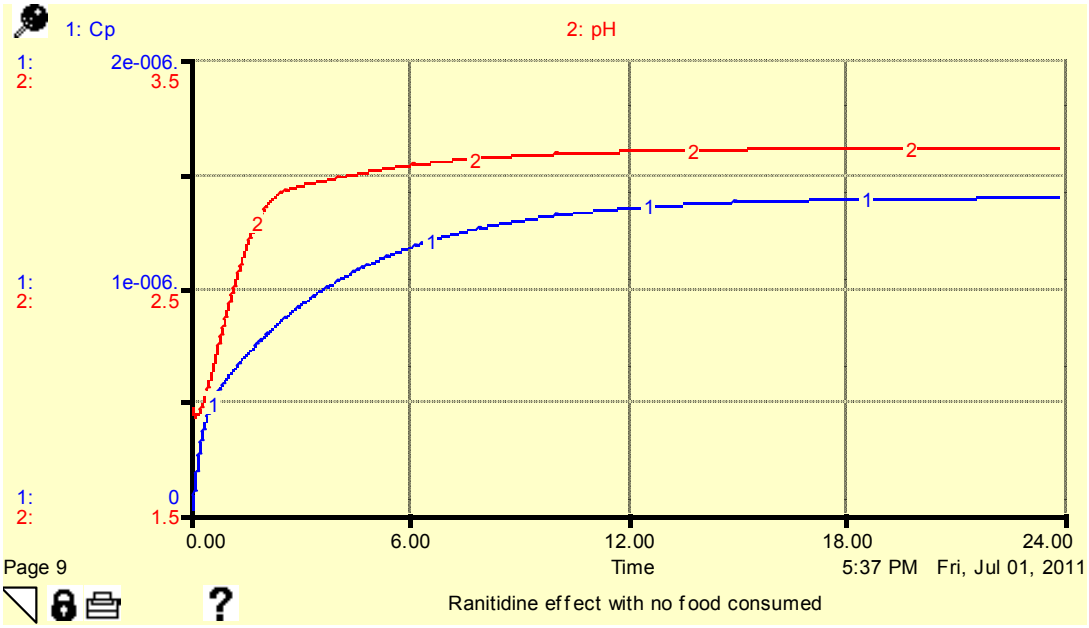

Figure 4-8 Ranitidine plasma concentration and gastric pH change.

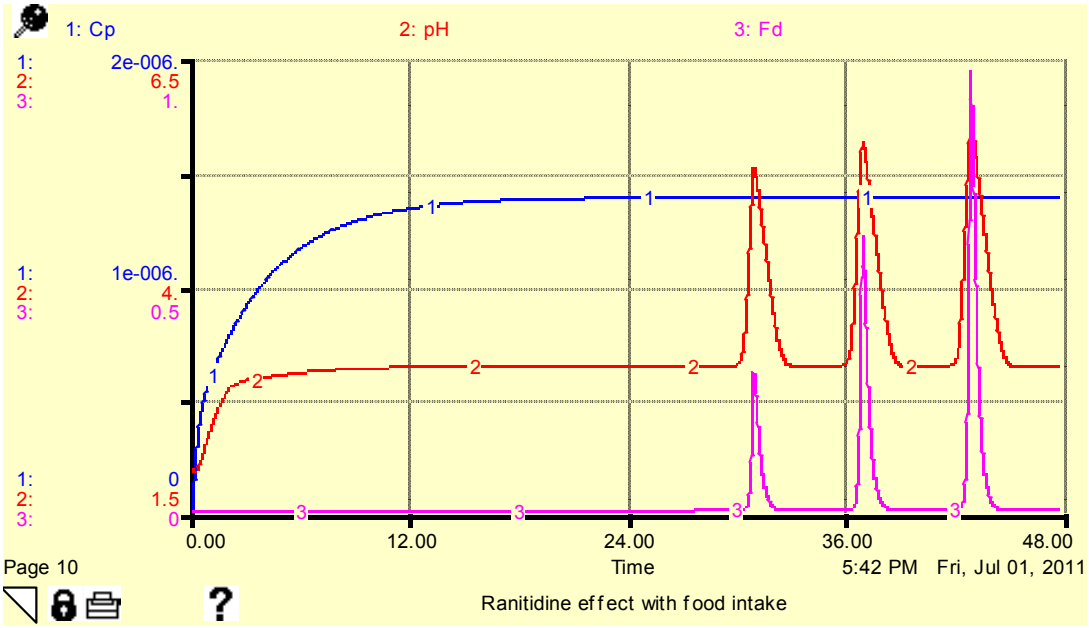

Figure 4-9 Ranitidine plasma concentration, gastric pH and the volume of food consumed over time.

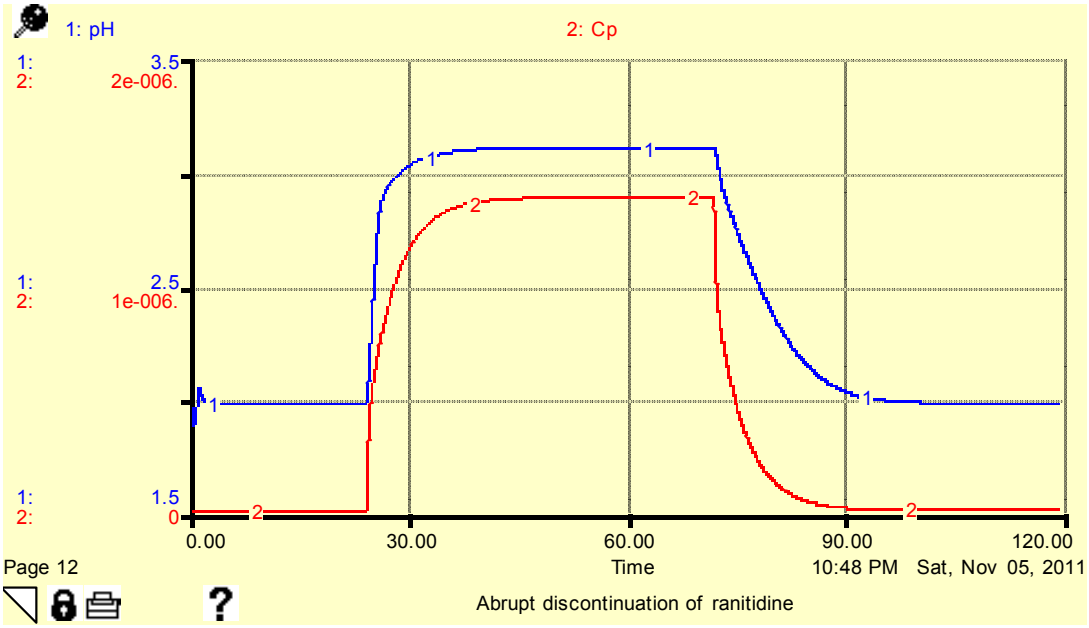

Figure 4-10 Gastric pH change when ranitidine infusion is discontinued

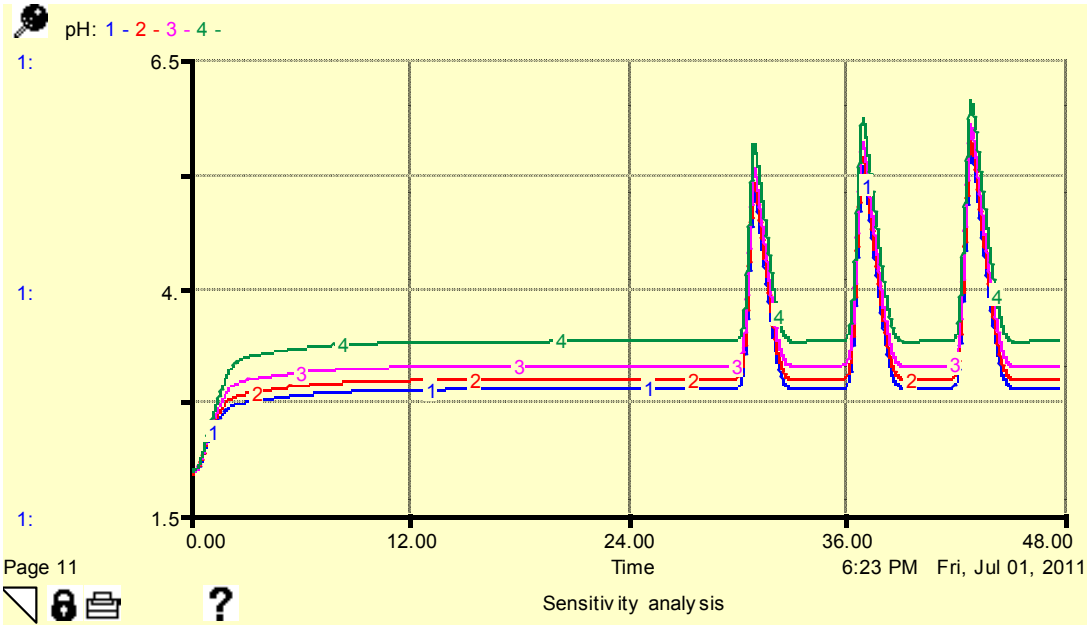

Figure 4-11 Sensitivity analysis. Gastric pH changes according to the different infusion rate of ranitidine. Line 1 is for infusion rate of 6.25 mg/hr, line 2, 8.33 mg/hr, line 3, 12.5 mg/hr and line 4, 25 mg/hr, respectively.

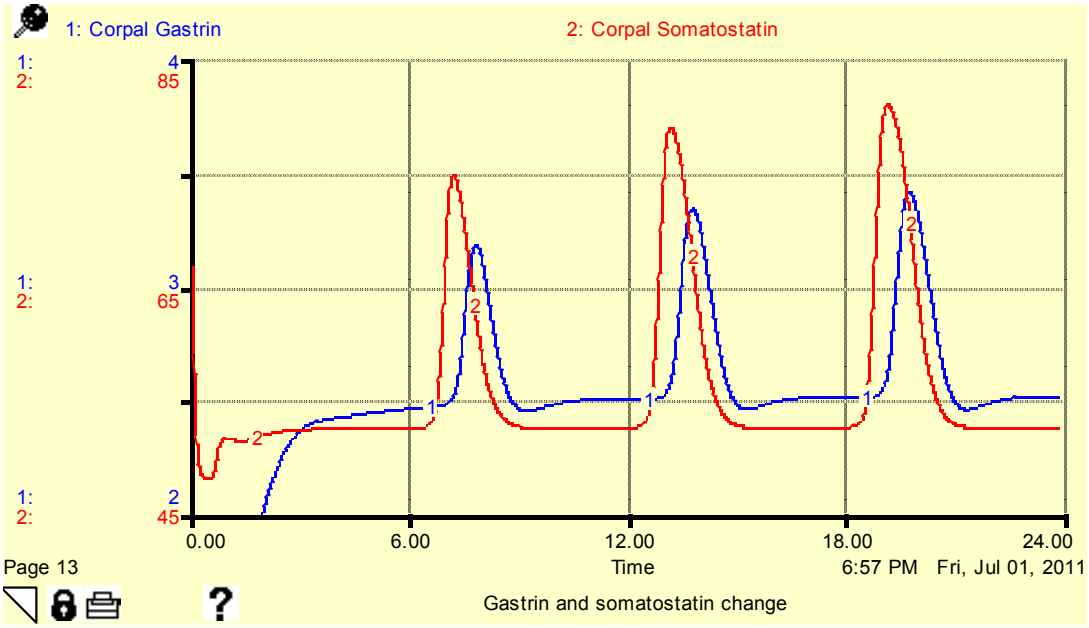

Figure 4-12 The reciprocal change of gastrin and somatostatin in corpus

Chapter 5

Summary and Future Direction

5.1 Pharmacokinetic-Pharmacodynamic Models of Ranitidine

The pharmacokinetics (PK) and pharmacodynamics (PD) of ranitidine have been investigated extensively using a traditional research approach. However, it is not only impractical but unethical to obtain multiple samples for the traditional PKPD analysis in a certain population such as critically ill patients. Thus, it has been common to develop PK and PD models with data from multiple individuals using a population approach. The specific aim of this research project was to model the PK-PD relationship of ranitidine in the sequential and the simultaneous approaches and to decide the important demographic or clinical characteristics for predicting PK or PD parameters. About 12 % of PD data were censored due to the technical limitation of the pH meter used in the trials. These censored data were excluded and Laplace estimation method was used to take into account the censoring issue in the analysis. The final PK models were identical in both approaches except one parameter included only in the sequential approach: the covariance between the interindividual variability of the clearance and the peripheral volume of distribution ($\omega_{CL,Vp}$). The final PK parameter estimates in the sequential approach were close to the corresponding values in the simultaneous approach. The

estimated PK parameters from both approaches agreed with the previously reported values. Creatinine clearance (CrCL) and patient's sex were identified to be the important covariates in the prediction of the ranitidine clearance and the peripheral volume of distribution, respectively. When patient's CrCL dropped, the ranitidine clearance was predicted to decrease as well. It was assessed that the final PK model predicted the actual observations well through simulation-based model evaluation plots. It was found that the PD parameter estimates in the sequential approach were more physiologically reasonable than in the simultaneous approach based on the actual data. In addition, the parameters were estimated more precisely when PK and PD models were built sequentially than simultaneously. None of the covariates were associated with any of the PD parameters. It was infeasible to use the simulation- or prediction-based model evaluation plots for evaluating PD model due to the censoring issue.

The investigation of the ranitidine PKPD relationship can be improved with the all PD values being reported because censoring explicitly means missing information. Although the fact of censoring was taken into account, it would have been better to have the actual PD data than the censored ones. Secondly, the PK sampling schedule also can be optimized for 2-compartmental PK model development in the future studies. In addition, the PK and PD of ranitidine can be evaluated in multiple doses as it is actually used in the future study.

5.2 Exposure-Response Analysis Using Time-To-Event Data of the Ranitidine

Most stress-related gastric bleeding is observed when the intragastric pH is less than 4. To achieve and maintain the gastric pH above the critical level is believed to be important in preventing possible gastric bleeding in critically ill patients. Complex modeling techniques such as time-to-event data analysis have not been applied to investigate the exposure-response relationship of ranitidine. The aim of this chapter was to apply the time-to-event data analysis on the development of exposure-response relationship of ranitidine using NONMEM. The plot of the response (the time to achieve gastric pH greater than 4) versus the exposure (the area under the time-concentration curve from the start of drug administration to the 2 hours, AUC_{0-2}) suggested that the sigmoid inhibitory E_{max} model was appropriate for the ranitidine time-to-event data. The event time was assumed to follow the Weibull distribution in the current analysis. The sigmoid inhibitory E_{max} model successfully described the exposure-response relationship of ranitidine. The estimated time to achieve gastric pH greater than 4 was 19.4 hours when ranitidine was not given. If ranitidine was given, the AUC_{0-2} of 0.000125 mg·hr/L was needed to achieve half of the maximal ranitidine effect. As a ranitidine dose, it was 0.00321 mg that was needed to achieve half of its maximal effect for a male subject with normal kidney function as presented with creatinine clearance of 90 ml/min. None of the demographic and clinical characteristics were associated with any of the time-to-event parameters. The ranitidine inhibitory effect was moderate as implied by the sigmoidicity coefficient, 0.423. The conditional probability of event increased with time as the

estimated shape factor (1.41) indicated. The precision of the estimated time-to-event parameters, EA_{50} and $Time\text{-}to\text{-}event_{NoDrug}$, were unsatisfactory and the final model over-estimated the survival probability compared to the actual observations as depicted in the Kaplan-Meier plot.

In the current study, we found fairly weak exposure-response relationship which is difficult to discern whether it is from true lack of relationship or insufficient range of exposure. The range of explored $AUC_{0\text{-}2}$ was not wide enough to discern the thorough exposure-response relation of ranitidine. Clearly, the exposure range needs to be extended in future studies. The metric of exposure to ranitidine, $AUC_{0\text{-}2}$ was chosen because it reflected the early exposure of a subject to ranitidine as well as it took into account the PK sampling schedule in the majority of patients. Although $AUC_{0\text{-}2}$ performed better than any other tested measures of exposure in the current analysis, other metrics should be considered and the sampling schedule needs to be adjusted depending upon possible choices. The study population in the future study can also be restricted to the critically ill patients who will experience stress ulcer and eventually receiving the study drug.

5.3 Food and Ranitidine Effect on Human Gastric Acid Secretion

The third aim of current research was to develop a mechanism-based mathematical model using STELLA® that could predict reasonable gastric pH and to test the food and

ranitidine effect on the gastric acid secretion. The mathematical modeling is free from the unexpected variability and non-invasive method that allows testing the system under the extreme conditions. In the current study, the following assumptions were made: 1) food intake alone could bring disturbance to the system 2) cell populations were at steady state 3) neuronal stimuli, endocrine and paracrine substances worked independently. The proposed physiologically-based simulation model successfully demonstrated observed human gastric acid regulation and the effect of food and ranitidine on gastric acid secretion. The observed fasting gastric pH agreed well with the literature value. The patterns of neuronal stimuli, endocrine and paracrine activities in response to the food intake agreed with the previous reports. The gastric acid secretion system was stable and returned to baseline quickly when it was disturbed. Ranitidine increased baseline as well as the peak gastric pH when food was taken. The gastric pH was restored to the previous steady-state level within 24 hours when ranitidine infusion was discontinued abruptly. However, none of the recommended ranitidine doses achieved a base gastric pH greater than 4. This model can be applied to simulate gastric acid secretion in a disease condition such as Zollinger-Ellison syndrome, *H. pylori* infection or partial gastrectomy when the relevant parts of this model affected by these conditions are identified. Gastric pH controlling agents other than histamine 2 receptor antagonist including proton pump inhibitor and antacid can also be incorporated into a simulation model.

Some of the assumptions in the current study can be relaxed in the future. The change of gastric cell population over time and the reported correlation between effectors can be

incorporated in the model. In addition to the dilution followed by food volume, different food contents or neuronal stimulations can be included as the reason of gastric pH change. Lastly, the parameters, cell populations and initial conditions adopted from experiments other than in human can be replaced by the corresponding values in human if available.

REFERENCES

Chapter 1

- Amaral MC, Favas C, Alves JD, Riso N, Riscado MV (2010) Stress-Related Mucosal Disease: Incidence of Bleeding and the Role of Omeprazole in its Prophylaxis. Eur J Intern Med 21(5):386-8.
- American Society of Hospital Pharmacist (1999), ASHP Therapeutic Guidelines on Stress Ulcer Prophylaxis. Am J Health Syst Pharm 56(4):347-79.
- Apte NM, Kamad DR, Medhekar TP, Tilve GH, Morye S, Bhave GG (1992) Gastric Colonization and Pneumonia in Intubated Critically Ill Patients Receiving Stress Ulcer Prophylaxis: a Randomized, Controlled Trial. Crit Care Med 20(5):590-3.
- Barletta JF, Erstad BL, Fortune JB (2002) Stress Ulcer Prophylaxis in Trauma Patients. Crit Care 6(6):526-30.
- Conrad SA, Gabrielli A, Margolis B, Quartin A, Hata SJ, Frank WO, Bagin RG, Rock JA, Hepburn B, Laine L (2005) Randomized Double-blind Comparison of Immediate-release Omeprazole Oral Suspension versus Intravenous Cimetidine for the Prevention of Upper Gastrointestinal Bleeding in Critically Ill Patients. Crit Care Med 33(4):760-5.
- Cook DJ, Fuller HD, Guyatt GH, Marshall JC, Leasa D, Hall R, Winton TL, Rutledge F, Todd TJ, Roy P, Lacroix J, Griffith L, Willan A and the Canadian Critical Care Trials Group (1994) Risk Factors for Gastrointestinal Bleeding in Critically Ill Patients. N Engl J Med 330(6):377-81.

- Cook DJ, Reeve BK, Guyatt GH, Heyland DK, Griffith LE, Buckingham L, Tryba M (1996) Stress Ulcer Prophylaxis in Critically Ill Patients. Resolving Discordant Meta-analyses. JAMA 275(4):308-14.
- Cook D, Guyatt G, marshall J, Leasa D, Fuller H, Hall R Peter S, Rutledge F, Griffith L, McLellan A, Wood G, Kirby A (1998) A Comparison of Sucralfate and Ranitidine for the Prevention of Upper Gastrointestinal Bleeding in Patients Requiring Mechanical Ventilation. N Engl J Med 338(12)791-7.
- Cook DJ, Griffith LE, Walter SD, Guyatt GH, Meade MO, Heyland DK, Kirby A, Tryba M, the Canadian Critical Care Trials Group (2001) The Attributable Mortality and Length of Intensive Care Unit Stay of Clinically Important Gastrointestinal Bleeding in Critically Ill Patients. Crit Care 5(6):368-75.
- Czaja MA, McAlhany JC, Pruitt BA Jr. (1974) Acute Gastroduodenal Disease after Thermal Injury. An Endoscopic Evaluation of Incidence and Natural History. N Engl J Med 291(18):925-9.
- Daley RJ, Rebuck JA Welae LS et al (2004). Prevention of Stress Ulceration: Current Trends in Critical Care. Crit Care Med 32:2008-13.
- Dial S, Alrasadi K, Manoukian C, Huang A, Menzies D (2004) Risk of Clostridium Difficile Diarrhea among Hospital Inpatients Prescribed Proton Pump Inhibitors: Cohort and Case-Control Studies. CMAJ 171(1):33-8.
- Dive A, Moulart M, Jonard P, Jamart J (1994) Gastroduodenal Motility in Mechanically Ventilated Critically Ill Patients: A Manometric Study. Crit Care Med22(3):441-7.

- Driks MR, Craven DE, Celli BR, Manning M, Burke RA, Garvin GM, Kunches LM, Farber HW, Wedel SA, McCabe WR (1987) Nosocomial Pneumonia in Intubated Patients given Sucralfate as Compared with Antacids or Histamine Type 2 Blockers. The Role of Gastric Colonization. N Engl J Med 317(22):1376-82.
- Eddleston JM, Vohra A, Scott P, Tooth JA, Pearson RC, McCloy RF, Morton AK, Doran BH (1991) A Comparison of the Frequency of Stress Ulceration and Secondary Pneumonia in Sucralfate or Ranitidine-Treated Intensive Care Unit Patients. Crit Care Med 19(12):1491-6.
- Erstad BL, Barletta JF, Jacobi J, Killian AD, Kramer KM, Martin SJ (1999) Survey of Stress Ulcer Prophylaxis Crit Care 3:145-9.
- Fennerty MB (2002) Pathophysiology of the Upper Gastrointestinal Tract in the Critically Ill Patients: Rationale for the Therapeutic Benefits of Acid Suppression. Crit Care Med 30(6) S351-5.
- Fogelman MJ, Garvey JM (1966) Acute Gastroduodenal Ulceration Incident to Surgery and Disease. Analysis and Review of Eighty-Eight Cases. Am J Surg 112(5):651-6.
- Grube RR, May DB (2007) Stress Ulcer Prophylaxis in Hospitalized Patients Not in Intensive Care Units. Am J Health Syst Pharm 64(13):1396-400.
- Gullotta R, Ferraris L, Cortelezzi C, Minoli G, Prada A, Comin U, Rocca F, Ferrara A, Curzio M (1997) Are We Correctly Using the Inhibitors of Gastric Acid Secretion and Cytoprotective Drugs? Results of a Multicentre Study. Ital J Gastroenterol Hepatol 29(4):325-9.

- Heyland DK, Tougas G, King D, Cook DJ (1996) Impaired Gastric Emptying in Mechanically Ventilated Critically Ill Patients. Intensive Care Med 22(12):1339-44.
- Kantorova I, Svoboda P, Scheer P, Doubek J, Rehorkova D, Bosakova H, Ochmann J (2004) Stress Ulcer Prophylaxis in Critically Ill Patients: a Randomized Controlled Trial. Hepatogastroenterology 51(57):757-61.
- Levy MJ, Seelig CB, Robinson NJ, Ranney JE (1997) Comparison of Omeprazole and Ranitidine for Stress Ulcer Prophylaxis. Dig Dis Sci 42(6):1255-9.
- Lin PC, Cahng CH, Hsu PI, Tseng PL, Huang YB (2010) The Efficacy and Safety of Proton Pump Inhibitors vs Histamine-2 Receptor Antagonists for Stress Ulcer Bleeding Prophylaxis among Critical Care Patients: A Meta-Analysis. Crit Care Med 38(4):1197-205.
- Lucas CE, Sugawa C, Riddle J, Rector R, Walt AJ (1971) Natural History and Surgical Dilemma of "Stress" Gastric Bleeding. Arch Surg 102:266-73.
- MacLaren R, Jarvis CL, Fish DN (2001) Use of Enteral Nutrition for Stress Ulcer Prophylaxis. Ann Pharmacother 35(12):1614-23.
- Marik PE, Vasu T, Hirani A, Pachinburavan M (2010) Stress Ulcer Prophylaxis in the New Millennium: A Systematic Review and Meta-analysis. Crit Care Med 38(11):2222-8.
- Miano TA, Reichert MG, Houle TT, MacGregor DA, Kincaid EH, Bowton DL (2009) Chest 136(2):440-7.
- Navab F, Steingrub J (1995) Stress Ulcer: Is Routine Prophylaxis Necessary? Am J Gastroenterol 90(5):708-12.

- Netzer P, Gaia C, Sandos M, Huluk T, Gut A, Halter F, Hüsler J, Inauen W (1999) Effect of Repeated Injection and Continuous Infusion of Omeprazole and Ranitidine on Intragastric pH Over 72 Hours. Am J Gastroenterol 94(2):351-7.
- Ojiako K, Shingala H, Schorr C, Gerber DR (2008) Famotidine versus Pantoprazole for Preventing Bleeding in the Upper Gastrointestinal Tract of Critically Ill Patients Receiving Mechanical Ventilation. Am J Crit Care 17(2):142-7.
- Peura DA, Johnson LF (1985) Cimetidine for Prevention and Treatment of Gastroduodenal Mucosal Lesions in Patients in an Intensive Care Unit. Ann Intern Med 103(2):173-7.
- Pham CQ, Regal RE, Bostwick TR, Knauf KS (2006) Acid Suppressive Therapy Use on an Inpatients Internal Medicine Service. Ann Pharmacother 40(7-8):1261-6.
- Prod'hom G, Leuenberger P, Koerfer J, Blum A, Chiolero R, Schaller MD, Perret C, Spinnler O, Blondel J, Siegrist H, Saghafi L, Blanc D, Francioli P (1994) Nosocomial Pneumonia in Mechanically Ventilated Patients Receiving Antacid, Ranitidine, or Sucralfate as Prophylaxis for Stress Ulcer. A Randomized Controlled Trial. Ann Intern Med 120(8):653-62.
- Quenot JP, Thiery N, Barbar S (2009) When Should Stress Ulcer Prophylaxis be Used in the ICU? Curr Opin Crit Care 15(2):139-43.
- Ran L, Khatibi NH, Qin X, Zhang JH (2011) Proton Pump Inhibitor Prophylaxis Increases the Risk of Nosocomial Pneumonia in Patients with an Intracerebral Hemorrhagic Stroke. Acta Neurochir Suppl 111:435-9.

- Schuster DF, Rowley H, Feinstein S, McGue MK, Zuckerman GR (1984) Prospective Evaluation of the Risk of Upper Gastrointestinal Bleeding after Admission to a Medical Intensive Care Unit. Am J Med 76(4):623-30.
- Selye H (1936) A Syndrome Produced by Diverse Nocuous Agents. Nature Jul 4;138(3479):32
- Skillman JJ, Bushnell LS, Goldman H, Silen W (1969) Respiratory Failure, Hypotension, Sepsis and Jaundice. A Clinical Syndrome Associated with Lethal Hemorrhage from Acute Stress Ulceration of the Stomach. Am J Surg 117(4):523-30.
- Simms HH, DeMaria E, McDonald L, Peterson D, Robinson A, Burchard KW (1991) Rose of Gastric Colonization in the Development of Pneumonia in Critically Ill Trauma Patients: Results a Prospective Randomized Trial. J Tauma 31(4):531-6.
- Spirt MJ, Stanley S (2006) Update on Stress Ulcer Prophylaxis in Critically Ill Patients. Crit Care Nurse 26(1):18-20, 22-8.
- Tryba M (1991) Sucralfate versus Antacids or H2-antagonists for Stress Ulcer Prophylaxis: A Meta-analysis on Efficacy and Pneumonia Rate. Cir Care Med 19(7):942-9.
- Zandstra DF, Stoutenbeek CP (1993) The Virtual Absence of Stress-Ulceration Related Bleeding in ICU patients Receiving Prolonged Mechanical Ventilation without any Prophylaxis. Intensive Care Med 20(5):355-40
- Zegerid Package Insert. Whitby, Ontario:Patheon Inc;2007

- Zeltsman D, Rowland M, Shanavas Z, Kerstein MD (1996) Is the Incidence of Hemorrhagic Stress Ulceration in Surgical Critically Ill Patients Affected by Modern Antacid Prophylaxis? Am Surg 62(12):1010-3.

Chapter 2

- Akaike, H (1974) A New Look at the Statistical Model Identification. IEEE Trans Auto Cont AC-19:716-23.
- Ariëns EJ, Simonis AM (1964) A Molecular Basis for Drug Action. J Pharm Pharmacol 16:137-57.
- Beal SL, Sheiner LB (1989). NONMEM Users Guides. ICON Development Solutions, Ellicott City, Maryland
- Byon W, Fletcher CV, Brundage RC (2008) Impact of Censoring Data below an Arbitrary Quantification Limit on Structural Model Misspecification. J Pharmacokinet Pharmacodyn 35(1):101-16.
- Colburn WA (1981) Simultaneous Pharmacokinetics and Pharmacodynamic Modeling. J Pharmacokinet Biopharm 9(3):367-88.
- Crommelin DJ, Sindelar RD, Meibohm B (2007) Pharmaceutical Biotechnology: Fundamentals and Applications. 3rd Edition. Informa Healtcare.
- Dayneka NL, Garg V, Jusko WJ (1993) Comparison of Four Basic Models of Indirect Pharmacodynamic Responses. J Pharmacokinet Biopharm 21(4):457-78.
- Duerksen DR (2003) Stress-related Mucosal Disease in Critically Ill Patients. Best Pract Res Clin Gastroenterol 17(3):327-44.

- Duval V, Karlsson MO (2002) Impact of Omission of Replacement of Data Below the Limit of Quantification on Parameter Estimates in a Two-Compartment Model. Pharm Res 19(12):1835-40.
- Garg DC, Baltodano N, Jallad NS, Perez G, Oster JR, Eshelman FN, Weidler DJ (1986) Pharmacokinetics of Ranitidine in Patients with Renal Failure. J Clin Pharmacol 26(4):286-91.
- Garg V, Khunvichai A (2007) Mechanistic Pharmacokinetic/Pharmacodynamic Models I. In: Ette EI, Williams PJ, eds. Pharmacometrics: The Science of Quantitative Pharmacology, John Wiley & Sons: 583-605.
- Food and Drug Administration, Center for Drug Evaluation and Research (2010). Guidance for Industry: Pharmacokinetics in Patients with Impaired Renal Function-Study Design, Data Analysis, and Impact on Dosing and Labeling. Rockville, MD.
- Karlsson MO, Savic RM (2007) Diagnosing Model Diagnostics. Clin Pharmacol Ther 82(1):17-20.
- McFadyen ML, Folb PI, Miller R, Keeton GR, Marks IN (1983) Pharmacokinetics of Ranitidine in Patients with Chronic Renal Failure. 25(3):347-51.
- McNeal JJ, Mihaly GW, Anderson A, Marshall AW, Smallwood RA, Louis WJ (1981) Pharmacokinetics of the H2-Receptor Antagonist Ranitidine in Man. Br J Clin Pharmacol 12(3);411-5.
- Meibohm B, Derendorf H (1997) Basic Concepts of Pharmacokinetic /Pharmacodynamic (PK/PD) Modeling. Int J Clin Pharmacol Ther 35(10):401-13.

- Pérez FJ, Olguín JH, Pérez FC, Guillé PG, Pérez GA, Vieyra CA, López TA, Portugal CM, Asseff LI (2003) Effects of Gender and Phase of the Menstrual Cycle on the Kinetics of Ranitidine in Healthy Volunteers. Chronobiol Int 20(3)485-94.
- Post TM, Freijer JI, Ploeger BA, Danhof M (2008) Extensions to the Visual Predictive Check to Facilitate Model Performance Evaluation, J Pharmacokinet Pharmacodyn 35(2):185-202.
- Proost JH, Schiere S, Eleveld DJ, Wierda JM (2007) Simultaneous versus Sequential Pharmacokinetic-Pharmacodynamic Population Analysis Using an Iterative Two-Stage Bayesian Technique. Biopharm Drug Disposition, 28(8);455-73.
- Sheiner LB, Stanski DR, Vozeh S, Miller RD, Ham J (1979) Simultaneous Modeling of Pharmacokinetics and Pharmacodynamics:application to d-Tubocurarine. Clin Pharmacol Ther 25(3):358-71.
- van Hecken AM, Tjandramaga TB, Mullie A, Verbesselt R, de Schepper PJ (1982) Ranitidine: Single Dose Pharmacokinetics and Absolute Bioavailability in Man. Br J Clin Pharmacol 14(2):195-200
- Zhang L, Beal SL, Sheiner LB (2003a) Simultaneous vs. Sequential Analysis for Population PK/PD data: Best-case Performance. J Pharmacokinet Pharmacodyn, 30(6):387-404.
- Zhang L, Beal SL, Sheiner LB (2003b) Simultaneous vs. Sequential Analysis for Population PK/PD data: Robustness of Methods. J Pharmacokinet Pharmacodyn, 30(6):405-16.

- Xu SX, Dunne A, Kimko H, Nandy P, Vermeulen A (2011) Impact of Low Percentage of Data Below the Quantification Limit on Parameter Estimates of Pharmacokinetic Models. J Pharmacokinet Pharmacodyn 38(4):423-32.

Chapter 3

- Cook DJ, Reeve BK, Guyatt GH, Heyland DK, Griffith LE, Buckingham L, Tryba M (1996) Stress Ulcer Prophylaxis in Critically Ill Patients: Resolving Discordant Meta-Analyses. JAMA 275(4):308-14.
- Cox EH, Veyrat-Follet C, Beal SL, Fuseau E, Kenkare S, Sheiner LB (1999) A Population Pharmacokinetic-Pharmacodynamic Analysis of Repeated Measures Time-to-Event Pharmacodynamic Responses: The Antiemetic Effect of Ondansetron. J Pharmacokinet Pharmacodyn, 27(6):625-44.
- Ette EI, Roy A, Nandy P (2007) Population Pharmacokinetic/Pharmacodynamic Modeling of Ordered Categorical Longitudinal Data. In: Ette EI, Williams PJ, Pharmacometrics: The Science of Quantitative Pharmacology, John Wiley & Sons: 655-72.
- Fennerty MB (2002) Pathophysiology of the Upper Gastrointestinal Tract in the Critically Ill Patients: Rationale for the Therapeutic Benefits of Acid Suppression. Crit Care Med 30(6):S351-5.
- Franceschi M, Di Mario F, Leandro G, magi S, Pilotto A (2009) Acid-Related Disorders in the Elderly. Best Pract Res Clin Gastroenterol 23(6):839-48.

- Gedeit RG, Weigle CGM, Havens PL, Werlin SL(1993) Control and Variability of Gastric pH in Critically Ill Children. Crit Care Med 21(12):1850-5.
- Gieschke R, Burger HU, Reigner B, Blesch KS, Steimer JL (2003) Population Pharmacokinetics and Concentration-Effect Relationships of Capecitabine Metabolites in Colorectal Can cer Patients. Br J Clin Pharmacol 55(3):252-63.
- Jönsson S, Kjellsson MC, Karlsson MO (2004) Estimating Bias in Population Parameters for Some Models for Repeated Measures Ordinal Data Using NONMEM and NLMIXED. J Pharmacokinet Pharmacodyn 31(4):299-320.
- Karlsson KE, Plan EL, Karlsson MO (2011) Performance of Three Estimation Methods in Repeated Time-to-event Modeling AAPS J 13(1):83-91.
- Kline JP, Moeschberger ML (1997) Survival Analysis: Techniques for Censored and Truncated Data. 2nd edition. New York, Springer: 21-56.
- Lee ET, Go OT (1997) Survival Analysis in Public Health Research. Annu Rev Public Health 18:105-34
- McFadyen ML, Folb PI, Marks IN, Wright JP, Lucke W (1981) The Pharmacokinetics of Ranitidine in Patients with Chronic Duodenal Ulceration. Scan J Gastroenterol Suppl 69:109-13.
- McNeil JJ, Mihaly GW, Anderson A, Marshall AW, Smallwood RA, Louse WJ (1981) Pharmacokinetics of the H2-Receptor Antagonist Ranitidine in Man. Br J Clin Pharmacol 12(3):411-5.

- Mignon M, Chau NP, Nguyen-Phuoc BK, Sauvage M, Leguy F, Bonfils S (1982) Ranitidine upon Meal-Induced Gastric Secretion: Oral Pharmacokinetics and Plasma Concentration Effect Relationships. Br J Clin Phrmacol 14(2):187-93.
- Netzer P, Gaia C, Sandos M, Huluk T, Gut A, Halter F, Hüsler J, Inauen W (1999) Effect of Repeated Injection and Continuous Infusion of Omeprazole and Ranitidine on Intragastric pH Over 72 Hours. Am J Gastroenterol 94(2):351-7.
- Russell TL, Berardi RR, Barnett JL, Dermentzoglou LC, Jarvenpaa KM, Schmaltz SP, Dressman JB (1993) Upper Gastrointestinal pH in Seventy-nine Healthy, Elderly, North American Men and Women. 10(2):187-96.
- Sheiner LB (1994) A New Approach to the Analysis of Analgesic Drug Trials, Illustrated with Bromfenac Data. Clin Pharmacol Ther, 56(3):309-22.
- Trocóniz IF, Wolters JM, Tillmann C, Schaefer HG, Roth W (2006) Modelling the Anti-Migraine Effect of BIBN 4096 BS. Clin Pharmacokinet, 45(7):715-28.
- van Hecken AM, Tjandramaga TB, Mullie A, Verbesselt R, de Schepper PJ (1982) Ranitidine: Single Dose Pharmacokinetics and Absolute Bioavailability in Man. Br J Clin Pharmacol 14(2):195-200.
- Yang YX, Lewis JD (2003) Prevention and Treatment of stress Ulcers in Critically Ill Patients. Semin Gastrointest Dis 14(1):11-9.

Chapter 4

- Amsden GW, Goss TF, Harrison NJ, D'Andrea DT, Schentag JJ (1994) Pharmacodynamics of Bolus Famotidine versus Infused Cimetidine, Ranitidine and Famotidine. J Clin Pharmacol 34(12):1191-8.
- Barocelli E, Ballabeni V (2003) Histamine in the Control of Gastric Acid Secretion: a Topic Review. Pharmacol Res 47(4):299-304.
- Borch K, Renvall H, Liedberg G, Andersen BN (1986) Relations between Circulating Gastrin and Endocrine Cell Proliferation in the Atrophic Gastric Fundic Mucosa. 21(3):357-63.
- Chew CS (1983) Inhibitory Action of Somatostatin on Isolated Gastric Glands and Parietal Cells. Am J Physiol 245(2):G221-9.
- Coruzzi G, Adami M, Pozzoli C, Bertaccini G (1996) Cardiac and Gastric Effects of Histamine H2 Receptor Antagonist: No Evidence for a Correlation between Lipophilicity and Receptor Affinity. Br J Pharmacol 118(7):1813-21.
- Cuvale RA (2009) Buffer Capacity of Bovine Serum Albumin. J Argentine Chemical Society 97(1):174-80.
- Debas HT, Carvajal SH (1994) Vagal Regulation of Acid Secretion and Gastrin Release. Yale J Biol Med 67(3-4):145-51.
- de Beus AM, Fabry TL, Lacker HM (1993) A Gastric Acid Secretion Model. Biophys J 65(1):362-78.
- Dressman JB, Berardi RR, Dermentzoglou LC, Russell TL, Schmaltz SP, Barnett JL, Jarvenpaa KM (1990) Upper Gastrointestinal (GI) pH in Young, Healthy Men and Women. Pharm Res 7(7):756-61.

- Dubios A, Erdewegh PV, Gardner JD (1977) Gastric emptying and secretion in Zollinger-Ellison Syndrome. J Clin Invest 59(2):255-63.
- Farhadi A, Fields JZ, Keshavarzian A (2007) Mucosal Mast Cells are Pivotal Elements in Inflammatory Bowl Disease that Connect the Dots: Stress, Intestinal Hyperpermeability and Inflammation. World J Gastroentrol 13(22):3027-30.
- Feurle GE (1994) Argyrophil Cell Hyperplasia and a Carcinoid Tumour in the Stomach of a Patient with Sporadic Zollinger-Ellison Syndrome. Gut 35(2):275-7.
- Feldman M (1983) Gastric Bicarbonate Secretion in Humans. Effect of Pentagastrin, Bethanechol and 11,16,16-Trimethyl Prostaglandin E2. J Clin Invest. 72(1):295-303.
- Feldman M (1985) Gastric H^+ and HCO_3^- Secretion in Response to Sham Feeding in Humans. Am J Physiol 248(2 Pt 1):G188-91.
- Grant SJ, Langtry HD, Brogden RN (1989) Ranitidine: An Updated Review of its Pharmacodynamic and Pharmacokinetic Properties and Therapeutic Use in Peptic Ulcer Disease and Other Allied Diseases. Drugs 37(6):810-70.
- Gedeit RG, Weigle CGM, Havens PL, Werlin SL(1993) Control and Variability of Gastric pH in Critically Ill Children. Crit Care Med 21(12):1850-5.
- Häkanson R, Larsson LI, Lieberg G, Oscarson J, Sundler F, Vang J (1976) Effects of Antrectomy or Porta-caval Shunting on the Histamine-storing Endocrine-like Cells in Oxyntic Mucosa of Rat Stomach. A Fluorescence Histochemical, Electron Microscopic and Chemical Study. J Physiol 259(3):785-800.
- Harty RF, Ancha HB (2006) Stress Ulcer Bleeding. Curr Treat Options Gastroenterol 9(2):157-66.

- Hersey SJ, Sachs G (1995) Gastric Acid Secretion. Physiol Rev 75(1):155-89.
- Johnson LR (2006) Gastrointestinal physiology. 7th edition. Philadelphia, Mosby Elsevier: 75-94.
- Joseph IM, Zavros Y, Merchant JL, Kirschner D (2003) A model for Integrative Study of Human Gastric Acid Secretion. J Appl Physiol 94:1602-1618.
- Kamolz T, Granderath FA, Bammer T, Pasiut M, Pointer R (2006) Psychological Intervention Influences the Outcome of Laparoscopic Antireflux Surgery in Patients with Stress-related Symptoms of Gastroesophageal Reflux Disease. Scand J Gastroenterol 36(8):800-5.
- Karam SM, Alexander G (2001) Blocking of Histamine H2 Receptors Enhances Parietal Cell Degeneration in the Mouse Stomach. Histol Histophthol 16(2):469-80.
- Kleveland PM, Waldum HL Larsson H (1987) Gastric Acid Secretion in the Totally Isolated, Vascularly Perfused Rat Stomach. Scand J Gastroenterol 22(6):705-13.
- Ličko V, Ekblad EBM (1992) What Dual-Action Agents Reveal about Acid Secretion: a Combined Experimental and Modeling Analysis. Biochim Biophys Acta 1137(1):19-28.
- Lin JH (1991) Pharmacokinetic and Pharmacodynamic Properties of Histamine H2-Receptor Antagonists. Relationship Between Intrinsic Potency and Effective Plasma Concentrations. Clin Pharmacokinet 20(3):218-36.
- Lindström E, Chen D, Norlén P, Andersson K, Håkanson R (2001) Control of Gastric Acid Secretion: the Gastrin-ECL Cell-Parietal Cell Axis. Comp Biochem Physiol A Mol Integr Physiol 128(3):503-11.

- Marino S, Ganguli S, Joseph IM, Kirschner DE (2003) The Important of an Inter-compartmental Delay in a Model for Human Gastric Acid Secretion. Bull Math Biol 65(6):963-90.
- Netzer P, Gaia C, Sandos M, Huluk T, Gut A, Halter F, Hüsler J, Inauen W (1999) Effect of Repeated Injection and Continuous Infusion of Omeprazole and Ranitidine on Intragastric pH Over 72 Hours. Am J Gastroenterol 94(2):351-7.
- Orenstein SR, Blumer JL, Faessel HM, McGuire JA, Fung K, Li BU, Lavine JE, Grunow JE, Treem WR, Ciociola AA (2002) Ranitidine, 75 mg, Over-the-counter dose: Pharmacokinetic and Pharmacodynamic Effects in Children with Symptoms of Gastro-oesophageal reflux. Aliment Pharmacol Ther 16(5):899-907.
- Peterson WL (1996), The Influence of Food, Beverages and NSAIDs on Gastric Acid Secretion and Mucosal Integrity. Yale J Biol Med 69(1):81-4.
- Puolanne E, Kivikari R (2000) Determination of the Buffering Capacity of Postrigor Meat. Meat Sci 56(1):7-13.
- Samuelson LC, Hinkle KL (2003) Insights into the Regulation of Gastric Acid Secretion through Analysis of Genetically Engineered Mice. Annu Rev Physiol 65:383-400.
- Sawchuk RJ (2010) Simulation of Pharmacokinetic Systems with STELLA®: Course Manual, Minneapolis, MN
- Schiller LR, Walsh JA, Feldman M (1980) Distention-Induced Gastrin Release: Effects of Luminal Acidification and Intravenous Atropine. Gastroenterology 78(5 Pt 1):912-7.

- Shankley NP, Welsh NJ, Black JW (1992) Histamine Dependence of Pentagastrin-Stimulated Gastric Acid Secretion in Rats. Yale J Biol Med 65(6):613-9.
- Tielemans Y, Axelson J, Sundler F, Willems G, Håkanson R (1990) Serum Gastri Concentration Affects the Self Replication Rate of the Enterochromaffin Like Cells in the Rat Stomach. Gut 31(3):274-8
- Zavros Y, Fleming WR, Shulkes A (1999) Concurrent Elevation of Fundic Somatostatin Prevents Gastrin Stimulation by GRP. Am J Physiol 276(1 pt 1):G21-7.
- Zavros Y, Rieder G, Ferguson A, Samuelson LC, Merchangt JL (2002) Hypergastrinemia in Response to Gastric Inflammation Suppresses Somatostatin. Am J Physiol Gastrointest Liver Physiol 282(1):G175-83.

APPENDIX

Chapter 2: Final sequential pharmacokinetic model of intravenous ranitidine

```
$PROBLEM    FINAL PK MODEL IN SEQUENTIAL APPROACH
$INPUT      C TRT ID DATE=DROP TIME AMT RATE DV CMT TYPE AGE SEX RACE
WT CRCL EVID MDV LIMI
; TRT = DOSING TYPE, 0=PLACEBO, 1=INFUSION WITH BOLUS, 2=INFUSION
; AMT = DOSE
; DV = PLASMA CONCENTRATION OR GASTRIC pH
; CMT = COMPARTMENT
; TYPE = OBSERVATION TYPE, 1=DOSING, 2=PK OBSERVATION, 3=PD OBSERVATION
; SEX, 1=MALE, 2=FEMALE
; RACE, 1=WHITE, 2=BLACK, 3=HISPANIC, 4=ASIAN, 5=AMERICAN INDIAN
; 6=OTHER
; WT = WEIGHT
; CRCL = CREATININE CLEARANCE
; LIMI = UPPER LIMIT OF OBSERVATIONS

$DATA       RAN_PKPD.CSV IGNORE=(C=C,TYPE=3)

$SUBROUTINE ADVAN3 TRANS4

$PK
   TVCL=THETA(1)*(CRCL/90)**THETA(5)
   CL=TVCL*EXP(ETA(1))

   TVV1=THETA(2)
   V1=TVV1*EXP(ETA(3))

   TVQ=THETA(3)
   Q=TVQ

   TVV2=THETA(4)
   IF(SEX.EQ.2)THEN
   TVV2=TVV2*THETA(6)
   ENDIF
   V2=TVV2*EXP(ETA(2))

   SC=V1/1000

$ERROR
   Y = F + F*ERR(1)+ERR(2)
   IPRED=F

$THETA
   (0,25) ; [CL]
   (0,16) ; [V1]
   (0,50) ; [Q]
```

```
   (0,60) ; [V2]
   0.5    ; [CRCL effect on CL]
   0.3    ; [SEX effect on V2]

$OMEGA BLOCK(2)
   0.1  ; [p] IIV on CL
   0.1  ; Interaction between CL and V2
   0.3  ; [P] IIV on V2

$OMEGA
   0.2  ; [p] IIV on V1

$SIGMA
   0.1  ; [P] sigma(1,1)
   1    ; [A] sigma(2,2)

$EST METHOD=1 INT PRINT=5 MAX=9999 SIG=3 MSFO=SEQPK.msf NOABORT

$COV PRINT=E

$TABLE ID TRT TIME CL V1 V2 ETA1 ETA2 ETA3 CWRES IPRED TYPE AMT WT AGE
SEX RACE CRCL ONEHEADER NOPRINT FILE=SEQPK.tab
```

Chapter 2: Final sequential pharmacodynamic model of intravenous ranitidine

```
$PROBLEM    FINAL PD MODEL IN SEQUENTIAL APPROACH
$INPUT      C TRT ID DATE=DROP TIME AMT RATE DV CMT TYPE AGE SEX RACE
WT CRCL EVID MDV LIMI
; TRT = DOSING TYPE, 0=PLACEBO, 1=INFUSION WITH BOLUS, 2=INFUSION
; AMT = DOSE
; DV = PLASMA CONCENTRATION OR GASTRIC pH
; CMT = COMPARTMENT
; TYPE = OBSERVATION TYPE, 1=DOSING, 2=PK OBSERVATION, 3=PD OBSERVATION
; SEX, 1=MALE, 2=FEMALE
; RACE, 1=WHITE, 2=BLACK, 3=HISPANIC, 4=ASIAN, 5=AMERICAN INDIAN
; 6=OTHER RACE
; WT = WEIGHT
; CRCL = CREATININE CLEARANCE
; LIMI = UPPER LIMIT OF OBSERVATIONS

$DATA        RAN_PKPD.CSV IGNORE=(C=C, TYPE=2)

$SUBROUTINES ADVAN6 TOL=5

$MODEL NCOMP=3
   COMP=(CENTRAL,DEFDOSE)
   COMP=(PERI)
   COMP=(EFFECT)

$PK
   CL=CLI
   V1=V1I
   Q=49.4
   V2=V2I

   K10=CL/V1
   K12=Q/V1
   K21=Q/V2

   TVKIN=THETA(1)
   KIN=TVKIN

   TVEC=THETA(2)
   EC=TVEC*EXP(ETA(2))

   TVEM=THETA(3)
   EM=TVEM+ETA(3)

   TVBS=THETA(4)
   BS=TVBS*EXP(ETA(1))
   A_0(3)=BS

$DES
   CONC=A(1)*1000/V1
```

```
   KOUT=KIN/BS

   DADT(1)=A(2)*K21-A(1)*(K10+K12)
   DADT(2)=A(1)*K12-A(2)*K21

   EFF=1+EM*CONC/(EC+CONC)
   DADT(3)= KIN*EFF-KOUT*A(3)

$ERROR
   YUP=LIMI
   PRB=PR_Y

   Y = F+F*ERR(1)
   IPRED=Y

$THETA
   (0, .1)  ;[KIN]
   (0, 50)  ;[EC50]
   (0, 8)   ;[EMAX]
   (0, 2)   ;[INITIAL GASTRIC pH]

$OMEGA
   .1       ;[p] IIV on Baseline gastric pH
   .1       ;[p] IIV on AUC when drug effect is half of its maximum
   .3       ;[a] IIV on maximal pharmacodynamic effect of ranitidine

$SIGMA
   .1       ;[p] sigma(1,1)

$EST METHOD=1 LAPLACIAN INT PRINT=5 MAX=9999 SIG=3 MSFO=seqpd.msf
NOABORT

$COV PRINT=E

$TABLE ID TRT TIME CL V1 V2 ETA1 ETA2 ETA3 PRB PRED CONC TYPE AMT WT
AGE SEX RACE CRCL ONEHEADER NOPRINT FILE=seqpd.tab
```

Chapter 2: Population simultaneous pharmacokinetic and pharmacodynamic model of intravenous ranitidine

```
$PROBLEM    FINAL PKPD MODEL IN SIMULTANEOUS APPROACH
$INPUT      C TRT ID DATE=DROP TIME AMT RATE DV CMT TYPE AGE SEX RACE
WT CRCL EVID MDV LIMI
; TRT = DOSING TYPE, 0=PLACEBO, 1=INFUSION WITH BOLUS, 2=INFUSION
; AMT = DOSE
; DV = PLASMA CONCENTRATION OR GASTRIC pH
; CMT = COMPARTMENT
; TYPE = OBSERVATION TYPE, 1=DOSING, 2=PK OBSERVATION, 3=PD OBSERVATION
; SEX, 1=MALE, 2=FEMALE
; RACE, 1=WHITE, 2=BLACK, 3=HISPANIC, 4=ASIAN, 5=AMERICAN INDIAN
; 6=OTHER RACE
; WT = WEIGHT
; CRCL = CREATININE CLEARANCE
; LIMI = UPPER LIMIT OF OBSERVATIONS

$DATA       RAN_PKPD.CSV IGNORE=C

$SUBROUTINES ADVAN6 TOL=5

$MODEL NCOMP=3
      COMP=(CENTRAL,DEFDOSE,DEFOBS)
      COMP=PERIPH
      COMP=EFFECT

$PK
   TVCL=THETA(1)*(CRCL/90)**THETA(9)
   CL=TVCL*EXP(ETA(1))

   TVV1=THETA(2)
   V1=TVV1*EXP(ETA(2))

   TVQ=THETA(3)
   Q=TVQ

   TVV2=THETA(4)
   IF(SEX.EQ.2)THEN
   TVV2=TVV2*THETA(10)
   ENDIF
   V2=TVV2*EXP(ETA(3))

   K10=CL/V1
   K12=Q/V1
   K21=Q/V2
   S1=V1/1000

   TVKIN=THETA(5)
   KIN=TVKIN*EXP(ETA(7))
```

```
   TVEC=THETA(6)
   EC=TVEC*EXP(ETA(5))

   TVEM=THETA(7)
   EM=TVEM*EXP(ETA(6))

   TVBS=THETA(8)
   BS=TVBS*EXP(ETA(4))
   A_0(3)=BS

$DES
   CONC=A(1)*1000/V1
   KOUT=KIN/BS

   DADT(1)=A(2)*K21-A(1)*(K10+K12)
   DADT(2)=A(1)*K12-A(2)*K21
   EFF=1+EM*CONC/(EC+CONC)
   DADT(3)= KIN*EFF-KOUT*A(3)

$ERROR
   IF(CMT.EQ.1)THEN
   Y=F+F*ERR(1)+ERR(2)  ; RUV of PK
   ELSE
   Y=F+F*ERR(3)         ;RUV of PD
   ENDIF
   IPRED=Y

$THETA
   (0, 20) ;[CL]
   (0, 20) ;[V1]
   (0, 40) ;[Q]
   (0, 50) ;[V2]
   (0, 1)   ;[KIN]
   (0,50)   ;[EC50]
   (0,8)    ;[EMAX]
   (0, 2)   ;[Initial gastric pH]
   (.5)     ;[CRCL effect on CL]
   (1)      ;[SEX effect on V2]

$OMEGA
   .1       ;[p] IIV on CL
   .1       ;[p] IIV on V1
   .1       ;[p] IIV on V2
   .1       ;[p] IIV on Baseline gastric pH
   .1       ;[p] IIV on AUC when drug effect is half of its maximum
   .1       ;[p] IIV on maximal ranitidine effect
   .1       ;[p] IIV on Kin

$SIGMA
   .1       ;[P] proportinal error of PK
   1        ;[a] additional error of PK
   .1       ;[P] proportional error of PD
```

```
$EST METHOD=1 INT PRINT=5 MAX=9999 SIG=3 MSFO=sim.msf NOABORT

$COV PRINT=E

$TABLE ID TIME CL V1 V2 Q BS EM EC KIN ETA1 ETA2 ETA3 ETA4 ETA5 ETA6
ETA7 CWRES CONC IPRED TYPE AMT WT AGE RACE SEX CRCL ONEHEADER NOPRINT
FILE=sim.tab
```

Chapter 3: Time-to-event analysis

```
$PROB RUN# TIME-TO-EVENT MODEL

$INPUT C TRT ID TIME DV AGE SEX RACE WT CRCL PSTS CLI MDV AUC EVID
; TRT = DOSING TYPE, 0=PLACEBO, 1=INFUSION WITH BOLUS, 2=INFUSION
; SEX, 1=MALE, 2=FEMALE
; RACE, 1=WHITE, 2=BLACK, 3=HISPANIC, 4=ASIAN, 5=AMERICAN INDIAN
; 6=OTHER RACE
; WT = WEIGHT
; CRCL = CREATININE CLEARANCE
; PSTS = PATIENT'S STATUS, 1=CRITICALLY ILL, 2=HEALTHY
; CLI = ESTIMATED INDIVIDUAL CLEARANCE
; AUC = AREA UNDER THE TIME-CONCENTRATION CURVE FROM START OF DRUG
; ADMINISTRATION TO 2 HOURS

$DATA tte.csv IGNORE=C

$PRED
   TVBS=THETA(1)
   BS=TVBS*EXP(ETA(1))  ;placebo effect

   TVEA=THETA(2)
   EA=TVEA              ;AUC when the effect is half of max

   SIG=THETA(4)         ;Sigmoidicity
   EFF=AUC**SIG/(EA**SIG+AUC**SIG)

   PHI=BS*(1-EFF)       ;median time to the event

   GAMMA=THETA(3)       ;shape factor
   CONST=.693

   T=TIME/PHI
   NUM=CONST*T**GAMMA
   DENSTY=GAMMA*NUM/TIME*EXP(-NUM)
   SURV=EXP(-NUM)

   IF(DV.EQ.1) THEN
   Y=DENSTY       ;FOR EVENT
   ELSE
   Y=SURV         ;FOR CENSORED
   ENDIF

$THETA
   (0,10)         ;[BASE]
   (0, .001)      ;[EA50]
   (0,1)          ;[GAMMA]
   (.5)           ;[SIGMOID]
```

```
$OMEGA
   0.1            ;omega(1,1)

$EST METHOD=COND LAPLACIAN LIKELIHOOD PRINT=5 SIG=3 MAX=9999
MSFO=tte.msf NOABORT

$COV PRINT=E

$TABLE ID TRT TIME BS EFF PHI WT AUC PSTS AGE RACE SEX CRCL SURV CWRES
ONEHEADER NOPRINT FILE=tte.tab
```